1-1-1996

Stabilization and destabilization of crystals of biopolymers initiated by the environment/

Chao-Cheng Chen
University of Massachusetts Amherst

STABILIZATION AND DESTABILIZATION OF CRYSTALS OF BIOPOLYMERS INITIATED BY THE ENVIRONMENT

A Dissertation Presented

by

CHAO-CHENG CHEN

Submitted to the Graduate School of the

University of Massachusetts Amherst in Partial Fulfillment

of the Requirements for the Degree of

DOCTOR OF PHILOSOPHY

February 1996

Department of Polymer Science and Engineering

STABILIZATION AND DESTABILIZATION OF CRYSTALS OF BIOPOLYMERS INITIATED BY THE ENVIRONMENT

A Dissertation Presented

by

CHAO-CHENG CHEN

Approved as to style and content by:

Shaw L. Hsu, Chair

David A. Tirrell, Member

Lynmarie Thompson, Member

Richard J. Farris Department Head

Polymer Science and Engineering

To my Wife

Mei-Wan

ACKNOWLEDGMENTS

First of all, I would like to acknowledge the guidance and support from my advisors, Professor Shaw Ling Hsu through the course of this research. And I want to thank Professor David A. Tirrell for providing the sample and also for his critical opinions in research. My sincere thanks are also due to Professor Lynmarie Thompson for her critical review of my thesis.

My special appreciation should be paid to Dr. Hun-Jan Tao, Dr. Hsing-Lung Chen, and Dr. Yunwa Wilson Cheung for their heartwarming assistance to me. I would also like to thank my group mates for their helpful discussion during my work, notably Professor Xiao-Zheng Yeng, Dr. Curtis W. Meuse, Dr. Mario Perez, Dr. Yuan Ren, Dr. Sunghoe Yoon, Zhaohui Su, Bert Chien, Thomas Hahn and Sophie Riou. I would like to express my gratitude to the Department for giving me the chance to study here and for providing the most advanced and stimulating research environment.

Finally I am greatly indebted to my wife and my parents for their love and support, which is beyond literal description.

ABSTRACT

STABILIZATION AND DESTABILIZATION OF CRYSTALS OF BIOPOLYMERS INITIATED BY THE ENVIRONMENT

FEBRUARY 1996

CHAO-CHENG CHEN, B.S., NATIONAL TAIWAN UNIVERSITY

M.S., NATIONAL TAIWAN UNIVERSITY

Ph.D.,UNIVERSITY OF MASSACHUSETTS AMHERST

Directed by : Professor Shaw Ling Hsu

Crystalline structure of biopolymers is shown to be greatly affected by the environment. The ubiquitous presence of moisture is found to disturb the crystalline structure of a biosynthesized model polypeptide. We propose a step-by-step mechanism to describe the process of hydration-induced structural changes. On the other hand, in the study of silk fibroin crystallization behavior, it is found that the presence of an oriented substrate can enhance the crystallization of silk II structure even from a dilute aqueous solution with or without salt. The mechanism of substrate-induced crystallization is discussed.

The model polypeptide used in the hydration study has a lamellar structure with uniform lamellar thickness, a folding surface decorated with functional groups and a crystalline core with β-sheet chain conformation. Its structure is changed by moisture sorption in a sequential way. The folding surface functionality is hydrated most quickly followed by the expansion of crystalline core in the intersheet distance. The crystalline chain conformation is the last to be changed. The expansion is proposed to be due to unfavorable surface energetics induced by the incorporation of water molecules on the folding surface. Comparison of hydration-induced structural changes between two

polypeptides with different lamellar thickness supports this explanation. The change in chain conformation is ascribed to the direct interaction of water and peptide units.

Silk fibroin known to be unable to crystallize from dilute aqueous solution with or without salt is found to crystallize in the silk II form on the poly(tetrafluoroethylene) oriented substrate. The orientation and chain conformation of silk fibroin crystals thus formed are characterized with external reflection infrared spectroscopy. Both lattice matching and surface topography are possible nucleation mechanisms.

The same oriented substrate is used in the study of crystallization of nylons from formic acid solution induced by nonsolvents. Different nonsolvents are found to induce different degree of orientation in the nylon crystals. Nylon 6 and nylon 66 exhibit different molecular arrangements on the oriented substrate. This difference in molecular arrangement is supposed to be due to the different phase separation behavior between these two polymers.

TABLE OF CONTENTS

LIST OF TABLES

LIST OF FIGURES

CHAPTER 1

INTRODUCTION

1.1 Objectives and Overview of This Work

One of our objectives in this thesis is to provide a detailed analysis of the structural destability of polymer materials caused by sorption of moisture. Although this has been an active research field, the complex polymer structure together with the various effects of moisture sorption still deter a thorough understanding of this problem. The other objective is, on the other hand, to examine a less appreciated area, i.e., the stabilizing effects of oriented polymer substrates on the formation of oriented nuclei and crystals of another polymer from aqueous media, especially when water-polymer interactions are dominant over polymer-polymer interactions. The orienting ability of the substrate will also be discussed. Later in this chapter the problem layout and related literature works will be reviewed.

In Chapter 2, we will investigate the effects of water sorption on the structure of a biosynthesized model polypeptide system. It is noted that the effects of moisture sorption on the polymer structure are complex and manifold. Therefore,with the advantage of uniform lamellar structure this polypeptide system provides us, we would like to contribute to the understanding of this process. Combination of different techniques, including isotope exchange, infrared spectroscopy, gravimetric method and wide angle X-ray diffraction, we are able to separate the hydration-induced structural changes into distinct events. We will establish that the hydration-induced structural changes are stepwise. In addition, the hydration behavior of two polypeptides with similar structure but with

different lamellar thickness will be compared. The comparison will lead us to conclude that these structural changes are triggered by the competition between different energetics, e.g. bulk energy vs. surface energy, or peptide-peptide hydrogen bonding vs. water-peptide hydrogen bonding.

In Chapter 3 and 4, we examine the substrate-induced crystallization behavior and morphology of silk fibroin and nylons. An friction-deposited oriented poly(tetrafluoroethylene) film will be used as the substrate. Its stabilizing effects on the formation of nuclei will be illustrated. Besides, the effects of surface characteristics, molecular configuration of the depositing polymer and non solvents, which have not been well characterized, will also be investigated in this part of study. We will show that these parameters control the resultant modes of deposition of polymer molecules and thus the spatial orientation of these molecules. Possible mechanism of the orienting ability of the substrate will be proposed. Summary of this thesis will be given in Chapter 5.

1.2 Hydration-Induced Structural Changes

Because of its small molecular size and propensity for forming hydrogen bonds, water is an effective penetrant and absorbate of macromolecules. The changes in the physical properties and structures of the macromolecules as a result of water uptake are of both technological and scientific importance. For example, when poly(methyl methacrylate) (PMMA) is used as the optical disk substrate in videodisks, computer memory units, and so on[1], bending of the disk caused by moisture sorption soon after melt molding is a troublesome problem in the production process. Water can induce proteins to minimize accessible hydrophobic surface area, and the relative strength of protein-protein versus protein-water interactions determines the ability of chains to fold into ordered three-dimensional structures. Therefore, a basic understanding of the water sorption

phenomenon and water-macromolecule interactions is of fundamental importance to both technological and scientific problems.

Effects of moisture on the modulus and elongation have been studied in detail on many polymers, most notably nylons[2], silk[3], and keratin[4], in which a network of hydrogen bonds is a major feature of the structure. Aging[5,6] and fatigue[7] characteristics are also influenced by the presence of moisture. Macroscopic dimensions of these materials also change with the absorption of moisture.[8] Moreover, microstructural changes in both amorphous and crystalline phases associated with moisture absorption have been identified in many macromolecular systems. For example, for synthetic polymers like Nylons, their glass transition temperature and relaxation characteristics associated with amorphous phase have been found to be greatly affected by the amount of water in the structure.[9] Table 1.1 lists the glass transition temperatures(T_g) of some textile fiber materials and their corresponding water contents. The decrease in glass transition temperature may cause major problems in dimensuional stability of these textile materials especially when they are subject to laundry.

Table 1.1 Changes in T_g for some textile materials with water contents.[9]

Polymer	T_g, ^oC	Water content, %
Silk	108-38	12.8-22.2
PET	71-57	6.4-6.8
Nylon 6	41-28	2.0-6.1
Nylon 66	40-29	1.9-6.1

On the other hand, the effects of water on crystalline phase are less documented. For Nylon 6, it has been found that a few water molecules in the interlamellar region may change the overall crystalline state[10]; and solid-solid state phase transitions in Nylon 66 have also been observed.[11] The chain conformation and crystal packing of polypeptides with ionic groups such as poly(L-lysine hydrochloride) or sodium poly(L-glutamate) are known to be particularly affected by the presence of moisture.[12-14] These polymers can exist in different conformations, e.g., β-sheet, α-helix, or disordered forms, depending on the relative humidity. In these cases quantatative relationships between water uptake and chain conformation can be established, as illustrated in Figure 1.1. However, in the case of lysozyme, which contains fewer ionic groups as compared to poly(L-lysine hydrochloride) or sodium poly(L-glutamate), the evidence is not as clear for changes in chain conformation. Since the onset of its enzyme activity depends on the amount of moisture uptake, this uncertainty about hydration-induced conformation change makes the determination of enzymatic mechanism difficult.[15-17]

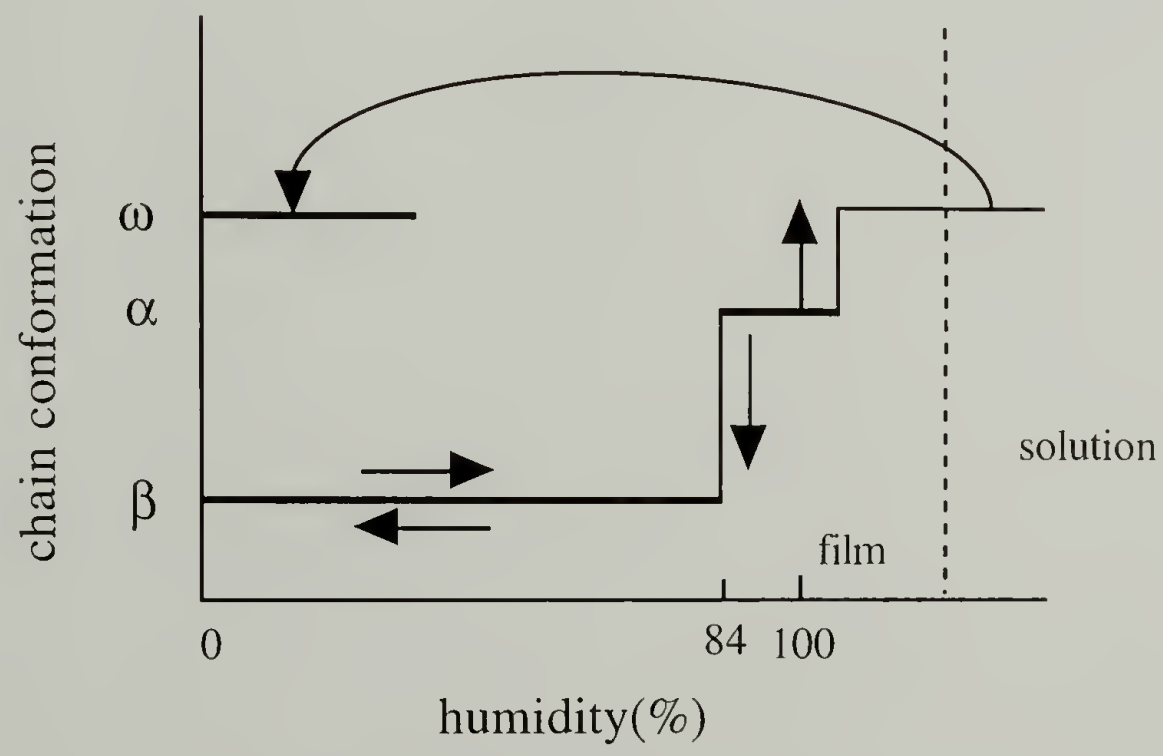

Figure 1.1 Schematic representation of the chain conformation changes as a function of humidity in poly(L-lysine hydrochloride). β, α and ω represent β-sheet, α-helix and disordered conformations respectively (from reference 14).

Although many of the above possibilities are well recognized, few are understood in detail. Especially at the molecular level, the details of water involvement in the mechanism of hydration-induced structural changes are poorly understood. A major reason for our incomplete knowledge is the complexity of the systems we are examining, and the consequent difficulty of separating out the different effects which water molecules have on the structure at different levels. For example, separate effects of moisture adsorption(on the surface of structure) and absorption(into the bulk of structure) have not been well appreciated, not to mention the separation of structural changes at various levels. It is the main purpose of this part of work to clarify these matters. A model polypeptide designed to have uniform lamellar crystalline structure is used so that separation of various hydration events is possible. Many works that have contributed to the understanding of water-macromolecule interactions will be reviewed next.

1.3 Water-Macromolecule Interactions

Investigation on water-macromolecule interactions can be categorized according to whether polymer solutions or polymer films and powders are studied. Solid samples allow variation of humidity over a wide range. Because of this advantage, experiments on such samples are the focus of this part of work.

The nature of interaction of water molecules with nylons has been studied by Puffr and Sebenda.[18] They claimed that as moisture sorption occurs in the amorphous phase of dry nylon, initially, the water molecule forms a double hydrogen bond between two carbonyl groups by means of free electron pairs on the oxygen atom. This is accompanied by a large evolution of heat and this water may be assessed as "firmly bound" (see Figure 1.2). Water molecules may also attach by replacing the hydrogen bonds between amide groups with negligible thermal effects. This may be classified as "loosely bound" water

(Figure 1.2). Further absorption can take place by multilayer formation of water molecules.[19]

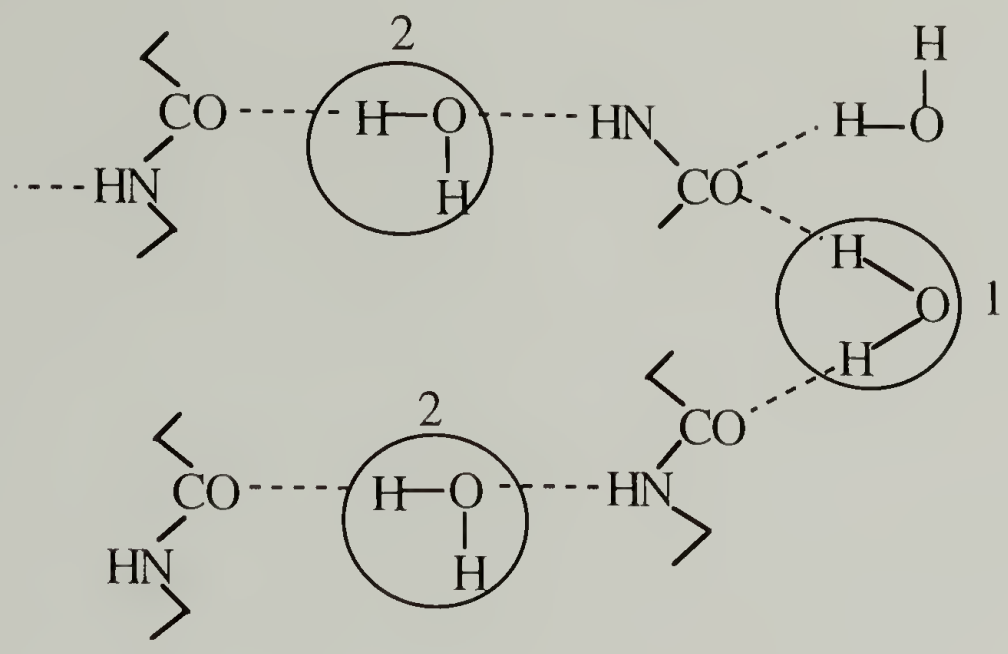

Figure 1.2 Interaction of water molecules with nylon: 1, firmly bound water; 2, loosely bound water (from reference 18).

Traditionally the water molecules associated with polymers are divided into three types: Structural, bound (firmly and loosely) and free (or bulk) water. The structural water is normally associated with the crystal and it can be described by a specific stoichiometry much as the hydrates of inorganic salts. Collagen has been shown to possess structural water to maintain its native tropocollagen triple helix conformation.[20] The best definition for bound water remains an operation one in which the bound water is considered as that having properties measurably different from those of bulk water measured by the same technique. This definition includes considerably more water than the structural water. Various techniques have been used to differentiate different types of water-macromolecule interactions. Electron density maps calculated from high resolution X-ray (or neutron) diffraction data have been widely used to locate bound water (including structural water) in protein crystals. Free water molecules are hard to detect with this technique because signals from these molecules are hardly distinguishable from noise mostly due to their high mobility.[21] Free water can be easily detected with DSC measurement, which is manifested by freezable water. The unfreezable water can be related to bound water. By and large, the

results from DSC and NMR regarding the amount of unfreezable water agree well.[22] Infrared spectroscopy is of particular value in the study of hydration at low moisture levels since it can characterize both water-water interactions and water-polymer interactions at molecular levels. With this technique a sequential hydration of different functional groups has been established for lysozyme.[17,23,24] Starting from dried lysozyme powder, the ionizable acid side chains are first fully hydrated ; then, the weaker binding sites, mostly carbonyl backbone, are gradually hydrated. Finally, only at higher hydration does multimolecular sorption take place.

1.4 Water Sorption Isotherm

One method of obtaining more information regarding the interaction of water with macromolecular systems is through the measurement of the sorption of water vapor. Sorption may be defined as the process in which vapor molecules are attached to sites in solids.[25] The terms "absorption' and "adsorption" have been used to describe the sorption process. Adsorption is the uptake of vapor at the surface of an insoluble solid, and absorption is generally taken to be the dissolving of the vapor molecules within a non-volatile material phase.[26] It has been suggested that absorption can be regarded as essentially internal adsorption, where the sorbate (water molecules) diffuses from the surface of the sorbent (polymer) into its interior via fine capillaries, crystal grain boundaries, and by penetration of vapor between the atoms of a crystalline network.[27] In our work only the word "sorption" will be used to include both effects. The two variables which have to be measured to obtain sorption isotherms are h, the amount of moisture sorbed, and p/p_0 the partial pressure or humidity. The water sorption isotherms for proteins, polypeptides, polyamides and many biological systems show the common feature of being sigmoids (S-Shaped), as represented in Figure 1.3.

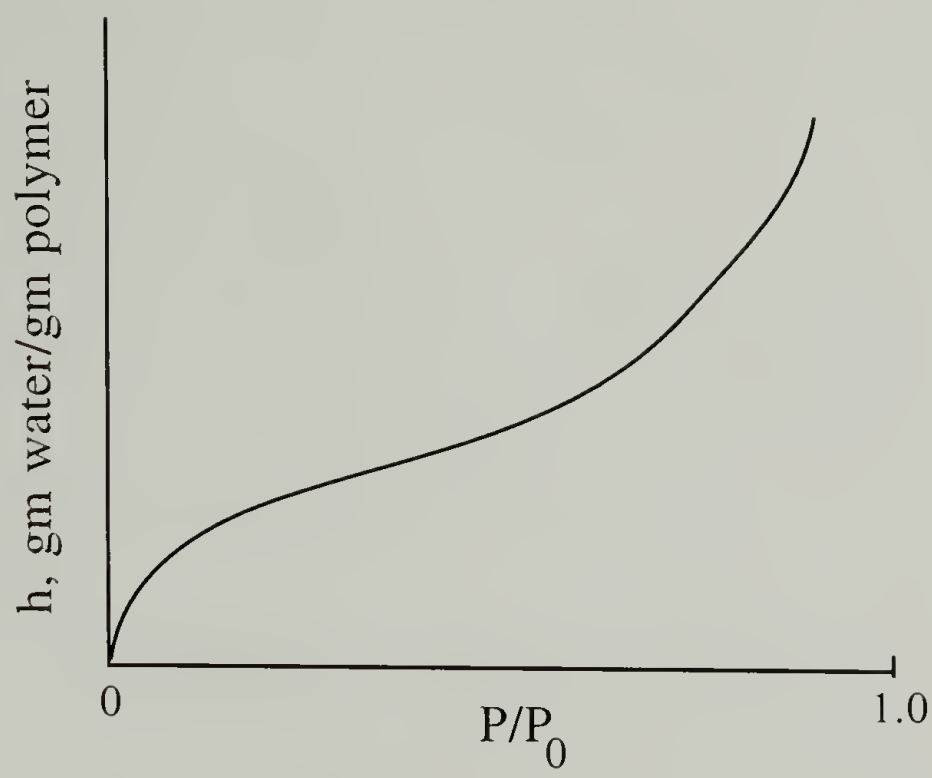

Figure 1.3 Schematic representation of a typical sorption isotherm for proteins, polypeptides, polyamides, etc., showing a sigmoidal curve.

As can be seen from Figure 1.3, the common features for such isotherms include the followings. First, at low partial vapor pressures, of the order $p/p_0 \leq 0.05$, the amount of moisture sorbed increases rapidly. Secondly, a distinct change of rate of sorption with partial vapor pressure, appearing as a "knee" in the isotherm, occurs at a partial vapor pressure of around 0.1, and up to $p/p_0 \sim 0.8$ the water content increases fairly slowly but steadily. Lastly, at partial vapor pressure greater than about 0.9, the water sorption again begins to increase rapidly and indeed the rate of sorption $dh/d(p/p_0)$ must approach an infinitely high value at partial vapor pressure of unity if the material exhibits any detectable water solubility.

This sigmoidal isotherms of water vapor with many natural and synthetic macromolecular substrates are not precisely described by simple isotherm equations. For example, Brunauer, Emmett and Teller[28] developed an isotherm (BET isotherm) taking into account the formation of multilayers of adsorbed vapor. However, outside the approximate range of 5-50% partial pressure serious discrepancies between experimental and predicted

isotherms frequently occur. Solution theories based on the principles of Flory[29] and Huggins[30] can give reasonable agreement with experimental data at high partial vapor pressure.[31] A theoretical isotherm developed by D'Arcy and Watt[32] has been used quite successfully in predicting the sigmoidal curve for the water sorption of both synthetic polymers and biopolymers. The predicted isotherm is a composite curve comprised of component isotherms arising from separate sorption processes at constant temperature, as presented by

$$h=\sum_i \frac{K'_i K_i P/P_0}{1+K_i P/P_0} + C P/P_0 + \frac{k'k P/P_0}{1-k P/P_0} \qquad (1.1)$$

Here P/P_o is the partial water vapor pressure. The first term refers to the monolayer adsorption by strongly binding sites(e.g. ionic or ionizable groups) and the subscript, i, indicates the possibility of heterogeneity in the binding capacity of these sites. The second term represents the monolayer adsorption by weakly binding sites(e. g. polar groups) and it has the same form as the Henry's Law. And the last term refers to the formation of a multilayer. The first two components have the form of Langmuir isotherms. The five parameters in this equation have the following interpretation: K' is proportional to the total number of strong binding sites; K is a measure of the affinity for water sorption on the strong binding sites; C is proportional to the product of the number of weak binding sites times the energy of interaction between water molecules with such a site; k' is the number of multimolecular sorption sites and k is the activity of this sorbed water molecules. Later in this part of work(Chapter 2) this theoretical isotherm will be used to analyze our sorption data obtained for the model polypeptide so that more insight can be gained into the effects of water on the structure of the model polypeptide.

1.5 Substrate-Induced Nueleation and Morphology

In eontrast to previous line of work, this part of work will investigate the possible stabilizing effects of foreign surfaees on the nuelei formation and erystal formation even from aqueous environment. The crystallization behavior of polymers is strongly influenced by the type of foreign surfaces and peeuliar morphologies are frequently obtained from various heterogeneity in systems. The addition of foreign partieles whieh aet as nueleating agents is thus a popular means to modify erystallization proeesses, but reeent attention has been foeused rather on what happens on erystalline substrates, often ealled epitaxy.[33]

The term "epitaxy" is generally applied to oriented growth of one erystalline substance on a substrate of a different substance. Early systematic attempts to understand the physical basis of epitaxy dates back to 19th eentury. Ionie erystals, eovalent erystals, and in particular, metals have been used in most studies on epitaxy.[34] Work involving polymeric systems is relatively new; henee the physical basis of epitaxy in polymers is less well understood. Although the eriteria of lattice matehing is eonsidered to be very important for any epitaxial growth, it is not the eontrolling factor.[35,36] To understand epitaxy it is necessary to have detailed knowledge of the mode of formation of the initial oriented nucleus on the substrate. Considerable variations in nueleation are possible and aeeordingly a variety of epitaxial effeets are expeeted. Depending on the depositing molecule-substrate pair, several faetors appear to be important in determining the nueleation proeess on a given surface, as reviewed in next sections.

1.6 Crystallization of Polymers on Inorganie Substrates

Based on the oriented erystallization of polyethylene on (001) faees of various alkali halides and also that of different polymers on sodium chloride, it has been eoncluded that lattiee matching with the substrate is not important. The epitaxial meehanism has been

attributed to the long range dipolar forces exerted by rows of like-charged ions on these surfaces.[37] Along this line of argument, after testing 2000 substances for their possible nucleating effects on the crystallization of polyolefins, Binsbergen[38] ruled out the lattice matching as the nucleation mechanism; instead, he proposed that a general feature of the crystal structure of the nucleating agents is responsible for their nucleating effects. The potential nucleating agents all show exposed faces of hydrocarbon groups arranged in rows or stacks. As a result, the faces show shallow ditches in which adsorbed polymer molecules can bc forced to assume a stretched conformation over some distance, making nucleation much easicr. On the other hand, for the case of epitaxial crystallization of nylon 6 on KCl, a two-dimensional lattice matching scheme was indeed established because of thc intermolecular hydrogen bonding requirements of the crystal lattice of nylon 6.[39] Consequently, in such a case the matching in lattice size between depositing polymers and substratcs is an crucial criterion in detcrmining the resultant epitaxial orientation. The matching of the two lattice periodicities is usually measured by

$$\Delta=100(d_p-d_s)/d_s \qquad (1.2)$$

where d_p and d_s are the matching distances of the polymer and the substrate, respectively. The usually accepted range of lattice mismatch for epitaxy is $\Delta\leq\pm15\%$.[40] In all cases above the closest packed plane of the overgrowth phase has been observed to be parallel to the substrate surface.[39,41,42]

1.7 Crystallization of Polymers on Polymers

In contrast to polymer-inorganic systems described above, interest in binary crystalline polymer systems has developed recently with the upsurge of technologically important polymer blends or alloys, or fiber-reinforced composite materials. The underlying assumption is that crystallographic interactions and more specifically epitaxy

may result in improved adhesion between the two (in general incompatible) phases and ultimately lead to a synergism of mechanical properties as illustrated for the iPP-PE system.[36,43,44] Various kinds of orientational relationships have been found in these binary crystalline polymer systems. Linear high polymers are particular susceptible to orientation-directing effects of the surface.[33] Because of their long-chain nature it is probable that initial adsorption of the polymer chain occurs so that the chain axis lies in the surface plane. Frequently the epitaxially grown crystals are, in accord with this geometrical condition, oriented with the chain axis parallel to the substrate surface. However, depending on the depositing molecule-substrate pair, several factors appear to be important in determining the resultant spatial orientation of each depositing molecule on a given surface. For example, polyethylene, nylon 6 and polycaprolactone were found to crystallized on drawn poly(tetrafluoroethylene) film with parallelism of chain axes, which was attributed to similarities in lattice dimensions between substrate and crystallizing polymers.[45] For the iPP-PE system a peculiar "cross-hatched" orientational relationship (Figure 1.4) has been observed.[36,43,44] The origin of this morphology is not entirely clear yet. It has been variously related to thermal shrinkage stresses[46], spherulite growth morphology[47], and various epitaxial relationships.[36,43,48]

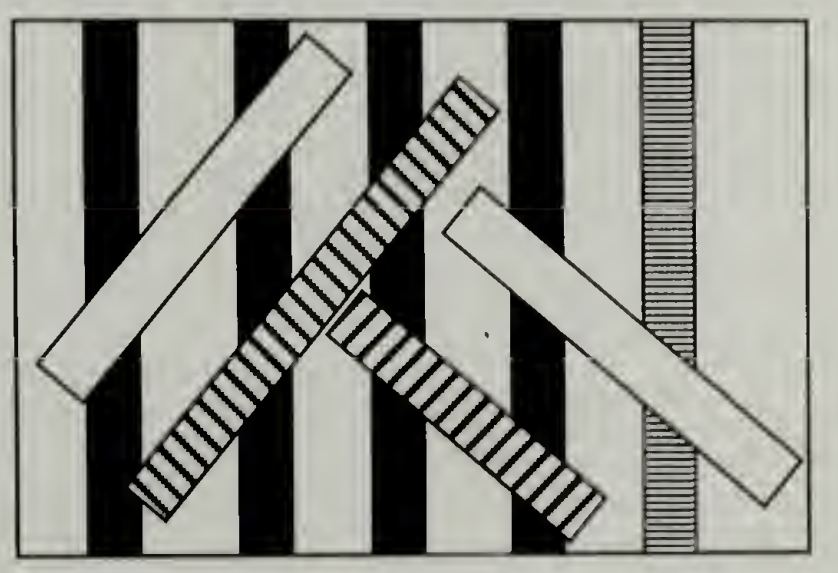

Figure 1.4 Schematic representation of crosshatch morphology observed in iPP-PE blend. PE crystals (on top) bridges several lamellar crystals of iPP. The black lines in the crystals indicate the chain directions.

The system of nylon 6/poly(p-phenylene terephthalamide) (PPTA) studied by Oono et al[49] is of particular interest, since it illustrates the importance and the role played by chemical interactions (e.g. hydrogen bonding) in epitaxial growth. These authors investigated, by microbeam X-ray diffraction, the crystal orientation in the nylon 6 transcrystalline layer and were able to distinguish an interfacial zone (near the substrate) and an intermediate zone a few microns away from the interface. The crystal orientation of nylon 6 at the interface differs significantly from that observed on non-polar substrates. Indeed. the contact plane is not the hydrogen-bond plane (ab plane) but rather the bc plane (a is hydrogen bonding direction; b is molecular axis). It was proposed to be due to that the amide groups of the first depositing nylon 6 chains strongly bond with the amide groups sticking out of the substrate surface. Further growth in nylon 6 occurs along the a axis away from the substrate. The growth of an epitaxial crystal has also been described to be a sequence of three steps. The initial layer of "adsorbed" molecules is arranged in conformity with the periodicities in the substrate surface. Above this zone a transition layer exists in which the lattice of the overgrowth substance starts to form, and it is mainly this region which contains dislocations and distortions. The final step involves the propagation of the oriented crystal phase. Depending on the relative interaction strengths of the molecules involved, the sizes of these zones will vary.[50]

The examples discussed so far not only demonstrate the orienting ability of the substrates but also the incompleteness of our understanding about the complex mechanism of substrate-induced oriented crystallization. This is partly due to the fact that the exposed faces of the substrates are not well characterized. A complete knowledge of the exposed surface should at least include the exposed crystallographic faces, surface topography and also the exposed functional groups, and so on. Another important parameter, which has not been fully appreciated, in this substrate-induced nucleation process is the molecular configuration of depositing macromolecules in the polymer liquid phase which could be changed by dilution, addition of salts or non solvents. Therefore, in this part of work, we

will investigate the effects of these parameters on the crystallization behavior of polymers on substrates. Especially, the work on crystallization of nylon on oriented substrate is part of our effort to understand the mechanism of forming a membrane with hydrophilic surface.

References

(1) Kusanagi, H.; Yukawa, S. *Polymer* **1994**, *35*, 5637.

(2) Reimschuessel, H. K. *J. Polym. Sci., Polym. Chem. Ed.* **1978**, *16*, 1229.

(3) Vollrath, F.; Edmonds, D. T. *Nature* **1989**, *340*, 305.

(4) Kitchener, A.; Vincent, J. F. V. *J. Mater. Sci.* **1987**, *22*, 1385.

(5) Verma, A.; Deopura, B. L.; Sengupta, A. K. *Text. Res. J.* **1984**, *54*, 92.

(6) Bubeck, R. A.; Kramer, E. J. *J. Appl. Phys.* **1971**, *42*, 4631.

(7) Michielsen, S. *J. Appl. Polym. Sci.* **1994**, *52*, 1081.

(8) Inoue, K.; Hoshino, S. *J. Polym. Sci., Polym. Phys. Ed.* **1976**, *14*, 1513.

(9) Fuzek, J. F. In *Water in Polymers*; S. P. Rowland, Ed.; ACS Symposium Series 127: Washington, D. C., 1980; pp 515.

(10) Murthy, N. S.; Stamm, M.; Sibilia, J. P.; Krimm, S. *Macromolecules* **1989**, *22*, 1261.

(11) Vergalati, C.; Imberty, A.; Perez, S. *Macromolecules* **1993**, *26*, 4420.

(12) Shmueli, U.; Traub, W. *J. Mol. Biol.* **1965**, *12*, 205.

(13) Lenormant, H.; Baudras, A.; Blout, E. R. *J. Am. Chem. Soc.* **1958**, *80*, 6191.

(14) Chirgadze, Y. N.; Ovsepyan, A. M. *Biopolymers* **1972**, *11*, 2179.

(15) Rupley, J. A.; Yang, P.-H.; Tollin, U. In *Water in Polymers*; S. P. Rowland, Ed.; ACS Symposium Series 127: Washington, D. C., 1980; pp 111.

(16) Kuntz, I. D.; Kauzmann, W. *Adv. Protein Chem.* **1974**, *28*, 239.

(17) Careri, G.; Giansanti, A. *Biopolymers* **1979**, *18*, 1187.

(18) Puffr, R. J.; Sebenda, J. J. *J. Polym. Sci. C.* **1967**, *16*, 79.

(19) Kawasaki, K.; Sekita, Y.; Kanoue, K. *J. Colloid Sci.* **1962**, *17*, 865.

(20) Pineri, M. H.; Escoubes, M.; Roche, G. *Biopolymers* **1978**, *17*, 2799.

(21) Teeter, M. M. *Annu. Rev. Biophys. Biophys. Chem.* **1991**, *20*, 577.

(22) Kuntz, I. D. *J. Am. Chem. Soc.* **1971**, *93*, 516.

(23) Pool, P. L.; Finney, J. L. *Biopolymers* **1983**, *22*, 255.

(24) Pool, P. L.; Finney, J. L. *Biopolymers* **1984**, *23*, 1647.

(25) McLaren, A. D.; Rowen, J. W. *J. Polym. Sci.* **1951**, *7*, 289.

(26) Pethig, R. *Dielectric and Electronic Properties of Biological Materials*; John Wiley and Sons: New York, 1979, pp 119.

(27) Hayward, D. O.; Trapnell, B. M. W. *Chemisorption*; Butterworths: London, 1964.

(28) Brunauer, S.; Emmett, P. H.; Teller, E. *J. Am. Chem. Soc.* **1938**, *60*, 309.

(29) Flory, P. J. *J. Chem. Phys.* **1942**, *10*, 51.

(30) Huggins, M. L. *Ann. N. Y. Acad. Sci.* **1943**, *44*, 431.

(31) Rowen, J. W.; Simha, R. *J. Phys. Chem.* **1949**, *53*, 921.

(32) D'Arcy, R. L.; Watt, I. C. *Trans. Faraday Soc.* **1969**, *66*, 1236.

(33) Wunderlich, B. *Macromolecular Physics, Crystal Structure, Morphology, Defects* Academic Press: New York, 1973; Vol. 1.

(34) Pashley, D. W. *Advan. Phys.* **1956**, *5*, 173.

(35) Broza, G.; Rieck, V.; Kawaguchi, A.; Petermann, J. *J. Mater. Sci.* **1985**, *23*, 2623.

(36) Gohil, R. M. *J. Polym. Sci. Polym. Phys. Ed.* **1985**, *23*, 1713.

(37) Koutsky, J. A.; Walton, A. G.; Baer, E. *J. Polym. Sci. A-2* **1966**, *4*, 611.

(38) Binsbergen, F. L. *Polymer* **1970**, *11*, 253.

(39) Willems, J. *Experientia* **1967**, *23*, 409.

(40) Wittmann, J. C.; Lotz, B. *J. Polym. Sci. Polym. Phys. Ed.* **1981**, *19*, 1837.

(41) Walton, A. G.; Carr, S. H.; Baer, E. *Polymer Preprints* **1968**, *9*, 603.

(42) Carr, S. H.; Colket, W. C. *J. Colloid Interf. Sci.* **1969**, *31*, 328.

(43) Gross, B.; Petermann, J. *J. Mater. Sci.* **1984**, *19*, 105.

(44) Lee, I. H.; Schultz, J. M. *J. Mater. Sci.* **1988**, *23*, 4237.

(45) Takahashi, T.; Teraoka, F.; Tsujimoto, I. *J. Macromol. Sci. -Phys.* **1976**, *B12*, 303.

(46) Nishio, Y.; Yamane, T.; Takahashi, T. *J. Macromolec. Sci. -Phys.* **1984**, *B23*, 17.

(47) Kojima, M.; Satake, H. *J. Polym. Sci. Polym. Phys. Ed.* **1984**, *22*, 285.

(48) Lotz, B.; Wittmann, J. C. *J. Polym. Sci. Polym. Phys. Ed.* **1986**, *24*, 1559.

(49) Oono, T.; Kumamaru, F.; Kajiyama, T.; Takayanagi, M. *Rep. Prog. Polym. Phys. Japan* **1981**, *24*, 193.

(50) Jesser, W. A.; Kuhlmann-Wilsdorf, D. *Phys. Stat. Solidi* **1967**, *19*, 95.

CHAPTER 2

EFFECT OF WATER ON THE STRUCTURE OF A MODEL POLYPEPTIDE

2.1 Introduction

Examples of hydration-induced structural changes are not rare. However, the mechanism has not been clarified yet. An early study on nylon 6 shows the anisotropic structural changes caused by moisture sorption.[1] Based on wide angle X-ray diffraction (WAXD) data it was found that the moisture-saturated sample, compared with a dried one, has better order in the hydrogen bonding direction accompanied by an expansion in the spacing but has worse order in the intersheet direction with a decreased spacing. Without other evidence, it was concluded that the crystalline structural changes were caused by penetration of moisture into the crystals. However, a more recent study on the same system, with the help of both infrared spectroscopy and WAXD, shows that water molecules do not enter the crystalline phase. Nonetheless, no clear explanation about the structural changes was offered.[2] A computer simulation study on nylon 66 hydration finds that without accessing the crystalline region, water molecules on the crystal surface can induce unit cell transition.[3] This conclusion indicates that the interaction with water on the crystal surface could be an important parameter in determining the structural changes upon hydration. More striking hydration-induced structural changes are found in polypeptides with ionic side chains, e.g.poly-L-lysine hydrochloride and sodium poly(L-glutamate).[4,5] Both crystal packing and chain conformation could be altered due to moisture sorption in these cases. Although the resultant electrostatic interaction was proposed to be the

underlying reason, no attempts were made to clarify if the changes in crystal packing and chain conformation occurred at the same time or separately.[4]

Although it is known that water can strongly influence the 3-dimensional states of proteins and polymers, it is necessary to specify the number and location of water molecules required to perturb macromolecular structures. Polymers seldom attain a high degree of crystallinity and will generally contain both amorphous and crystalline regions. In most instances water will preferentially interact with functional groups in the amorphous regions of a semicrystalline polymer, because of restricted mobility of water to permeate crystalline regions as readily. From the microscopic viewpoint, hydration may also be a stepwise process because hydration of ionizable and ionic groups is expected to be completed before that of other polar sites, and because non-polar sites are the last to be hydrated.[6-8]

The exact mechanism of the structural changes induced by water in polymers is not clear. Vibrational spectroscopy is an ideal tool to analyze the amount of water present and to characterize the chain conformations of polymers. The bands used for analyzing chain conformations are in general well understood and it is also possible to follow both water uptake and water location by using D_2O instead of H_2O. Specific vibrational frequencies affected by hydrogen-deuterium exchange may be exploited to determine sites where exchange occurs most rapidly. Based on spectroscopic studies, it is possible to: 1. utilize the kinetics of hydration in order to characterize the structure of polymers and proteins; 2. identify conformational and packing changes as a function of water content; 3. identify surface-bound water; and 4. clarify the relationship between surface structure and crystalline packing.

The polymer system described herein is a model polypeptide(**1**) prepared via bacterial expression of an artificial gene.[9]

1 $-((Ala\ Gly)_n\ Glu\ Gly)_m-$

The repeating alanylglycine dyads were chosen as the basis of the design because alanylglycine-rich polypeptides are known to exist as β-sheet structures in the solid state.[10] The glutamic acid residue was thought to be sufficiently bulky as to be excluded from the crystalline interior, and would therefore be expected to be confined either to the fold surface or to the amorphous phase. Glycine has the conformational flexibility needed for completion of the reverse turn and should allow the chain to fold back on itself, forming antiparallel β-sheets between the repeating alanylglycine dyads. The observed solid state structure of this polymer is consistent with chain folding at glutamic acid, bearing surfaces decorated with carboxylic acid groups[9], as illustrated in Figure 2.1.

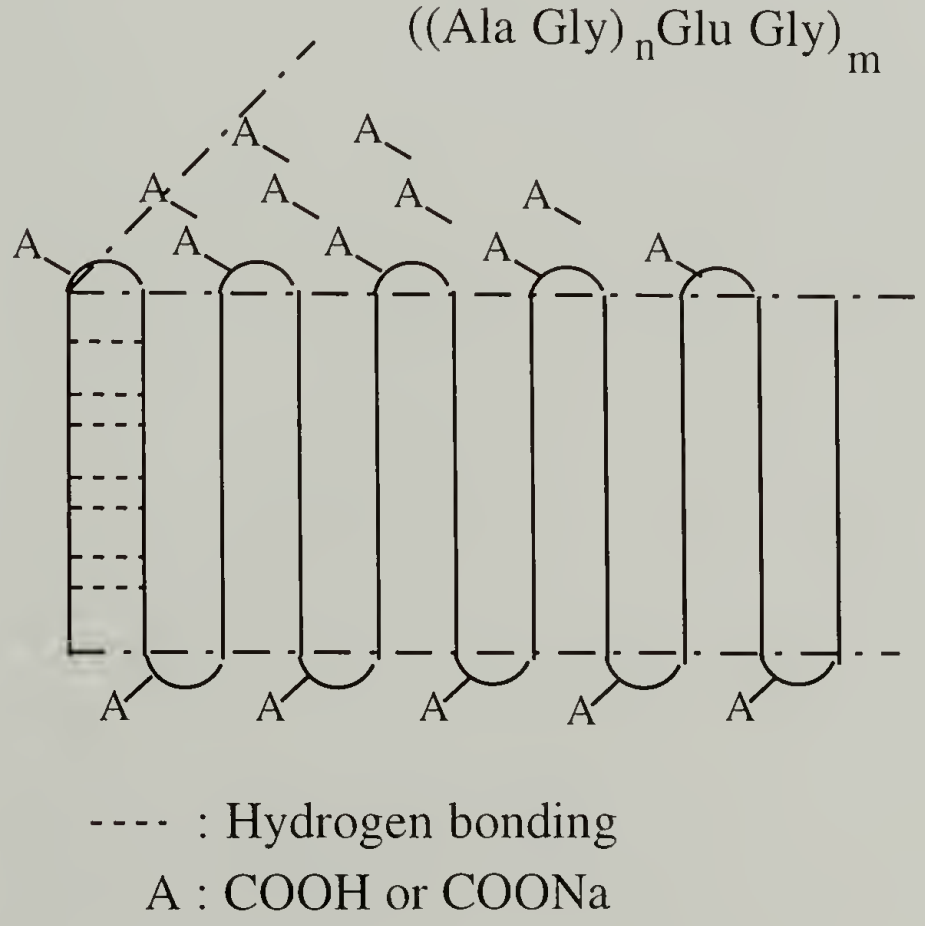

Figure 2.1 Schematic representation of the lamellar structure of the model polypeptide.

Therefore, in addition to its regular tertiary and secondary structure, this polypeptide system offers the possibility of studying the effects of strong interactions between water

and accessible ionizable groups. It is also possible to change the surface functionality from carboxylic acid groups (COOH) to sodium carboxylate groups (COONa).

The use of such model polypeptides provides a unique opportunity to characterize the kinetics of the hydration process by following the H→D exchange rate, in both amorphous and crystalline regions. By carrying out simultaneous gravimetric measurements it is also possible to determine the exact amount of the water present. By following the vibrations characteristic of the carboxylic acid one can then characterize the changes in the environment of these highly polar groups. This combination of information provides an opportunity to investigate hydration effects on protein and polymer structures at a level of detail not available previously. We show herein that the hydration of **1** is a three-step process. First, water penetrates into the most easily accessible amorphous (or fold surface) regions containing the most strongly interacting functional groups. Further hydration induces separation of the hydrogen-bonded sheets, and then finally one observes changes in the secondary structures of the polypeptide chains. Moreover, through the comparison of hydration behavior between two polypeptides with different crystalline stem lengths, we infer that the relative importance of surface energy vs. bulk energy is crucial for the stability of the crystalline structure upon sorption of water.

2.2 Experimental Section

The polypeptide was prepared via bacterial expression of the corresponding artificial gene, as described previously.[9] The chain conformation in the crystalline regions can be controlled by the procedure selected for sample preparation. If the polymer is dissolved in aqueous formic acid solution (70% v/v) and precipitated with methanol, the powder obtained has the silk II, or β chain conformation. On the other hand, dissolution in aqueous lithium bromide solution (60%), and precipitation by dialysis against

progressively diluted lithium bromide solutions, affords the silk I structure. The chain conformation for samples prepared in this manner is still undefined although distinct spectroscopic features have been observed. In this study, we have examined only samples with the β conformation, with crystalline features close to those proposed for *Bombyx mori* silk fibroin and poly(L-alanylglycine).[11,12] Fibroin has the following orthogonal unit cell dimensions: a axis : 9.4 Å (inter-β-strand or hydrogen bonding direction); b axis : 9.2 Å (intersheet spacing); c axis : 6.9 Å (peptide repeat). Two polypeptides with different stem lengths were used, as described in table 2.1.

Table 2.1 Unit cell dimensions of two model polypeptides.

Sample	Stem length n	Chain length m	Unit cell dimensions(Å) a	b	c
AG3	3	36	9.48	10.10	6.95
AG6	6	14	9.71	9.82	6.95

Ionization of the sample is accomplished by treating the polypeptide with dilute sodium methoxide-methanol solution(~0.1% w/v). No changes in the vibrational spectra or wide angle X-ray diffraction pattern are found after this treatment except for the disappearance of the absorption for carboxylic acid groups and the corresponding appearance of the carboxylate group absorption in the infrared spectrum. Therefore, the change in surface functionality from COOH to COONa does not affect either the chain conformation or the structure of the hydrogen-bonded sheets.

Hydration or deuteration was achieved by sorption of water or deuterium oxide(D_2O) vapor at room temperature. It is possible to vary the equilibrium H_2O or D_2O content by altering the relative humidity (RH) of the sample environment using various saturated salt solutions. The salts used in this experiment to control the humidity are listed in Table 2.2.[13]

Table 2.2 Saturated aqueous salt solutions for controlling the humidity at 25°C.

R.H.(%)	5	12	22	32	44	56	76	86	94
Salt	NaOH	LiCl	CH_3COOK	$CaCl_2$	K_2CO_3	NaBr	NaCl	KCl	Na_2SO_4

The samples were equilibrated in the humidity-controlled environment for a month. Then, water uptake was obtained by measuring the weight gain of the sample between two AgCl windows, which were used to avoid loss of water during measurement, directly on a balance or by measuring the weight loss of the sample on a Perkin-Elmer TGS-2 thermogravimetric analyzer (TGA). When the difference between these two measurements exceeded 10%, the TGA data were used for the analysis.

All infrared spectra (2 cm^{-1} spectral resolution) were obtained using a Nicolet IR-38 spectrometer in the 4000-400 cm^{-1} region with a DTGS detector. To prevent loss of water during transfer and measurement, samples were sealed between two AgCl windows. Raman spectra (4 cm^{-1} spectral resolution) were taken on a Bruker FRA 106 spectrometer with a N_d:Yag laser (1064 nm wavelength) as the irradiation source. A back scattering collection geometry was used. Samples were sealed in capillaries and the dead space above the sample was made as small as possible to reduce loss of water due to heating by the laser. Wide angle x-ray diffraction (WAXD) powder patterns were recorded on a Statton

camera to follow crystal packing changes, especially changes in the intersheet spacing. The same precautions as in the Raman experiment were taken to prevent loss of water during exposure.

Intensities of vibrations were calculated using a Lab Calc software package, based on the deconvoluted area associated with each absorption . For the Amide I region (1710-1610 cm^{-1}) three peaks were considered. Three vibrations were also considered in the region between 1610 and 1500 cm^{-1}. A combination of Gaussian and Lorenzian band shapes was used. Frequency, width at half-height, intensity and percentage of Gaussian or Lorenzian band, were varied to obtain the best fit. The resulting χ-square values were on the order of 10^{-3}-10^{-4}. Estimations of error are based on 3 independent measurements. The underlying water absorption in the Amide I region may introduce errors which are difficult to account for. The frequencies of the the three components in Amide I and II regions are, 1698, 1651, 1625 cm^{-1} and 1575, 1545, 1526 cm^{-1}, respectively.

2.2.1 IR and Raman Characterization of the Model Polypeptides

Table 2.3 lists some important vibrational frequencies which are useful in characterization of polypeptide chain conformation.

Table 2.3 Characteristic vibrational frequencies (cm^{-1}) of polypeptides.[14,15]

	β-sheet	α-helix	disordered
Amide I(IR)	1630, 1698	1653	~1655
Amide I(Raman)	*1665*	*1655*	*~1655-1670*
Amide II(IR)	1523	1545	~1550

It should be noted that although the vibrational frequencies of α-helix and disordered conformations are very close, it is still possible to distinguish these two conformations with band width. For example, the band half-width of Amide I for a α-helix is found to be about 16 to 33 cm^{-1}; on the other hand, 38 to 48 cm^{-1} for the disordered state.[16]

The infrared spectra of AG3 polypeptide are shown in Figure 2.2. The potential energy distribution of characteristic bands involving peptide are tabulated in Table2.4.

Table 2.4 Potential energy distribution of characteristic bands.[2,14]

Amide A	NH stretch (99%)
Amide B	Fermi resonance between Amide A and the overtone of Amide II
Amide I	CO stretch (78%) + CN stretch (20%)
Amide II	NH bending (55%) + CN Stretch (25%)

In the Amide I and II region (Figure 2.2.a), the dominant 1623 cm^{-1} band and a weak absorption band at 1698 cm^{-1} indicate that this sample has a antiparallel pleated sheet,i.e. β-sheet, chain conformation. The amide II band position at 1523 cm^{-1} also corroborates this assignment. The Amide I and II vibrations at 1623 and 1523 cm^{-1} respectively have long been recognized as due to out-of-phase vibrations of adjacent amide groups involved in an antiparallel β pleated sheet.[17] The weak band at about 1690 cm^{-1} was assigned as the Amide I vibration in which adjacent groups in antiparallel β pleated sheet move in phase with one another.[17] The splitting between the in-phase and out-of-phase vibrations has been explained by including a transition dipole coupling between adjacent groups.[17-20]

Two small shoulders at 1710 and 1740 cm^{-1} are due to the absorption of carboxylic acids on the lamellar surface. The broad band centered at 1655 cm^{-1} is assigned to the disordered component. Figure 2.2.b shows the higher frequency region where Amide A at 3290 cm^{-1} and Amide B at 3070 cm^{-1}. The band shape of Amide A band suggests that the sample is an extensively hydrogen-bonded system even though the Amide I region shows appreciable amount of disordered component. Figure 2.3 show the Raman spectrum of the same sample in the Amide I region. It again supports the β-sheet conformation assignment.

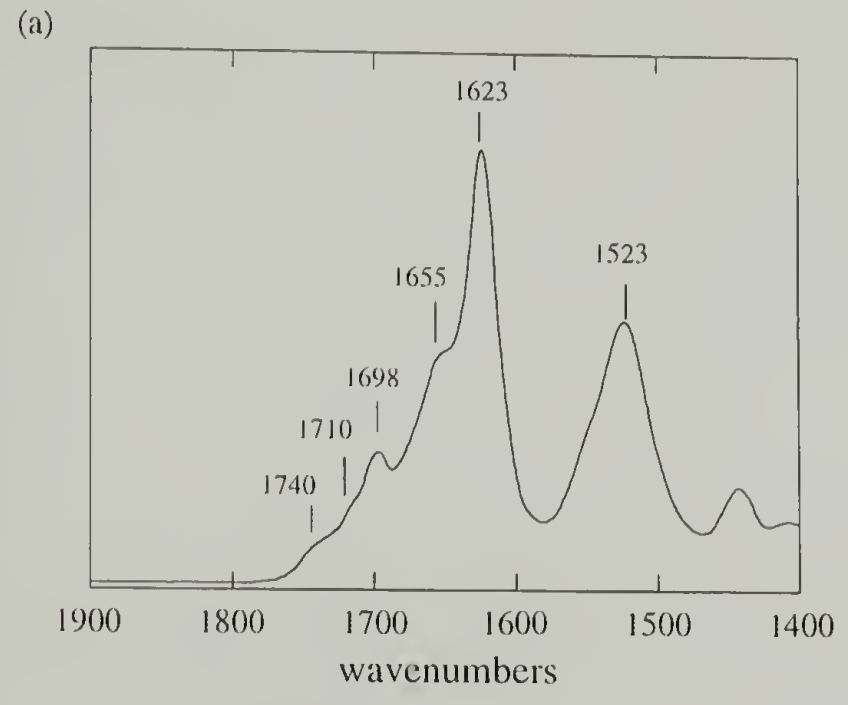

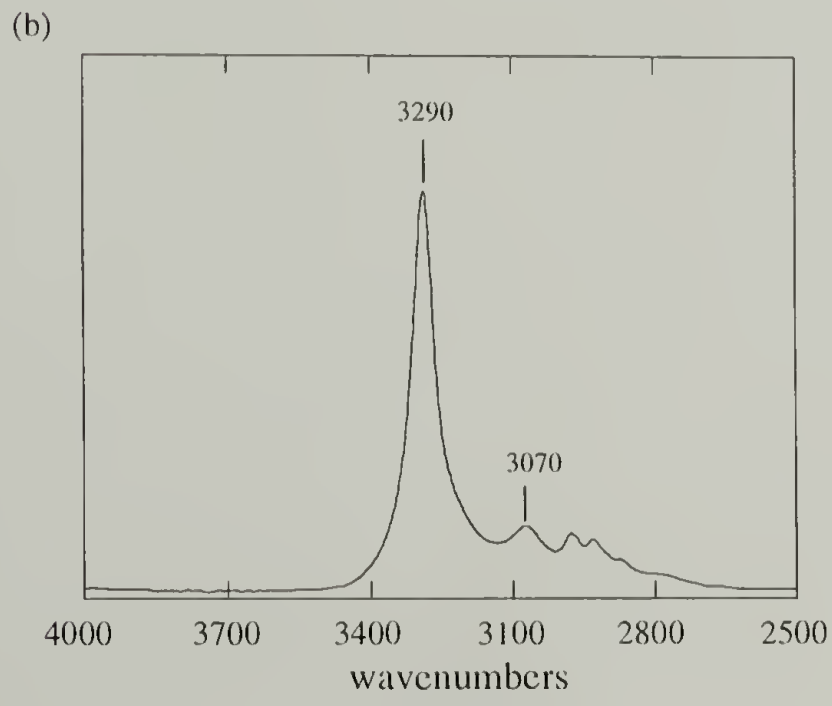

Figure 2.2 Infrared spectra of AG3 sample. (a) Amide I and Amide II region. (b) Amide A and Amide B region.

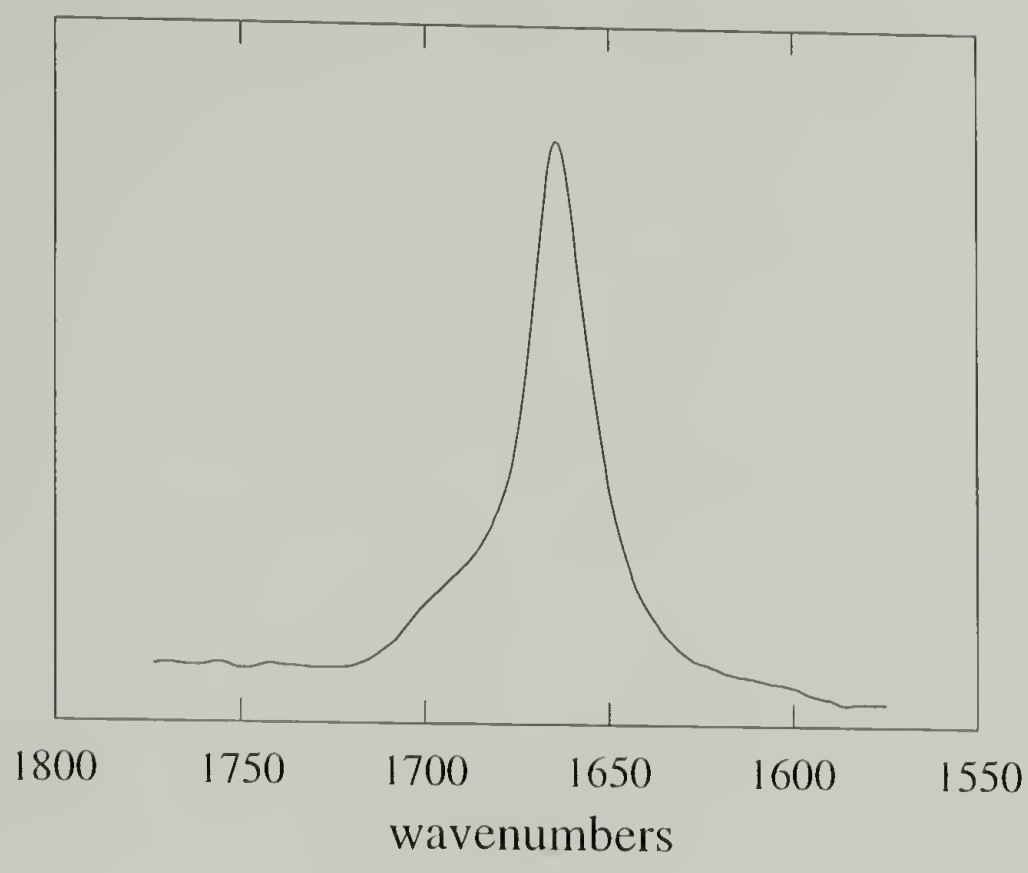

Figure 2.3 Raman spectrum of AG3 sample in the Amide I region.

The infrared spectra in the Amide I and Amide II regions of AG3 and AG6 samples are compared in Figure 2.4. Although the AG6 sample shows characteristic bands of β-sheet conformation as AG3 sample does, there are some spectral differences between these two polypeptides. Indicated by the smaller disordered band at about 1655 cm^{-1}, it is obvious that the AG6 sample has higher β-sheet content as we expect from its chemical composition. This point will also be confirmed later by following the deuteration kinetics. It should also be noted that the AG6 sample has a little higher Amide I and Amide II frequencies (1626 and 1529 cm^{-1} vs. 1623 and 1523 cm^{-1}), suggesting a weaker hydrogen bonding strength in this sample. This is in agreement with the WAXD data (Table 2.1) that the hydrogen bonding distance of AG6 is larger than that of AG3. However, that the band width of Amide II of AG6 sample is greater than that of AG3 sample is not clear.

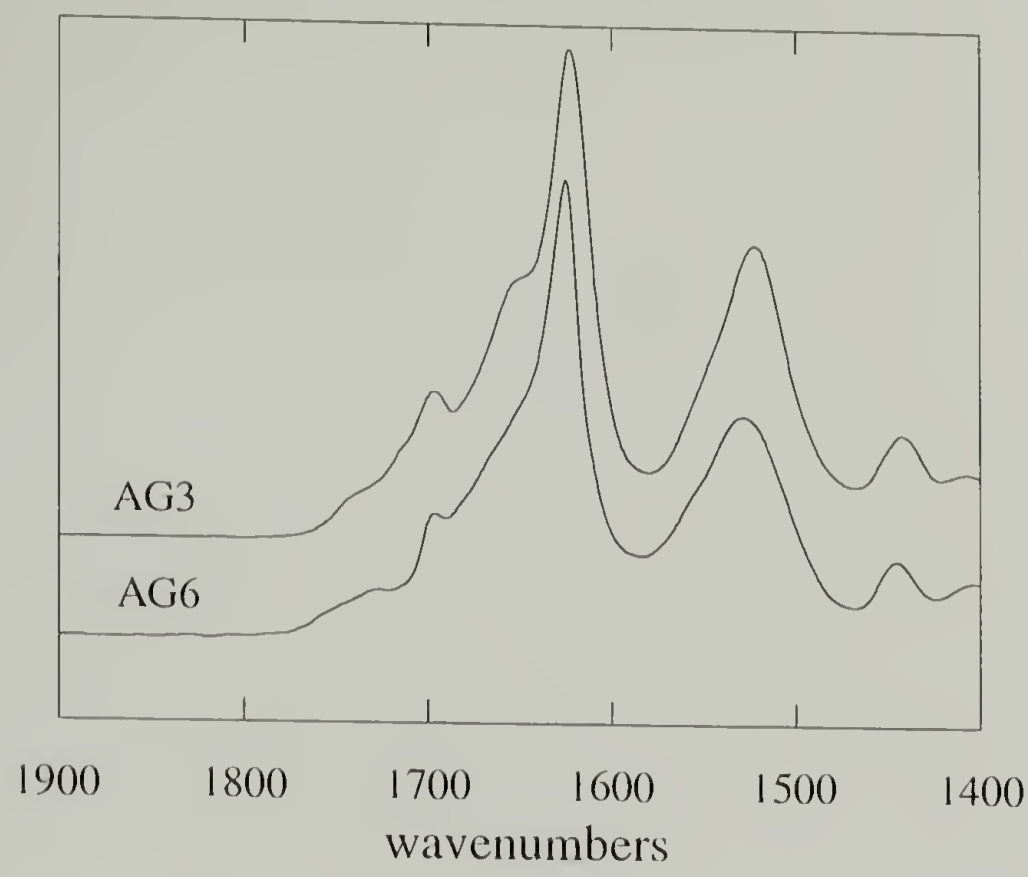

Figure 2.4 Comparison of infrared spectra of AG3 and AG6 samples in the Amide I and Amide II region.

2.3 Results and Discussion

2.3.1 Deuteration studies

The dramatic changes in the infrared spectra obtained for the model polypeptide when D_2O is introduced are shown in Figures 2.5 and 2.6. Virtually all vibrations involving internal coordinates affected by the H→D substitution will exhibit changes in frequency and intensity. The Amide I vibration is dominated by C=O stretching and therefore is only slightly perturbed by the H→D substitution. On the other hand, the Amide A and Amide II vibrations have significant contributions from the N-H stretch and in-plane-bending internal coordinates, respectively. Therefore, as H→D exchange takes place when D_2O is introduced, we expect to observe significant changes in the 3200-1400

cm^{-1} regions. The Amide A and Amide II vibrations are expected to be shifted to the 2400 and 1440 cm^{-1} regions, respectively. In Figure 2.5 we do observe these expected spectral changes. The decreases in intensity of Amide A and Amide II bands are accompanied by the occurrence of a doublet at about 2420 cm^{-1} and 2450 cm^{-1} which can be ascribed to the Fermi resonance bands between Amide A' and Amide II' vibrations (see Table 2.4) and by the growth of 1440 cm^{-1} region due to Amide II' (and probably also HDO bending) absorption (the superscript indicates deuterated bands). On the other hand the Amide I absorption frequency (1623 cm^{-1} β-sheet chain conformation) does not change with deuteration. The observed changes in the Amide I and Amide II regions are also shown in Figure 2.6. In Figure 2.7 and Figure 2.8 these spectral changes will be quantified to assist us in the understanding of the various events induced by the sorption of water (or D_2O) molecules.

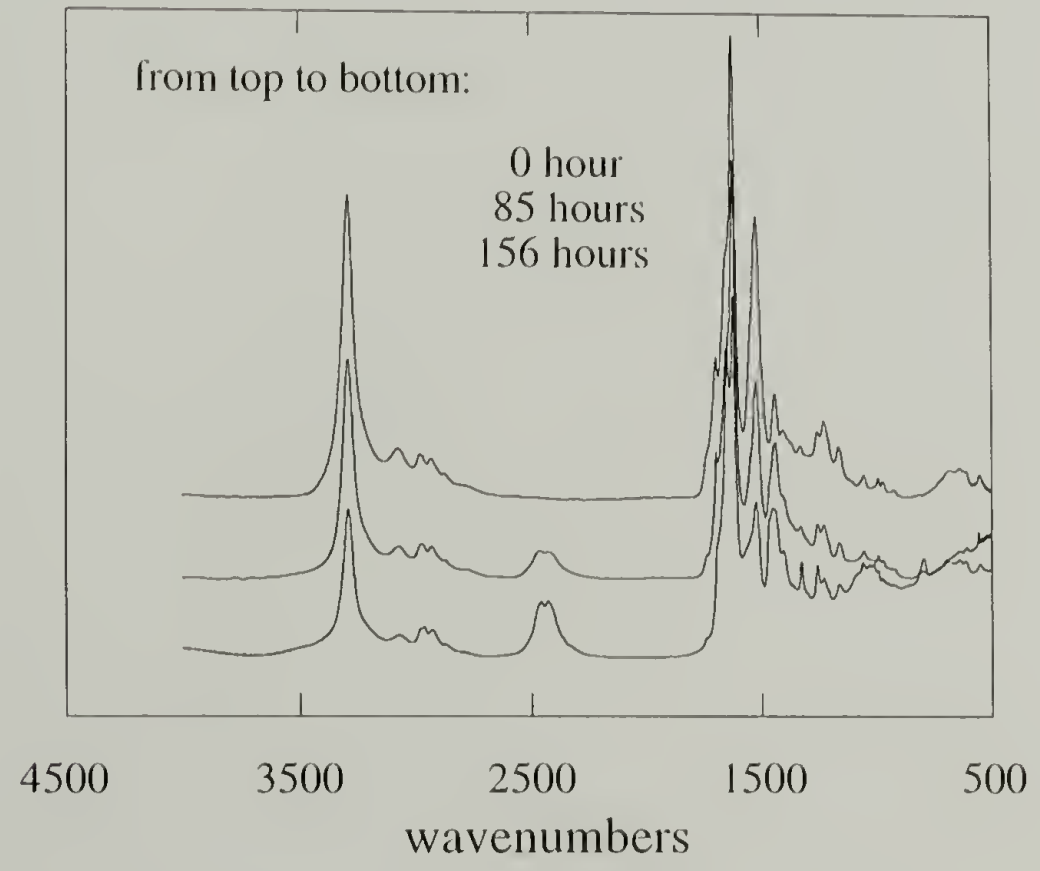

Figure 2.5 Infrared spectra of progressively deuterated AG3 sample in the 500-4000 cm^{-1} region.

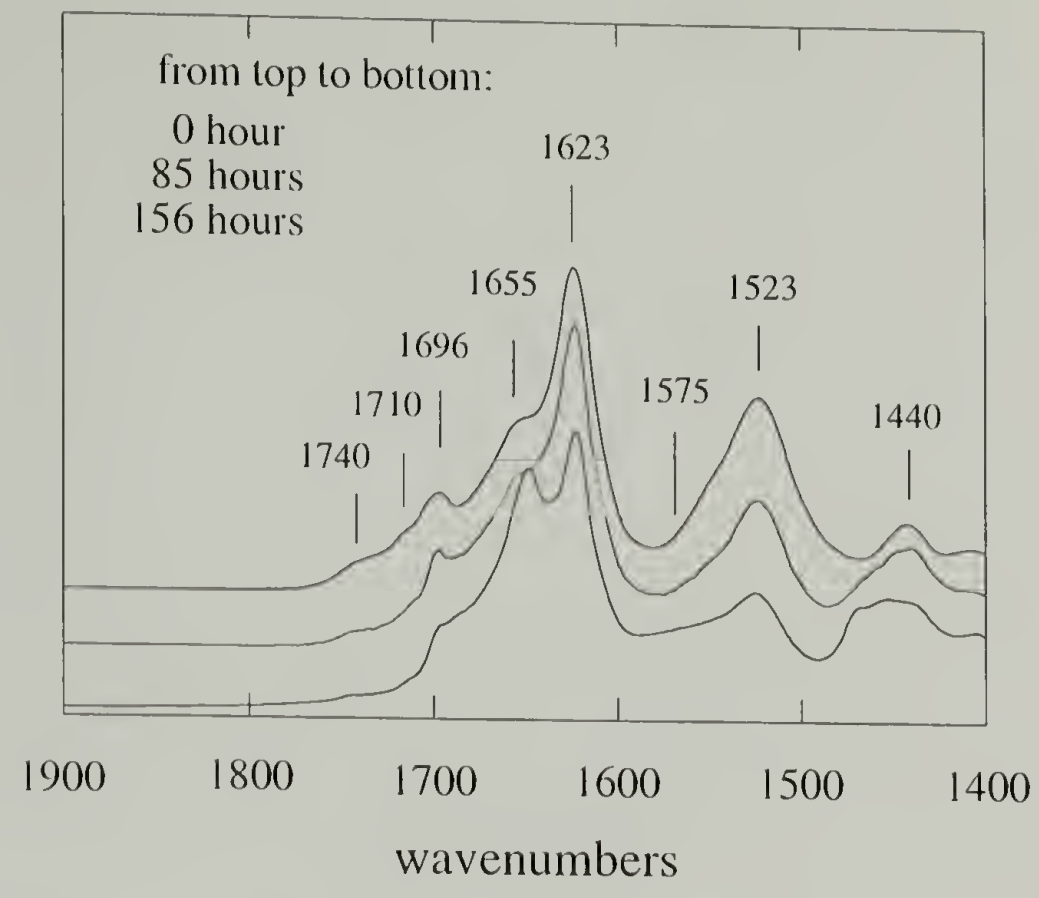

Figure 2.6 Infrared spectra of progressively deuterated AG3 sample in the Amide I and Amide II region.

The difference in accessibility between crystalline and disordered phases in polymers has been well recognized,[2,3,21-23] and the protons of acid groups on the lamellar surfaces should be exchanged most easily. The absorptions associated with carboxylic acids at 1710 and 1740 cm^{-1} decreased with the introduction of D_2O, with a corresponding growth of the hydrated carboxylate band at 1575 cm^{-1}. Upon the introduction of D_2O vapor, the amide groups on the fold surface are also expected to be deuterated, while amide groups in the β-sheet crystalline region should remain unchanged. This expectation is confirmed by following the deuteration kinetics as shown in Figure 2.7. For the sample in the carboxylic acid form, the intensity of the Amide II band decreases within the first 10 hours, and then remains constant for up to 3 days as shown by the top curve of Figure 2.7, indicating its crystalline region not accessible to D_2O molecules. During this period, no conformational change is detected since the Amide I band remains unchanged. For this sample, approximately three of the eight constituent amino acids are located at the fold and

should be easily accessible.[9] The plateau shown in Figure 2.7 represents approximately 32% deuteration; thus although the sample may not be fully crystalline, the fraction of amide protons readily accessible to D_2O vapor suggests that the degree of crystallinity is high. For the sample in the carboxylate form, the introduction of D_2O causes far more significant changes in the intensity of Amide II band in the infrared spectra. As shown in Figure 2.7, the amide protons of this sample seem to be much more accessible to D_2O molecules as compared to those in the original material in carboxylic acid form since the sample in the carboxylate form can be exchanged at a much faster rate. For the sample in the carboxylate form the fast rate of H→D exchange did not diminish as a function of time for up to 50 hours. This is an indication that its crystalline region has been accessible to the D_2O molecules.

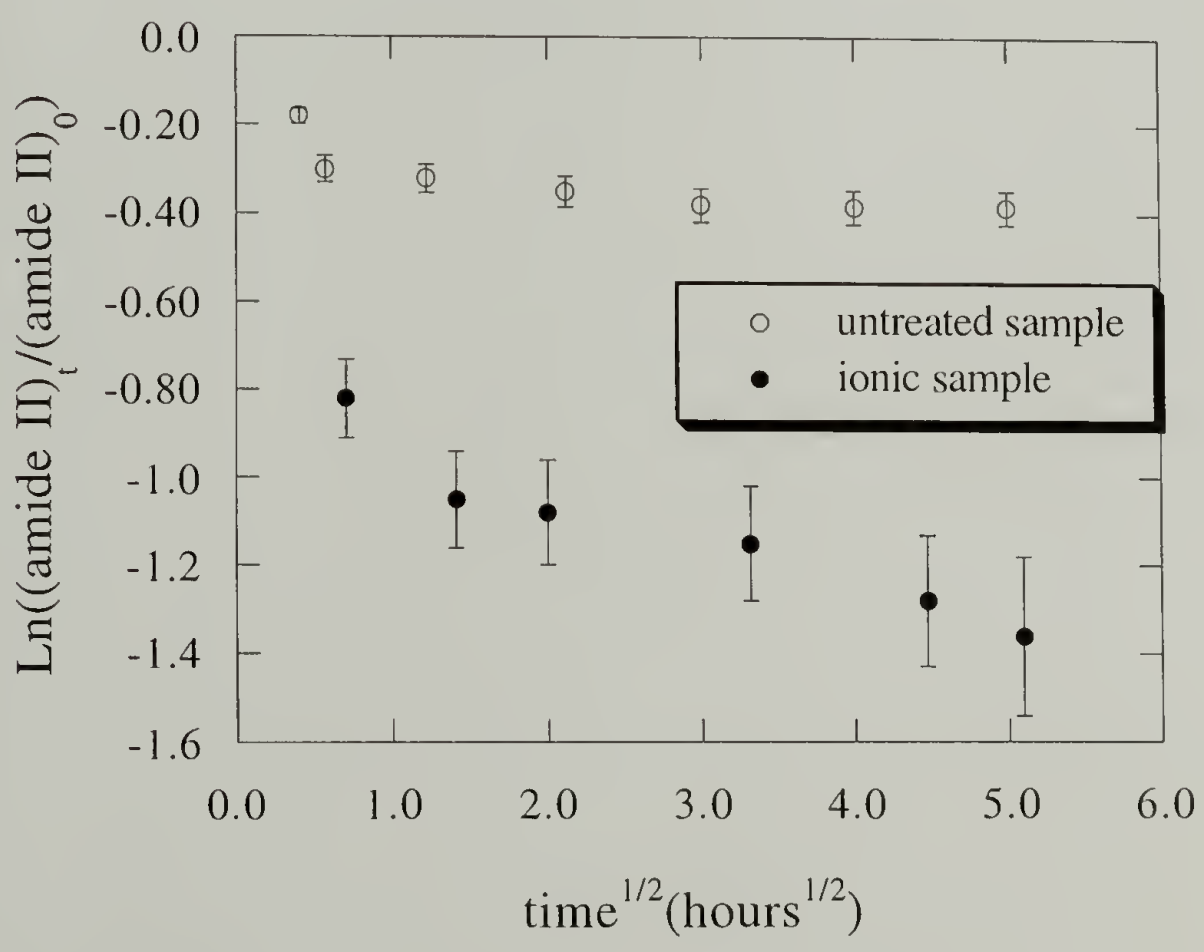

Figure 2.7 Rate of deuteration of AG3 sample in the carboxylic acid and carboxylate forms calculated from the rate of decrease of total Amide II intensity.

For the AG3 sample in the carboxylate form exposed to D_2O vapor for longer than 50 hours, the Amide II vibration decreased dramatically in intensity, indicating that the structure has " opened up ", making more of the amide groups accessible to the H→D substitution. This is also true for the AG3 sample containing carboxylic acids, but in this case, the required time of exposure to " open up " the structure is much longer. This increase in accessibility may involve changes in both crystal packing and chain conformation. We can clarify this point later by comparing the rate of changes in accessibility and chain conformation. It is possible, however, to distinguish changes in the environment of amide groups versus changes in chain conformation. The conformational change is readily identified by the relative intensity changes for the Amide I bands, while the decrease in the Amide II band intensity can be used to monitor the accessibility of the amide units. As mentioned previously, changes in the carboxylic acid bands are also readily analyzed by monitoring the increase in 1575 cm^{-1} band intensity.

The relative intensities of 3 types of vibrations observed for progressively deuterated AG3 sample are shown in Figure 2.8. Data as a function of time are expressed as a percentage of the band intensity measured at the longest time of D_2O exposure. The degree of ionization of the carboxylic acid is calculated using the 1575 cm^{-1} band. As mentioned earlier, based on the Amide II intensity measurements, approximately 32% of the amide units can been deuterated readily. Because of the slow diffusion, the crystalline regions are not expected to be deuterated easily. The slow change in Amide II intensity beyond 50 hours reflects this restricted deuteration of amide units in crystalline regions of the sample. The accessibility of NH groups in crystalline phase is calculated in terms of incremental percentage change from the plateau value, 68%, shown in Figure 2.7. Finally, the degree of conformational change is calculated from the decrease in intensity of the 1623 cm^{-1} crystalline Amide I band.[24,25] It is clear from these data that changes in different parts of the structure occur at very different rates.

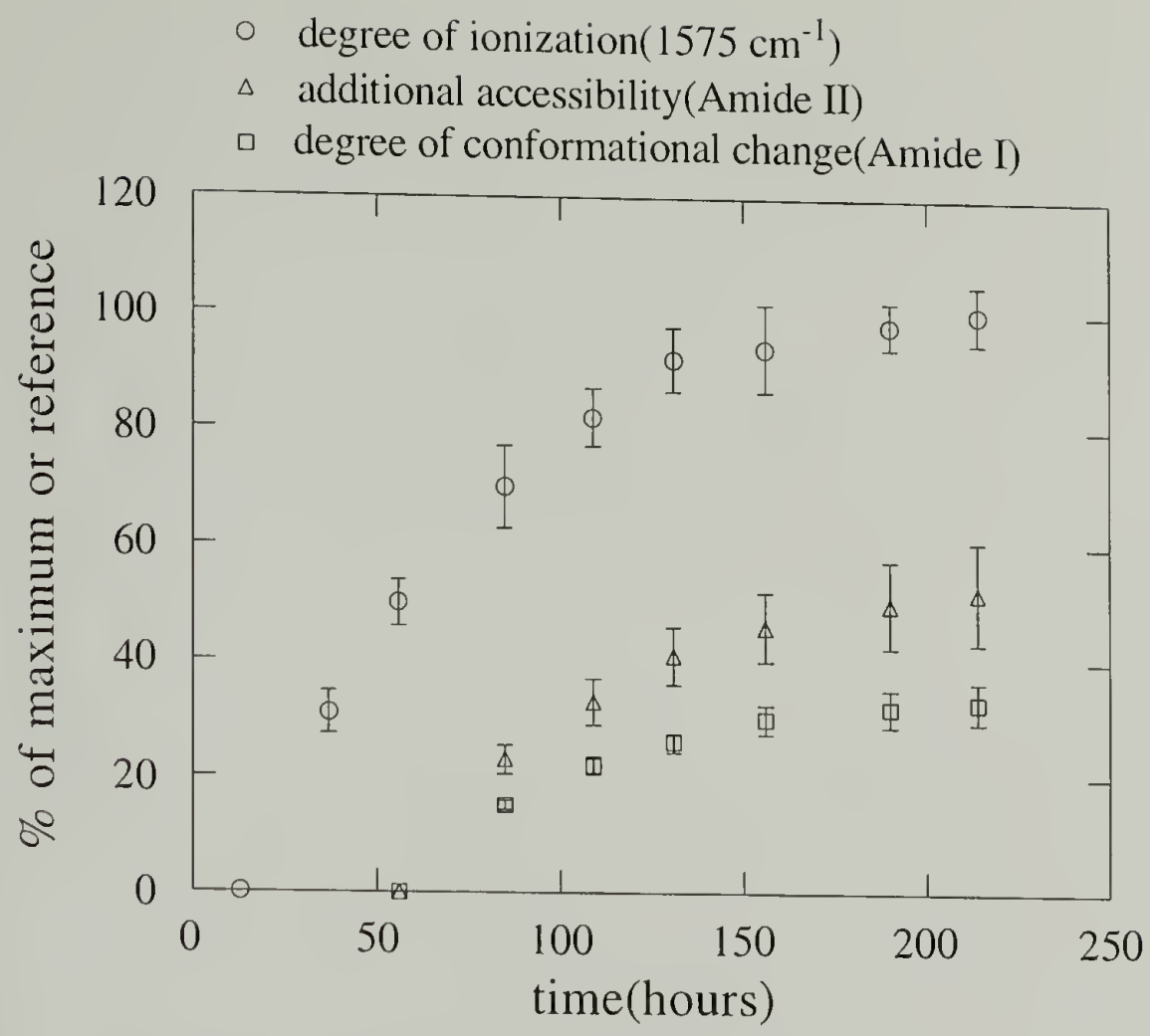

Figure 2.8 Comparison of rates of changes as a function of time for the Amide II and Amide I bands.

The intensity of the band at 1655 cm^{-1} attributed to disordered or folded structures increases at the expense of the crystalline β-sheet band as the hydration process progresses. If a change in chain conformation is the only mechanism for increasing the number of accessible NH groups beyond those on the fold surface, then the change in Amide I band intensity should evolve at the same or higher rates than the additional change in Amide II band intensity. Instead, it is evident that the rate of increase in accessibility represented by the Amide II vibration is higher than that of conformational change represented by the changes in the Amide I region. In this analysis, small errors associated with band deconvolution procedure exist, and the water band in the Amide I region was not taken into account. Nevertheless, our data still serve to indicate that the hydration-induced structural changes proceed in a stepwise fashion. Therefore, from these data we propose that water first interacts with ionic and polar groups predominantly in the interlamellar region. Subsequent hydration of the ionic groups then causes changes in the underlying crystal

packing. Only in the later stages of hydration are the interchain spacing and chain conformation changed. However, the answer for why the crystalline region would become accessible to water molecules cannot be obtained in this deuteration experiment.

2.3.2 Hydration studies

To test this hypothesis, the sample in the carboxylate form proved to be especially instructive. As mentioned previously, the X-ray and vibrational spectroscopic data indicate that neither the chain conformation nor the inter-sheet packing is altered by conversion of the surface-bound side chains from the protonated state to the sodium salt form, thus we are actually dealing with the same structure. With this form of sample the experiment is simplified since it is then not necessary to be concerned about the degree of dissociation of the carboxylic acid groups during hydration. The effects of hydration on the carboxylate form of the polypeptide are shown in Figure 2.9. The disordered Amide II band at 1550 cm^{-1},[14] not observable in the deuteration experiments described above (Figure 2.6) can now be observed. This supports the idea that chain conformation changes only after water molecules have penetrated the crystalline region, otherwise we would have observed the disordered Amide II band in Figure 2.6.

Figure 2.10 shows that the symmetric COO^- stretching vibration at 1400 cm^{-1} gradually shifts to lower frequency (1391 cm^{-1}) when the sample in the carboxylate form is progressively hydrated, and that interaction between water and the carboxylate groups is readily detected even at low levels (e.g. 1%) of hydration. Similar spectral changes have been observed for hydrated ionomers.[26,27] In the absence of water, the sodium-carboxylate can be regarded as a contact ion pair due to strong electrostatic interactions. With water present around the ions, the anion-cation interaction is perturbed,[26] and a hydration-mediated dissociation equilibrium between the ions is gradually established.

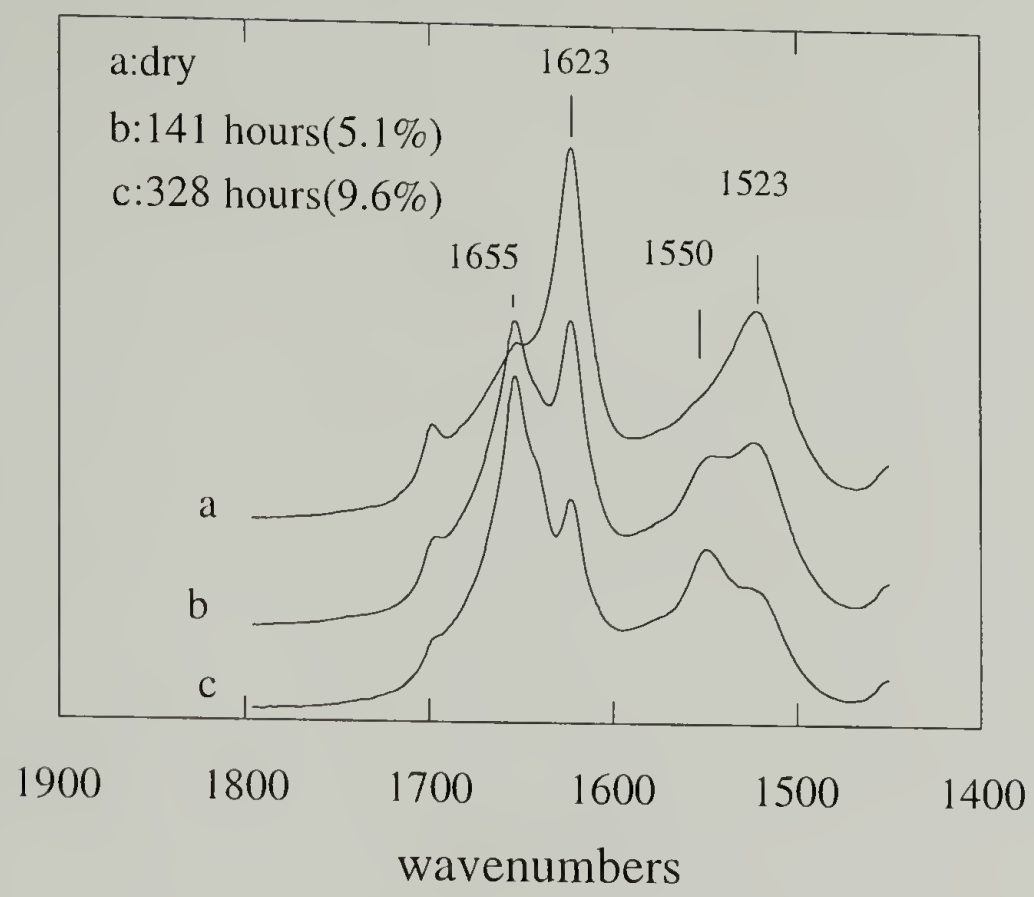

Figure 2.9 Effect of hydration on the conformation of the AG3 samples in its carboxylate form manifested in the Amide I and Amide II region of the infrared spectrum.

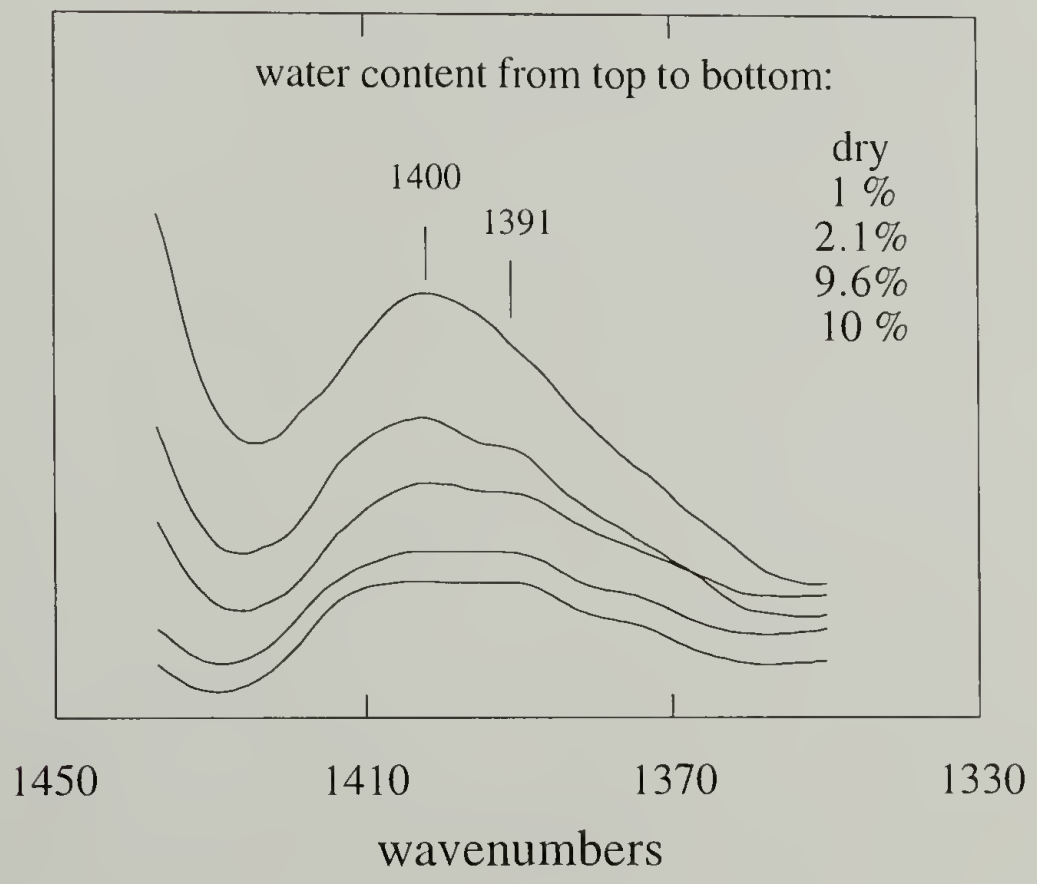

Figure 2.10 Effect of hydration on the symmetric COO^- band in the infrared spectrum.

Based on the spectroscopic evidence presented above, it is clear that water molecules penetrate into the interlamellar regions of the polymer quite readily. For the AG3 polypeptide in the carboxylic acid form, hydration of the acid groups is slower than that measured for the sample in the carboxylate form. For the latter sample, water can potentially interact with 2 ionic centers, COO^- and Na^+, making the interlamellar regions much more accessible as compared to the sample in the carboxylic acid form. We propose that the hydrated ions, either because of increasing steric interactions resulting from the requirement to accommodate the sorbed water molecules on the lamellar surface or through long range electrostatic interactions between themselves, change the interlamellar regions, and in turn perturb the crystalline core to such an extent that water molecules are now able to penetrate the crystalline region causing chain conformation changes. It has been demonstrated both experimentally and theoretically that a few water molecules on the lamellar surface can perturb the crystalline structure of nylons without penetrating the crystalline phase.[2,3]

The experimental results shown so far have principally dealt with the kinetics of structural perturbation of AG3 sample when water is sorbed into the system. It is also important to relate the total amount of water uptake to changes in the structure. Equilibrium sorption experiments would provide us this information. AG3 samples in the carboxylate form were subjected to hydration at a variety of partial vapor pressures to examine the extent to which water molecules penetrate into different morphological regions during hydration.[22] The results as a function of humidity obtained from infrared spectroscopy (in the Amide I and Amide II regions), the equilibrium water content from gravimetric measurements, and the intersheet distance determined via wide angle X-ray diffraction, are shown in Figures 2.11, 2.12, and 2.13, respectively. Combination of these techniques can make it possible to separate structural changes at different levels as a function of water content.

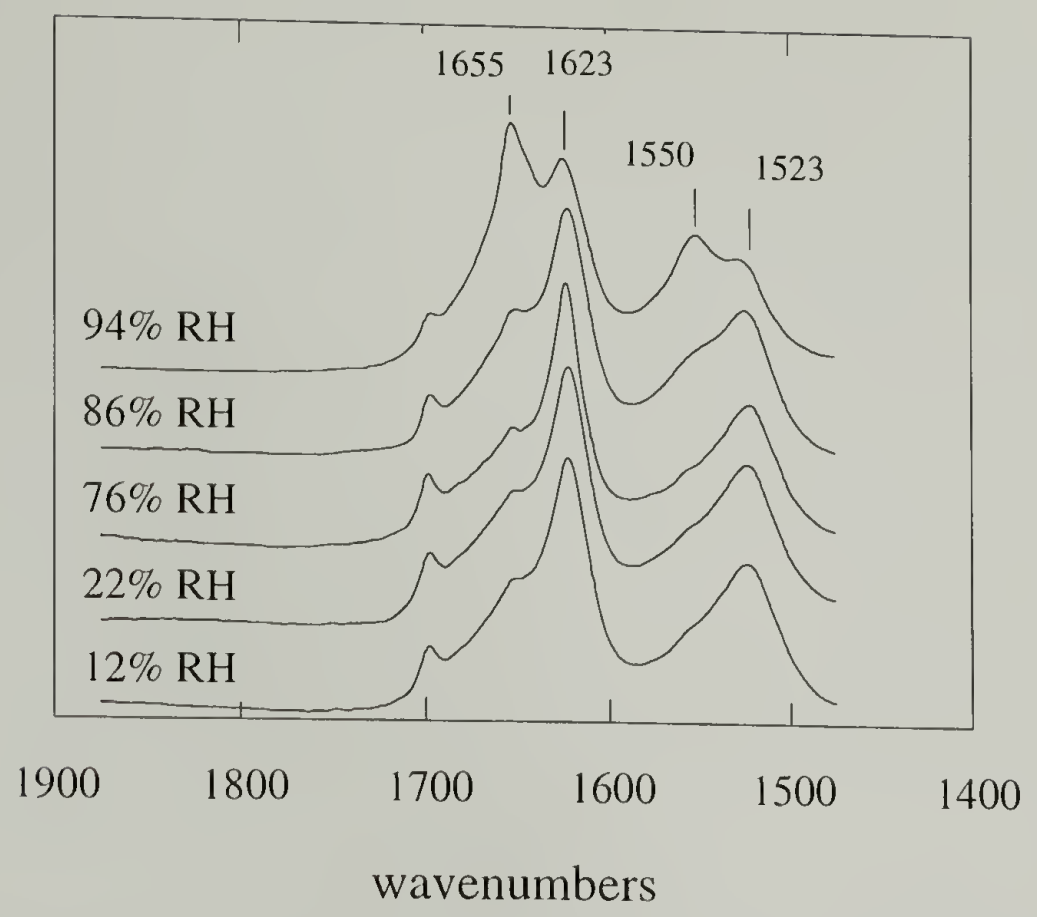

Figure 2.11 Infrared Amide I and Amide II region of AG3 samples equilibrated with various humidity environments.

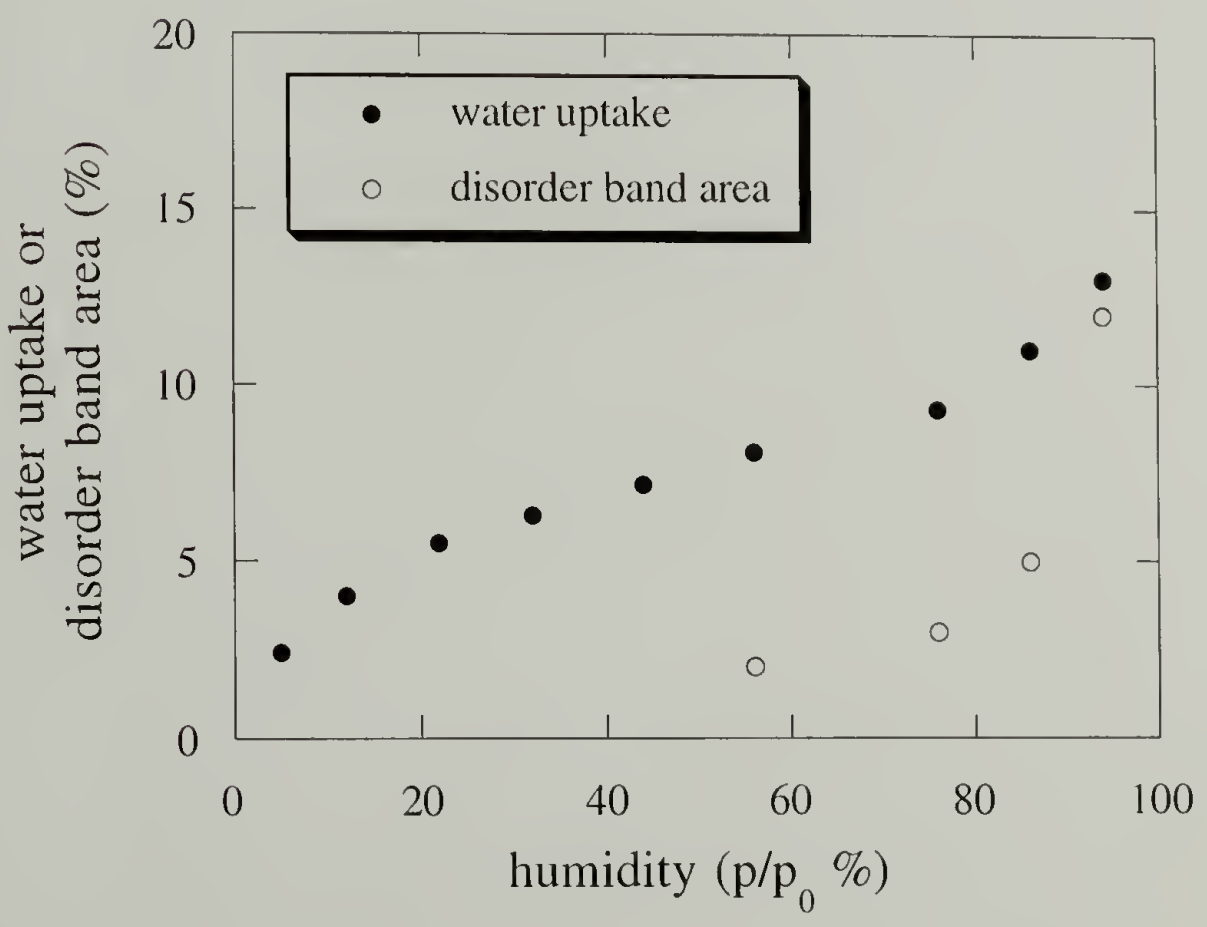

Figure 2.12 Water content and relative increases in the disordered band of the hydrated samples in Figure 2.11.

For samples exposed to low partial water vapor pressures, no chain conformational changes can be observed even for samples exposed for long times as seen in Figure 2.11. No changes in the conformation-sensitive infrared bands are found when the partial water vapor pressures are lower than 76%. In these same samples, however, the inter-sheet distance plotted as a function of partial water vapor pressure or humidity in Figure 2.13 has increased and the COO^- symmetric stretch band has already shifted to a lower frequency even at low partial vapor pressures, indicating hydration of the ionic groups and expansion of the crystals. Therefore, the changes in chain conformation occur *after* the intersheet spacing has expanded, i.e. after the crystalline region has become accessible to water. That water could access the crystalline regions has been confirmed by previous deuteration experiments presented above. We thus infer that the conformational disordering effect of water molecules on the polypeptide occurs most probably through the competition for hydrogen bonding with the amide groups.

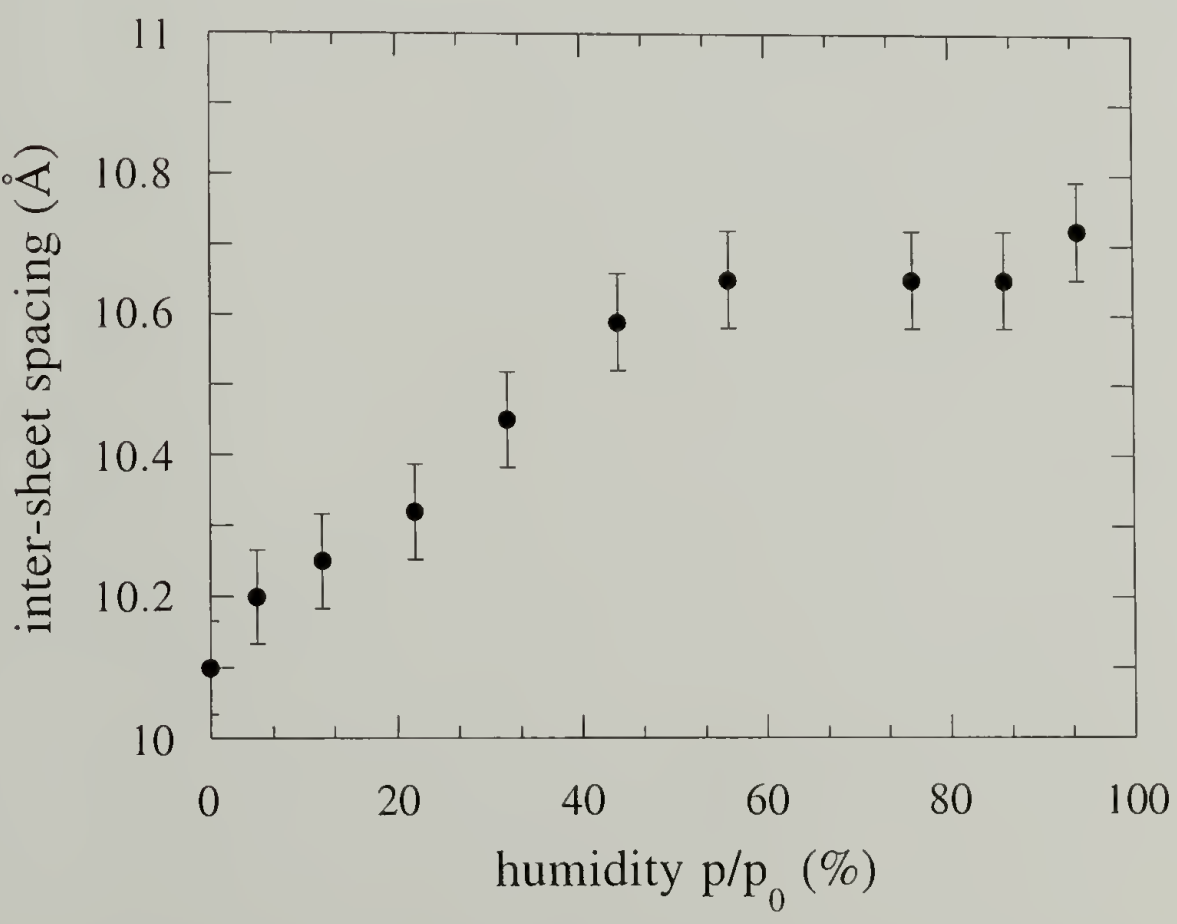

Figure 2.13 Changes in intersheet spacing induced by hydration of AG3 samples in Figure 2.11 and Figure 2.12.

The sorption isotherm shown in Figure 2.14 exhibits the typical sigmoid shape uaually found for synthetic polymers and biopolymers. The sorption data are fitted with D'Arcy and Watt equation as discussed previously in Chapter 1. The fitted sorption isotherm and various sorption components are shown in Figure 2.14 and 2.15. Values of the parameters associated with each sorption component are given in Table 2.5, together with literature values for related materials. Reiteration with the parameters for silk from Table 2.5 as the initial values was used to obtain the best fit. Reasonable fitting of the isotherm can be obtained with the following equation:

$$h = \frac{1.38\ P/P_0}{1+37\ P/P_0} + 0.072\ P/P_0 + \frac{0.0014\ P/P_0}{1-0.995\ P/P_0} \qquad (2.1)$$

Table 2.5 Isotherm parameters for various polymers

polymer	K'_i	K_i	C	k'	k
AG3	0.037	37	0.072	0.0014	0.995
silk[a]	0.0235	20.6	0.079	0.00868	0.976
nylon 6[b]	0	0	0.0812	0.00482	0.868
polyacrylic acid[c]	0.0131	25.4	0	0.0766	0.945
keratin[d]	0.039	20.2	0.120	0.02098	0.906

a. from reference 28

b. from reference 29

c. from reference 29

d. from reference 29

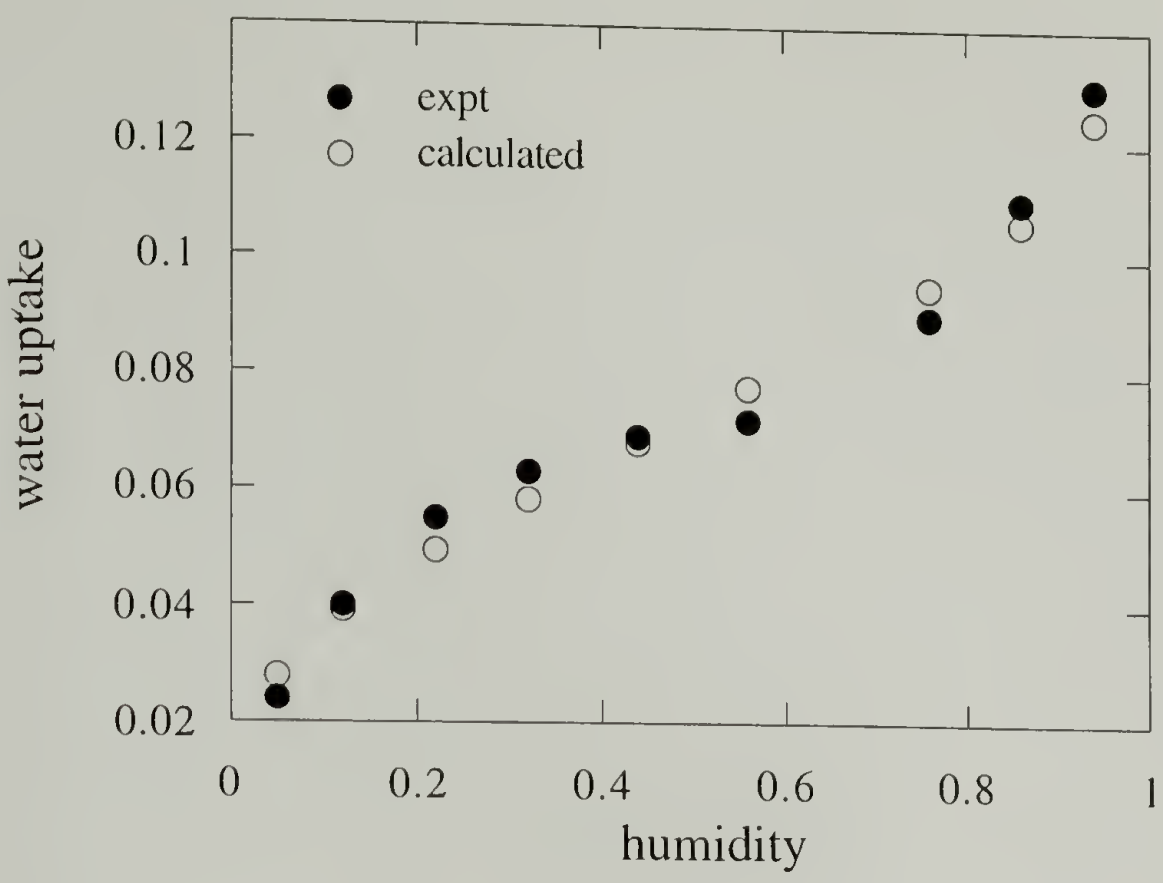

Figure 2.14 Comparison of experimental and calculated isotherm.

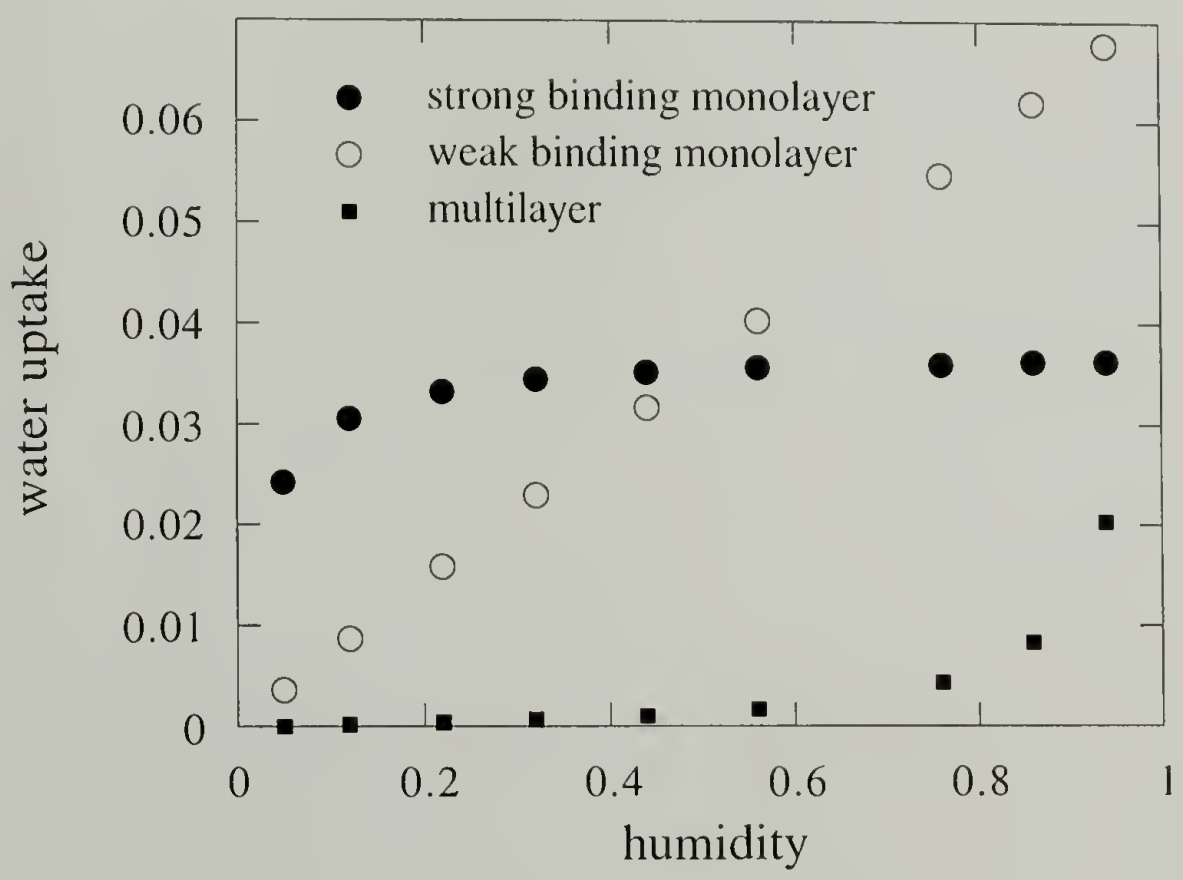

Figure 2.15 Various contributions to the calculated isotherm.

From Figure 2.15 it is clear that the strong binding monolayer component(the first term in the equation) reaches its limiting value at low humidities. This contribution can be attributed to the sorption of carboxylate groups on the lamellar surface in AG3 sample. The weak binding monolayer component(the second term in the equation) can be ascribed to the sorption of peptide groups, especially at the folding surface. It is interesting to note that the starting humidity for multilayer formation(the last term in the equation) roughly corresponds to that when chain conformation change occurs. The isotherm parameters for AG3 sample are comparable with related materials, e.g. silk, except that silk seems to have many more multimolecular formation sites (larger k'). Also from Table 2.5, values of K_i and K'_i for nylon 6 are zero, indicating that there is no contribution from the formation of a monolayer on highly reactive sites. Besides, for the water-soluble polyacrylic acid its value of C is zero.

It is also interesting to speculate how "disordered" the chain conformation really is. This issue can be resolved by comparing the infrared and Raman spectra of hydrated samples. Raman spectra of a series of hydrated samples in the carboxylate form are shown in Figure 2.16. There is only one Raman-active Amide I band (at 1666 cm^{-1}) for the β-sheet conformation and the small broad band centered at about 1690 cm^{-1} in Figure 2.16 is assigned to amides on the lamellar fold surface.[14] With hydration, the 1666 cm^{-1} band shifts to lower frequency, and broadens slightly; it is centered at 1664 cm^{-1} for samples containing about 5% water. This frequency shift is due to the increase in intensity of the band at 1660 cm^{-1}, as seen from the band convolution shown in the inset. This band (1660 cm^{-1}) in the Raman spectrum should have the same structural origin as the 1655 cm^{-1} band in the infrared spectrum, since both of their intensities increase upon hydration. The frequency difference between Raman and infrared Amide I bands has been calculated for "disordered" polypeptides previously.[15] It was argued that because of steric interactions along the chain, the probability of finding truly random chain conformations is quite small, and the distribution of ϕ and ψ in the regions associated with well characterized

chain conformations in fact is narrow. Therefore, even for " disordered " polypeptides, individual peptide units may still maintain dihedral angles close to those of a few allowed stable states. Assuming nearest -neighbor interactions only, it was found that the frequency difference between the Raman and infrared maxima should be of the order of 5 cm^{-1} for " disordered " polypeptides with local β-sheet dihedral angles, which was close to the experimental values.[15] What we observe here (1660 cm^{-1} vs. 1655 cm^{-1}) is also close to the calculation. Therefore, we conclude that the conformational change upon hydration involves the loss of long-range correlation in dihedral angles, but that the peptide units maintain dihedral angles close to those of the β-sheet.

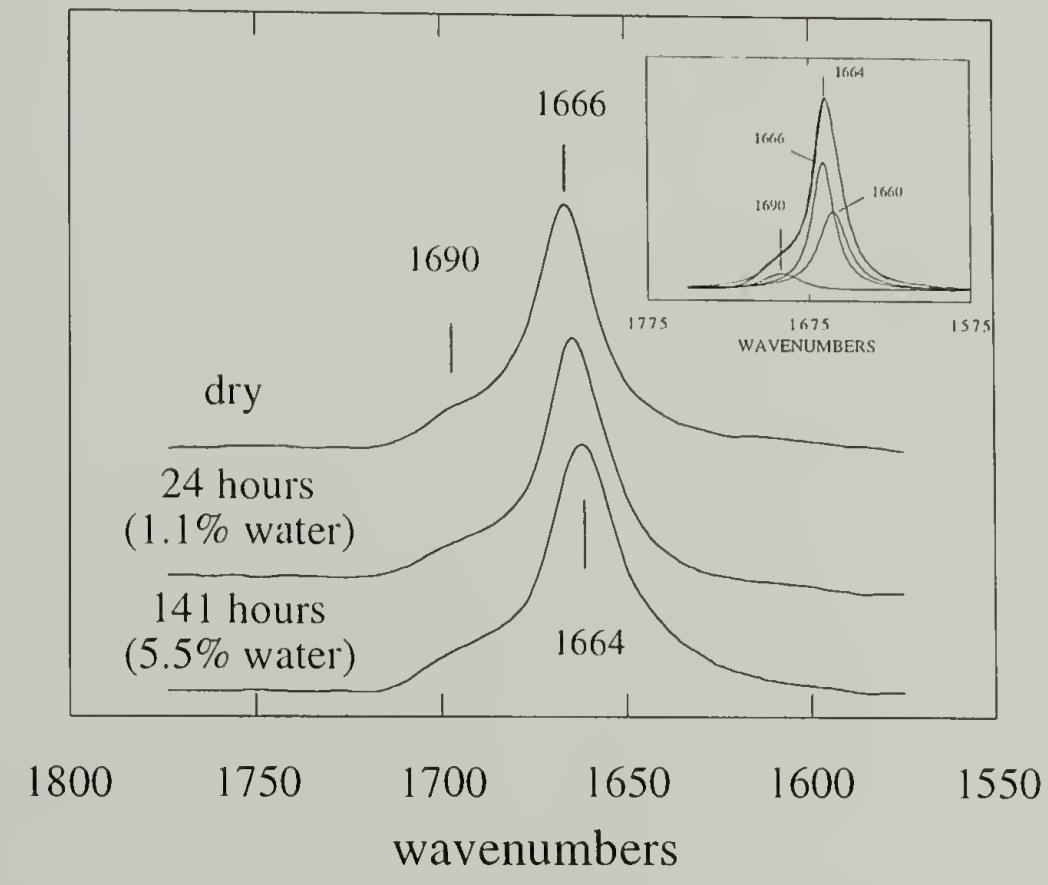

Figure 2.16 Raman spectra of progressively hydrated ionic AG3 samples.

Because the AG3 polypeptide has a relatively thin lamellar structure (thickness about 30 Å), unfavorable interactions on the lamellar surface can account for a considerable part of the overall energy. Upon hydration, the surface interactions become comparable to the cohesive energy in the crystalline phase and drive the observed structural changes. This

is especially true for the intersheet spacing since the hydrogen-bonded sheets are binded only by weaker Van de Waal's interaction in contrast to the stronger hydrogen bonding in the sheets. With this picture in mind we would expect that a thicker lamellar crystal like that of the AG6 polypeptide should show much less structural change upon hydration. This expectation is confirmed when we compare the hydration behavior of AG3 and AG6 samples. The infrared spectra of progressively deuterated AG6 samples in the carboxylic form are shown in Figure 2.17.

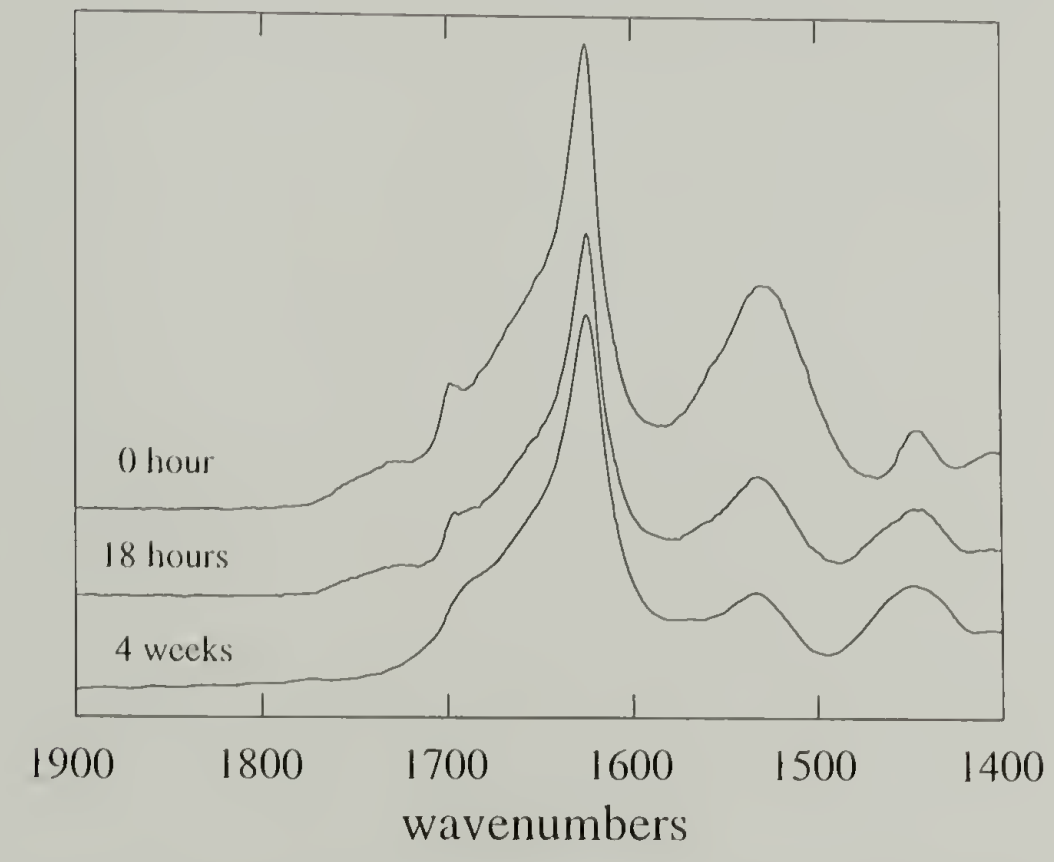

Figure 2.17 Infrared spectra of progressively deuterated AG6 samples in the Amide I and Amide II regions.

Figure 2.18 shows the deuteration kinetics of AG6 polypeptide in its carboxylic acid and carboxylate forms. In contrast to what we found for the AG3 sample, where deuteration of the carboxylate form proceeded much faster than that of carboxylic acid form and conformational changes occur, for the AG6 sample the deuteration rate and accessibility of its carboxylate form are only a little larger than those of the carboxylic form. Besides, no conformational change is detected in the Amide I region and a plateau in the

deuteration curve is found for the carboxylate form of AG6 sample. This suggests that the lamellar crystalline structure of AG6 is much more stable than that of AG3 in terms of hydration effects on its crystalline chain conformation. Moreover, the accessibility of the AG6 sample to D_2O can be estimated to be about 27% from the plateau value, which is lower than the value, 32%, obtained for the AG3 sample. This is consistent with the structure of the model polypeptide that the AG6 sample consists of smaller proportion of folding surface than the AG3 sample.

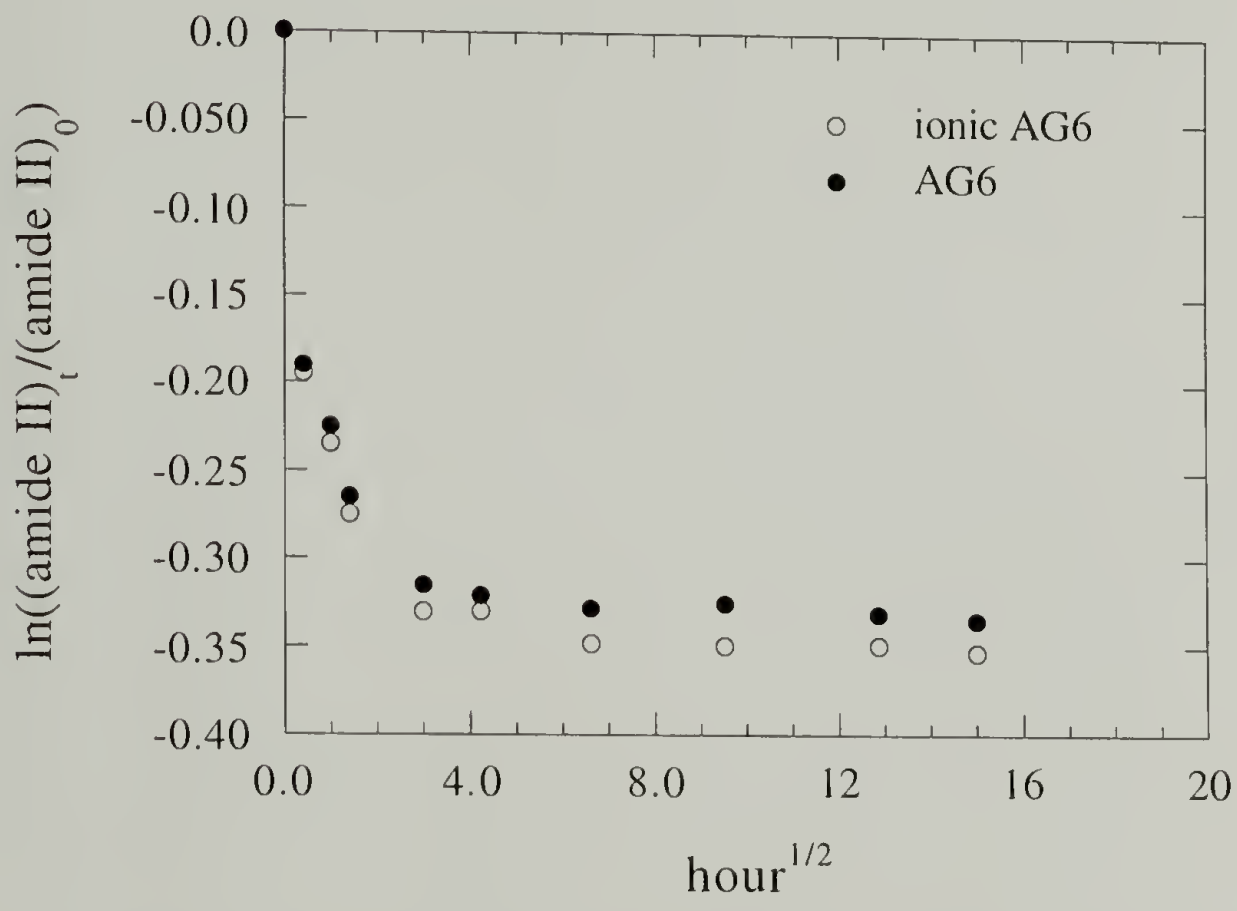

Figure 2.18 Rate of deuteration of AG6 samples in the carboxylic and carboxylate forms calculated from the rate of decrease of Amide II intensity.

More supporting evidence comes from the changes in intersheet distance with hydration obtained from WAXD experiment. As also shown in Figure 2.19, AG6 exhibits much smaller changes than AG3 even at the highest level of hydration. With this WAXD data and previous finding that water molecules do not access the crystalline core of the AG6 sample, it is inferred that the unfavorable interaction on the lamellar surface caused by

hydration is limited, compared with the bulk energy, such that the expansion in intersheet distance is not large enough to make the crystalline region accessible. Therefore, the comparison of hydration behavior between two lamellar crystals with different thickness confirms our hypothesis that surface energy is an important determinant of structural stability against hydration especially in the case of thin crystals.

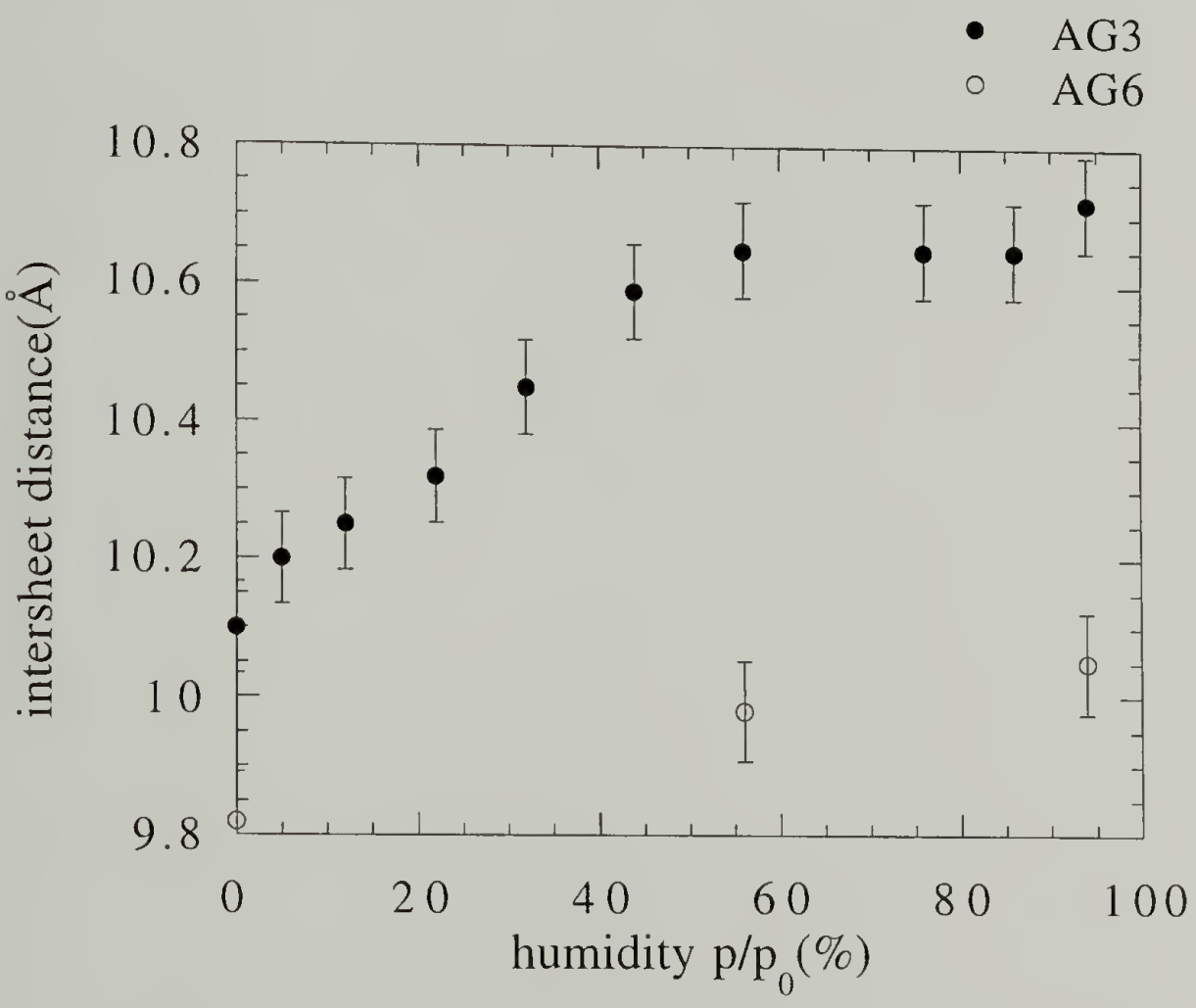

Figure 2.19 Comparison of intersheet spacing changes in AG3 and AG6 samples in their carboxylate forms when they are subject to various humidity environments.

2.4 Conclusions

Kinetic and equilibrium information derived from vibrational spectroscopy and wide angle X-ray diffraction has been used to establish that the hydration of polypeptide **1** is a stepwise process. Polypeptides such as **1**, with well-defined β-sheet conformations

and uniform lamellar structures with fold surfaces decorated with functional groups, serve as good model systems for examination of the mechanism by which water affects polymer structure at different levels. Each step of the structural change occurring as a function of water content can be characterized. At low water contents, changes in inter-sheet spacing are caused by hydration of the ionic groups on the fold surface, without involving water directly in the crystalline region. Consequently, crystalline regions become increasingly accessible to water and susceptible to changes in chain conformation. The extent of inter-sheet expansion is a function of water content. Comparison of infrared and Raman spectra obtained for hydrated samples suggests an increase in long-range disorder with retention of local order, i.e. a structure with local β-sheet dihedral angles, in which long-range correlation has been lost due to the interaction with water. Because the AG3 polypeptide has a relatively thin lamellar structure (thickness about 30 Å), unfavorable interactions on the lamellar surface can account for a considerable part of the overall energy. Upon hydration, the surface interactions become comparable to the cohesive energy in the crystalline phase and drive the observed structural changes. The investigation of deuteration and hydration behavior of AG6 sample confirm this proposal. In this case the AG6 sample, with thicker lamellae with similar structure and thus relatively unimportant surface energy, upon sorption of moisture shows only limited intersheet spacing expansion and no chain conformation changes were observed.

The sequential hydration-induced structural changes can be illustrated in Figure 2.20. The essential mechanism can be boiled down to 1. the competition between surface energy and bulk energy, which determines the extent of expansion of the crystals and thus the accessibility to water molecules; 2. the competition between peptide-peptide hydrogen bonding and water-peptide hydrogen bonding, which causes the changes in chain conformation.

Structural Changes with Water Content

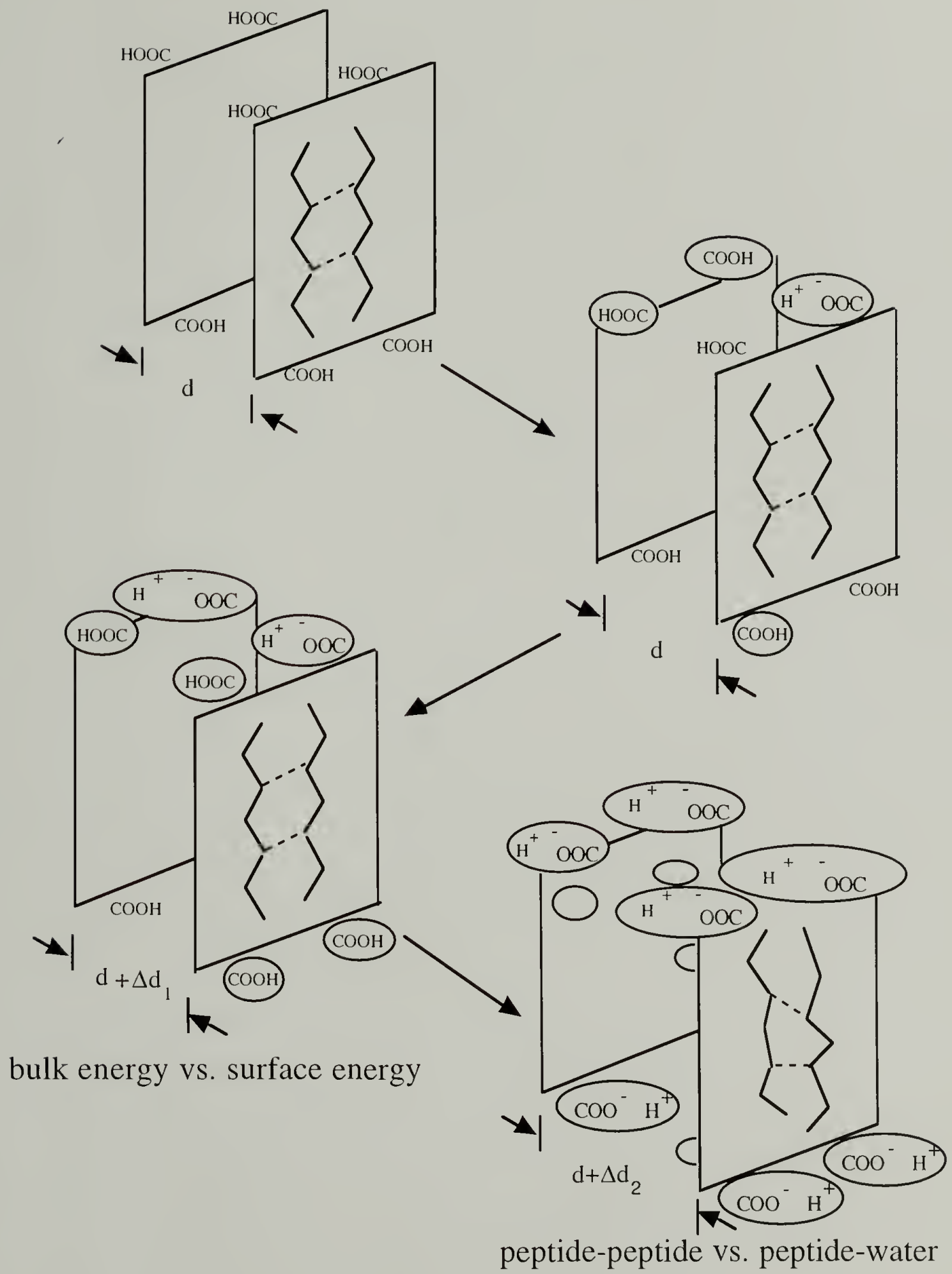

Figure 2.20 Schematic representation of sequential hydration events in the model polypeptides.

References

(1) Campbell, G. A. *J. Polym. Sci. B* **1969**, *7*, 629.

(2) Murthy, N. S.; Stamm, M.; Sibilia, J. P.; Krimm, S. *Macromolecules* **1989**, *22*, 1261.

(3) Vergalati, C.; Imberty, A.; Perez, S. *Macromolecules* **1993**, *26*, 4420.

(4) Shmueli, U.; Traub, W. *J. Mol. Biol.* **1965**, *12*, 205.

(5) Lenormant, H.; Baudras, A.; Blout, E. R. *J. Am. Chem. Soc.* **1958**, *80*, 6191.

(6) Careri, G.; Giansanti, A. *Biopolymers* **1979**, *18*, 1187.

(7) Bolton, B. A.; Scherer, J. R. *J. Phys. Chem.* **1989**, *93*, 7635.

(8) Rupley, J. A.; Yang, P.-H.; Tollin, U. In *Water in Polymers*; S. P. Rowland, Ed.; ACS symposium Series 127: Washington, D. C., 1980; pp 111.

(9) Krejchi, M. T.; Atkins, E. D. T.; Waddon, A. J.; Fournier, M. J.; Mason, T. L.; Tirrell, D. A. *Science* **1994**, *265*, 1427.

(10) Fraser, R. D. B.; MacRae, T. P. *Conformation in Fibrous Proteins*; Academic Press: New York, 1973.

(11) Marsh, R. E.; Corey, R. B.; Pauling, L. *Biochim. Biophys. Acta* **1955**, *16*, 1.

(12) Fraser, R. D. B.; MacRae, T. P.; Stewart, F. H. C.; Suzuki, E. *J. Mol. Biol.* **1965**, *11*, 706.

(13) Greenspan, L. *J. Res. Nat. Bur. Standards* **1977**, *81A*, 89.

(14) Krimm, S.; Bandekar, J. *Adv. Protein Chem.* **1986**, *38*, 181.

(15) Painter, P. C.; Coleman, M. M. *Biopolymers* **1978**, *17*, 2475.

(16) Chirgadze, Y. N.; Brazhnikov, E. V.; Nevskaya, N. A. *J. Mol. Biol.* **1976**, *102*, 781.

(17) Miyazawa, T.; Blout, E. R. *J. Am. Chem. Soc.* **1961**, *83*, 712.

(18) Miyazawa, T. *J. Chem. Phys.* **1960**, *32*, 1647.

(19) Abe, Y.; Krimm, S. *Biopolymers* **1972**, *11*, 1817.

(20) Moore, W. H.; Krimm, S. *Biopolymers* **1976**, *15*, 2465.

(21) Tirrell, D.; Grossman, S.; Vogl, O. *Makromol.Chem.* **1979**, *180*, 721.

(22) Puffr, R. *Kolloid-Z. Z. Polym* **1968**, *222*, 130.

(23) Tsuboi, M.; Nakanishi, M. *Adv. Biophys.* **1979**, *12*, 101.

(24) Susi, H.; Timasheff, S. N.; Stevens, L. *J. Biol. Chem.* **1967**, *242*, 5460.

(25) Blout, E. R.; DE Loze, C.; Asadourian, A. *J. Am. Chem. Soc.* **1961**, *83*, 1895.

(26) Lowry, S. R.; Mauritz, K. A. *J. Am. Chem. Soc.* **1980**, *102*, 4665.

(27) Kutsumizu, S.; Nagao, N.; Tadano, K.; Tachino, H.; Hirasawa, E.; Yano, S. *Macromolecules* **1992**, *25*, 6829.

(28) Bull, H. *J. Am. Chem. Soc.* **1944**, *64*, 751.

(29) D'Arcy, R. L.; Watt, I. C. *Trans. Faraday Soc.* **1969**, *66*, 1236.

CHAPTER 3

CHARACTERIZATION OF SILK CRYSTALLIZATION BEHAVIOR ON HIGHLY ORIENTED SUBSTRATES

3.1 Introduction

In many instances, substrates are found to be able to affect the crystallization behavior of the depositing polymers, depending on the nature of the substrate and the casting conditions. Many such examples can be found in the literature. For example, when a solution of nylon 6 yarn in formic acid is spread on to a plane glass surface and the solvent evaporated, it is found that the α-crystalline form predominates in the resultant film. On the other hand, when the same polymer solution is spread on to the (100) faces of either sodium chloride or potassium bromide at 35°C, the resultant cast film is largely in the γ-crystalline form[1], which is less stable than the α-crystalline form.[2] Crystallization of nylon 6, 66 copolymer solution in the presence of a large amount of foreign material was shown to all occur on the foreign surfaces as long as the surfaces are hydrophilic, indicating the nucleating ability of the surfaces.[3] A similar phenomenon has also been observed for the crystallization of silk fibroin from its aqueous solution on different substrates. For example, more amorphous structure is obtained on hydrophobic substrates like poly(tetrafluoroethylene) and polyethylene than on hydrophilic substrates like nylons.[4] It would be particularly interesting to investigate the possible stabilizing effects of oriented substrates on the crystallization behavior of dilute aqueous silk fibroin solution because of the extensive interaction between water and silk molecules normally preventing crystallization from occurring.[5] This part of study will also further demonstrate the

competition between the various interactions among polymer, water and substrate. The review of the crystallization behavior of silk fibroin is in order because of its versatility under various conditions.

The silk fibers produced by spiders and silkworms exhibit many impressive physical and mechanical properties, which has inspired numerous attempts to spin such fibers from silk solutions *in vitro* .[6,7] It is particularly interesting that silk originates from an aqueous solution. In the spinning process water-soluble silk fibroin is converted at room temperature to insoluble high performance fibers by a physical rather than chemical process. The only by product is water.

The structure of silk can be quite complex. *Bombyx mori* cocoon silk is known to be composed of two proteins, fibroin and sericin. A double filament of fibroin is enveloped by an outer layer of sericin. Fibroin is the protein that gives silk its unique physical and chemical properties and mainly consists of (Gly-Ala-Gly-Ala-Gly-Ser) repeating units in the crystalline regions. In these crystalline regions, chain conformation has been established to be planar β-pleated sheet packed in an antiparallel fashion, sometimes referred to as silk II. The less stable water-soluble form is called silk I. Either silk I or II can be obtained from solution depending on the crystallization conditions. In the substantial silk literature dealing with the mechanism of crystallization, parameters such as solvent, concentration, temperature, drying rate, substrate, and so on are found to be important in determining the chain conformation of silk.[6,8-10] Mechanical stress accompanying flow of the aqueous silk solution has been found to be particularly important in causing silk fibroin to precipitate into crystalline forms. Based on experiments on a steady-state flow of regenerated silk fibroin from *Bombyx mori* , Yamaura[11] proposed that nucleation occurs in flow-induced oriented silk fibroin adsorbed to the solution surface. The oriented molecules associate to produce fibrillar crystals. *Bombyx mori* silk fibroin crystallizes to form fibers in solution. Iizuka[12] showed that the critical shear rate for such

crystallization changes with different ionic strength, pH, and fibroin concentration. It has also been found that growth of β-form spherulites can be promoted on the surface of well-oriented β-form silk filaments immersed in fibroin solution.[13] These and earlier studies indicate that segmental orientation is crucial to the crystallization of β-form silk crystals from solutions of silk fibroin.

Orientation of silk molecules can be accomplished by many means, for example, by shearing silk fibroin solution[11,12] or by adsorption at the air-water interface.[14] In the present work, the influence of an oriented substrate on the crystallization behavior of silk from aqueous solution or aqueous LiBr solution is investigated by casting a film of silk from solution on a highly oriented poly(tetrafluoroethylene) substrate under conditions normally unfavorable for crystallization of silk II structure. It has been reported that by using this highly oriented poly(tetrafluoroethylene) substrate, oriented molecular crystals, polymers, or even certain inorganic materials can be formed from the melt, solution or from the vapor phase.[15-17]

Infrared vibrational spectroscopy is used in this work to characterize silk films. When bands are properly assigned and the polarization state is well defined, vibrational spectroscopy provides a measure of structures and preferred segmental orientation at the localized level. Indeed, transmission infrared spectroscopy has been used to characterize silk films since the early 1950s, and this pioneering work served to establish many assignments and band polarizations.[18] For the reason of in-situ examination, external reflection infrared spectroscopy was chosen to characterize both the microstructure and preferred segmental orientation of the substrate and that of the silk crystals formed. The oriented poly(tetrafluoroethylene) surface proved able to induce crystallization even under conditions normally regarded unfavorable. The results obtained in the present investigation are reported here.

3.2 Experimental Section

Silk cocoon was degummed by boiling in deionized water with sodium dodecyl sulfate (0.5%). Degummed silk was then dissolved in aqueous 9.3 M LiBr solution at 50 °C. The undissolved residue was removed by filtering with paper filters. Then the solution was dialyzed against Millipor deionized water for 72 hours with 12,000-14,000 MW cut-off Spectrapor membrane. Water was changed every 24 hours. That rapid transport of LiBr to the dialysate was established was determined via conductivity measurements of the silk solutions. Dialyzed solution was then filtered with 0.45 mm Millipore filters. All silk solutions were stored at 5 °C. We used a solution concentration of 0.5 g/l (or 0.05%) obtained by dilution of the original dialyzed solution. The silk concentration of the latter had to be determined by drying at 50°C in vacuum to obtain the actual amount of silk after the solution was prepared due to the presence of insoluble material. The 9.3 M LiBr/silk solution was prepared by addition of required amount of LiBr.

The procedure used to prepare smooth highly oriented substrates followed the one described by Wittman et al.[15] as illustrated in Figure 3.1. It has also been pointed out that in terms of film smoothness and continuity, and orientation-inducing ability, poly(tetrafluoroethylene) is superior to other possible materials, e.g. polyethylene and liquid crystalline polyester.[19] Besides, it also offers the advantage of thermal and chemical resistance. Therefore, in our experiment we chose poly(tetrafluoroethylene) as the oriented substrate. The preparation procedure involved rubbing one face of a commercial grade, melt-crystallized poly(tetrafluoroethylene) block back and forth 4 times on a glass microscopy slide at a controlled temperature (300 °C) and pressure (40 N/cm^2). The temperature used, which is about 0.9Tm of poly(tetrafluoroethylene), has been determined to be optimum in obtaining continuous films.[17]

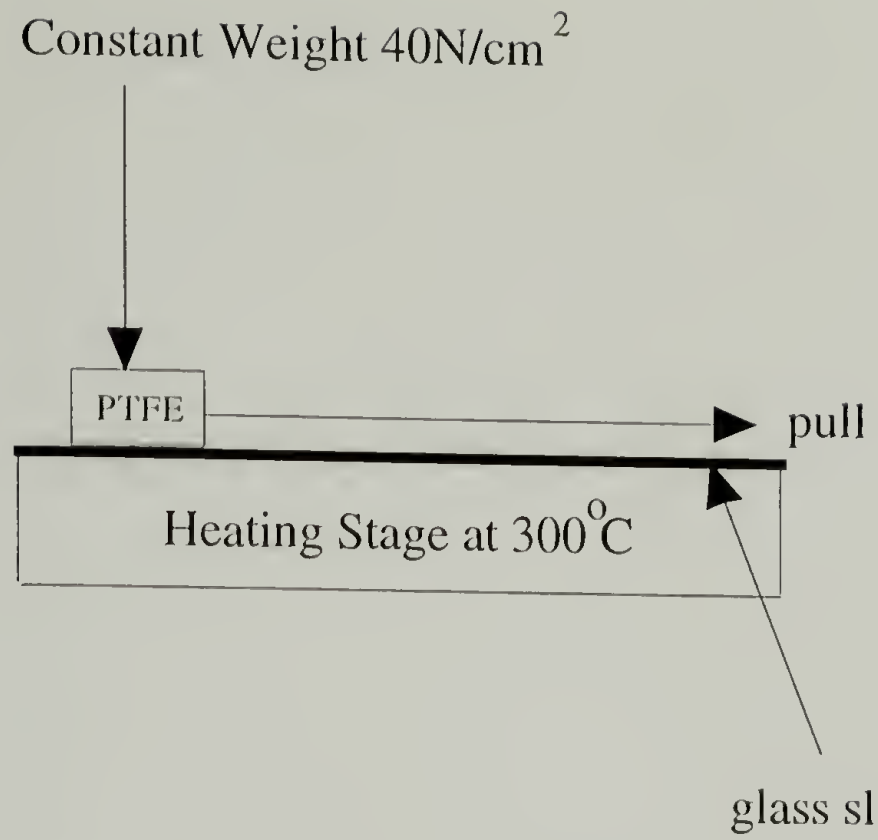

Figure 3.1 Schematic representation of the procedure to prepare the oriented poly(tetrafluoroethylene) film.

Wide angle X-ray diffraction experiments in reflection geometry were carried out using Siemens D500 diffractometer using Ni filtered CuKα radiation operated at 30 mA and 40 kV. A 1° divergence slit and a 0.4 mm receiving slit were used to collimate the beam. A scan step of 0.1° per second was chosen. The sample was rotating around the rubbing direction with detector scanning synchronously from 5° to 35°. Although this experiment can characterize the thin films in situ, it does not provide as much information as transmission experiments. Therefore, electron diffraction experiments were attempted. The thin poly(tetrafluoroethylene) films can be lifted from glass by immersion in water. 300 mesh copper grids were then used to pick up the films from water surface; the films were then air-dried and examined with a JEOL 100 CX instrument operated at 100 kV with a corresponding wavelength of 0.0375Å. The size of the beam is about 0.5 μm. The sample-film distance was calibrated by using sputtered gold thin films.

Silk fibroin films were cast on bare or oriented poly(tetrafluoroethylene)-coated glass slides and also on isotropic poly(tetrafluoroethylene) surface from silk solution (0.05%) at room temperature and then dried in vacuum. To cast films from 9.3 M LiBr silk solution (also with 0.05% of silk fibroin), the solution on substrates was first equilibrated for two days with saturated aqueous solution of LiBr. Silk fibroin could then deposit on the substrates without co-precipitation of LiBr crystals. After two days, the glass slides were then rinsed with deionized water for one minute and quickly dried in a stream of dry air.

Reflectance spectra were obtained with a Perkin-Elmer 2000 FTIR spectrometer equipped with both wide and narrow band MCT detectors, using an external reflection cell purchased from Graesby Specac in Waterbury, Connecticut. The incident angle of the infrared beam was chosen at 30 degrees relative to the surface normal, as shown in Figure 3.2. This angle has been specifically chosen because for reflection experiments on dielectric substrates like glass or polymers, this condition has been found to yield the best signal-to-noise ratio.[20]

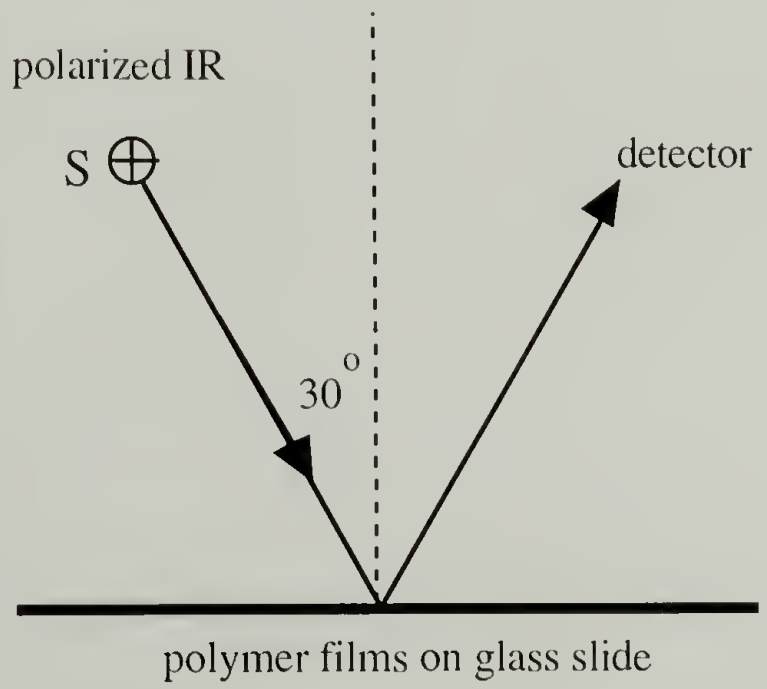

Figure 3.2 Schematic illustration of reflection IR experiment.

The refleetance absorbanee is defined as -log(R/R_o), where R_o is the refleetivity of a bare glass, and R is the refleetivity of a film deposited on glass. In general, the intensity of a refleetance speetrum depends on the polarization state of incident radiation, angle of ineidence, and the thiekness of the films being studied. Since in this experiment only in-plane orientation of poly(tetrafluoroethylene) and silk fibroin on glass slides is of interest, only s polarization (eleetrie veetor of incident light perpendieular to the seattering plane defined by the ineident and exit radiation; see also Figure 3.2) was used. A gold-grid polarizer was placed immediately before the glass sample. To probe the moleeular orientation eharacteristics of poly(tetrafluoroethylene) or silk fibroin , the glass slide was rotated relative to the polarizer by 90 degrees. In this study, the parallel and perpendicular spectra are defined by orienting the ineident polarization parallel and perpendieular to the rubbing direction. For isotropie films on glass, the rotation was found to produee minimal changes in the spectrum.

There are several bands assoeiated with the amide group whieh can be used to charaeterize chain conformation. For example the Amide I bands are found at 1660, 1645, and 1630 cm^{-1} for α, disordered, and β struetures respeetively (See also Chapter 2, Table 2.2). To charaeterize the segmental orientation of both silk and poly(tetrafluoroethylene), we need to know the characteristie polarization of these bands, as tabulated in Table 3.1 and Table 3.2. The bands observed for silk films prepared often exhibit asymmetrie broad band shapes suggesting multiple structures. Band deconvolution (Lab Calc^{TM}) was used to assess quantitatively the amount of eaeh eomponent. The 1710-1600 em^{-1} and 1600-1500 cm^{-1} regions were each deeonvoluted into three contributions. A eombination of Gaussian and Lorentzian band shape was used. Frequeney, width at half height, intensity and percentage of Gaussian or Lorentzian band eontribution to the contour were varied to obtain the best fit.

Table 3.1 Conformation-sensitive frequencies (cm^{-1}) of poly(tetrafluoroethylene), and their polarization characteristics. ⊥: transition dipole moment perpendicular to the molecular axis; ||: parallel to the molecular axis.[21, 22]

15_7 helix	1210 (⊥), 1150 (⊥), 637 (||)
Trans	624 (||)

Table 3.2 Conformation-sensitive frequencies (cm^{-1}) of silk, and their polarization characteristics. ⊥: transition dipole moment perpendicular to the molecular axis; ||: parallel to the molecular axis.[23, 24]

	silk II	silk I	α-helix	disordered
Amide I	1630 (⊥)	1660 (⊥)	1650 (||)	~1655
Amide II	1530 (||)	1540 (||)	1545 (⊥)	~1535

3.3 Results and Discussion

3.3.1 Characterization of the Oriented Substrate

The polarized external infrared reflection spectra of a friction deposited poly(tetrafluoroethylene) thin film are displayed in Figure 3.3. The bands at 637, 1150, and 1210 cm^{-1} are characteristic of a 15_7 helical chain conformation and the 624 cm^{-1} band is a defect band with trans chain conformation.[21,22] These spectra were obtained in s polarization with the electric vector of the light incident on the polymer surface oriented either along or perpendicular to the rubbing direction, depending on the sample orientation.

The different signs of absorbance for those bands with different polarization characteristies can only be understood if the poly(tetrafluoroethylene) chains lie parallel to the film surface.[20] The spectra shown in Figure 3.3 suggest that the preferred segmental orientation along the rubbing direction in the poly(tetrafluoroethylene) thin film deposited on glass slides seems to be extremely high. The orientation funetion estimated from the dichroie ratio for the 1150 cm^{1} band is 0.62. This value is eomparable to the plateau value, which is also obtained from infrared dichroism, found in mechanieally drawn bulk poly(tetrafluoroethylene) film.[25] It should also be noted that even though the crystalline chains are highly oriented, the 850 cm^{-1} band assigned to the amorphous structure[26] exhibits no orientation.

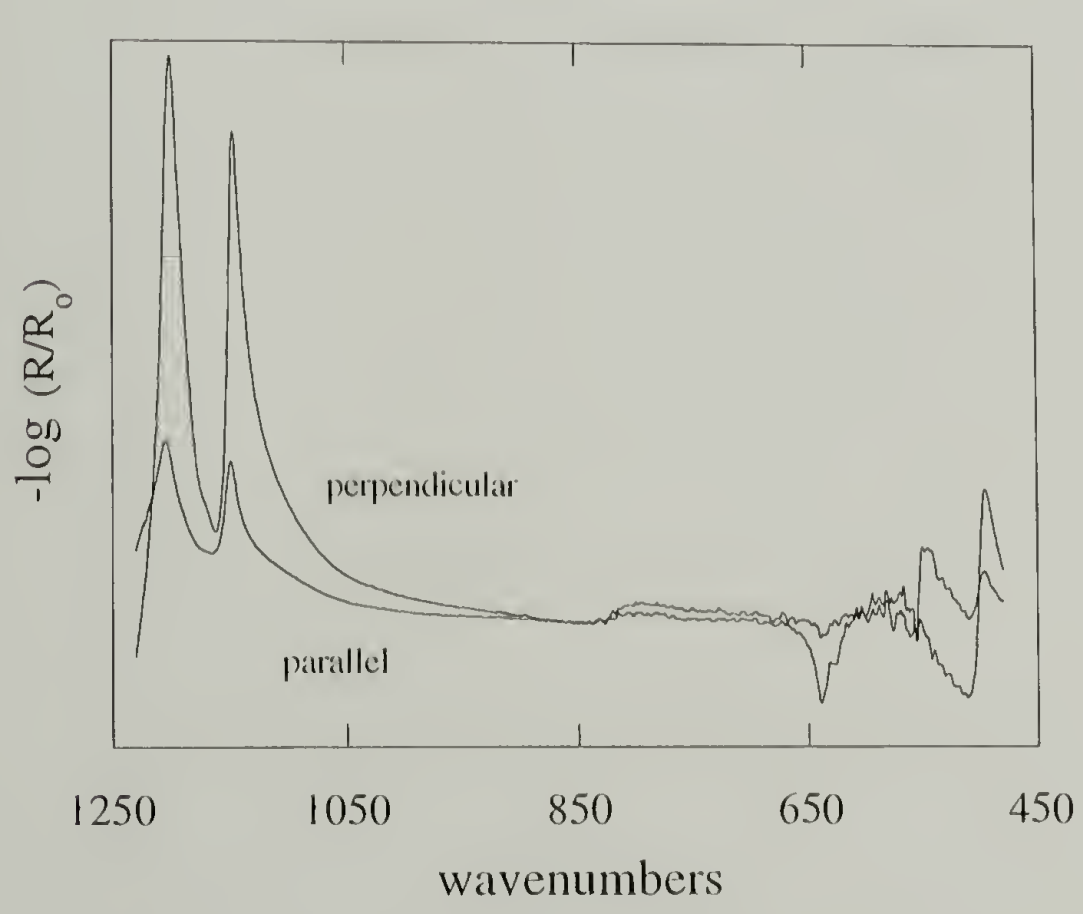

Figure 3.3 Reflectance infrared speetra of friction-deposited poly(tetrafluoroethylene) film on glass slide, with the infrared beam polarized parallel and perpendicular to the rubbing direction.

To further ascertain whether the deposited thin film of poly(tetrafluoroethylene) has the same crystalline structure as conventional bulk material, wide angle X-ray diffraction and electron diffraction experiments were conducted. Figure 3.4 shows the only one peak observed in the wide angle X-ray diffractometer trace. This would be understandable if the poly(tetrafluoroethylene) molecules are arranged lying on the surface as shown in Figure 3.5.a and if the unit cell is pseudohexagonal as seen in Figure 3.5.b. This can be explained by the Ewald sphere construction shown in Figure 3.6, where it shows that the diffraction normal to the sample surface is detected.[17] Therefore, this data supports the aforementioned inference from reflection infrared experiment that the poly(tetrafluoroethylene) molecules lie parallel to the surface, although the X-ray diffraction in reflection geometry could not characterize the in-plane orientation of the poly(tetrafluoroethylene) molecules. Thus, transmission experiment is necessary to obtain the unit cell dimensions.

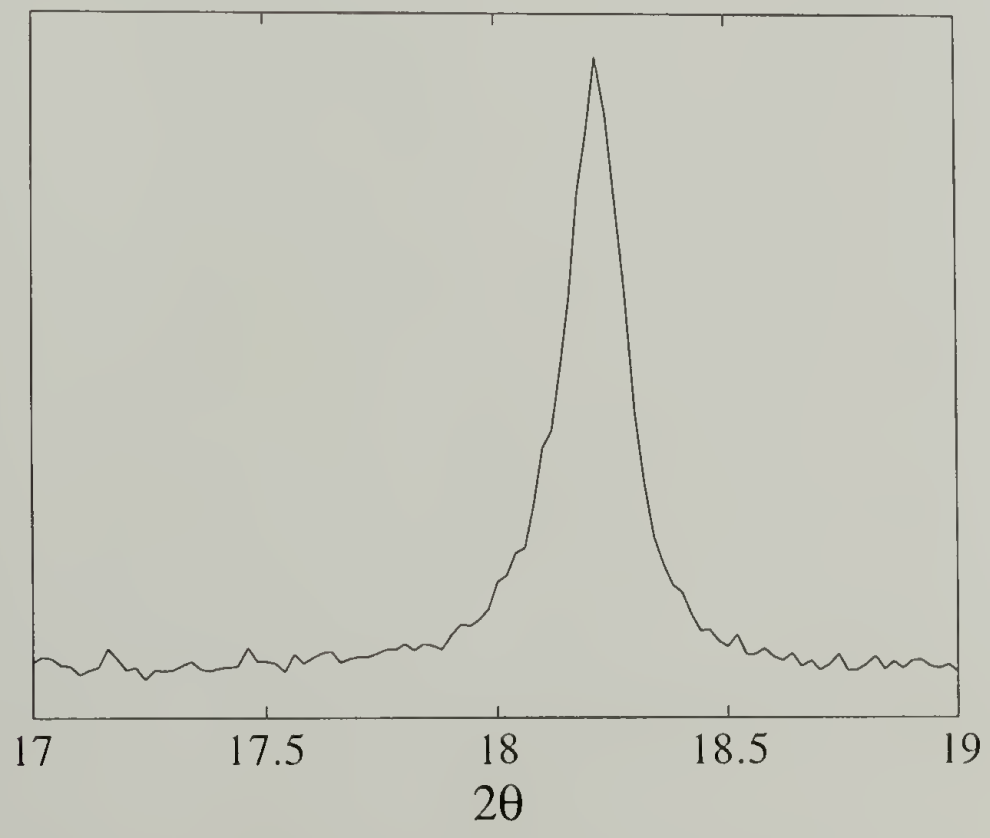

Figure 3.4 Wide angle X-ray diffractometer trace of friction-deposited poly(tetrafluoroethylene) film on glass slide.

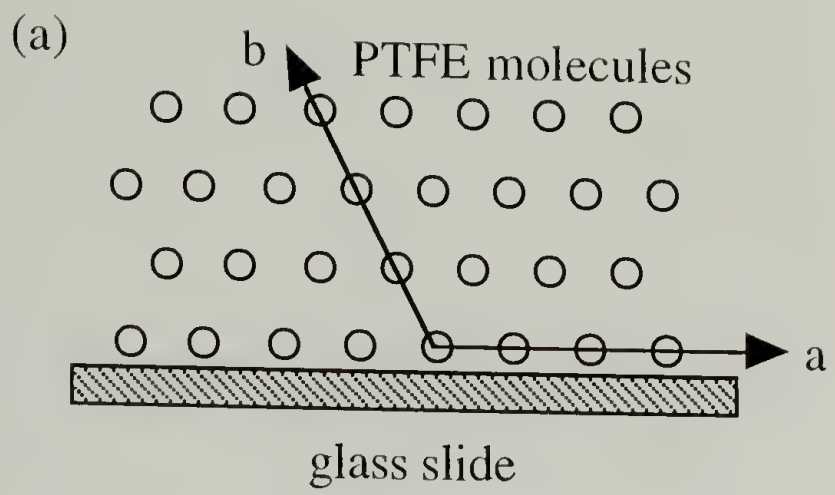

Figure 3.5 Structure model of the poly(tetrafluoroethylene) thin film. (a) Schematic arrangement of poly(tetrafluoroethylene) molecules on the glass surface. Molecular axes are into the plane of paper. (b) Distribution of structural factors corresponding to the arrangement in (a) (from reference 17).

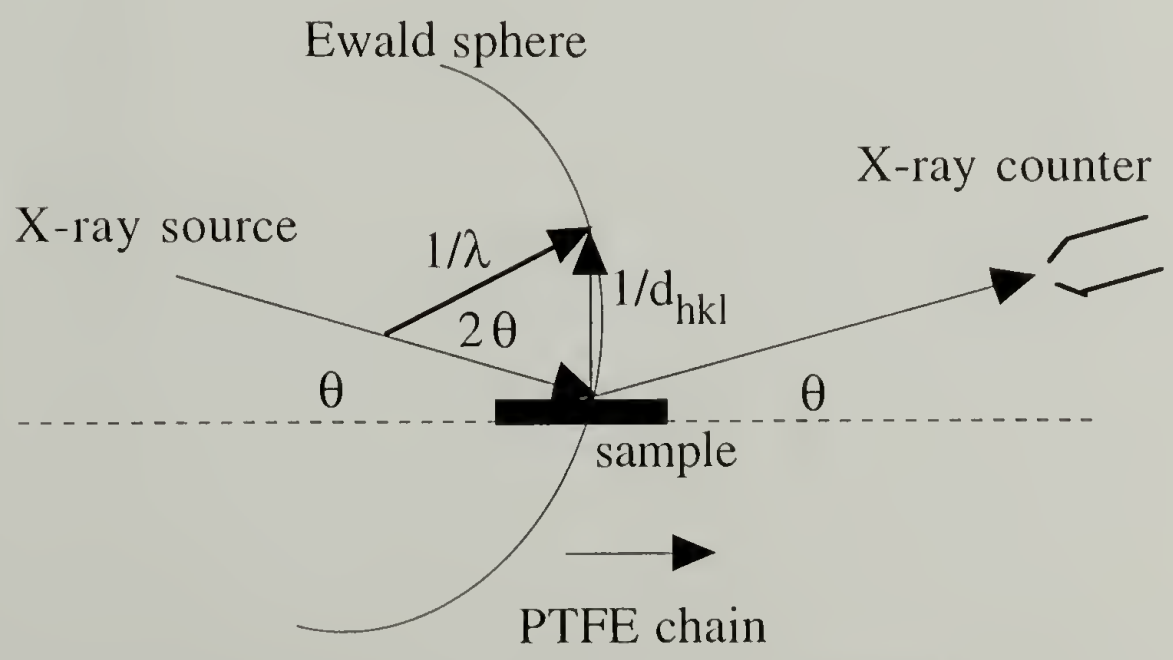

Figure 3.6 Ewald sphere construction of the X-ray diffractometer in the reflection mode (from reference 17).

Since the poly(tetrafluoroethylene) films are too thin for wide angle X-ray experiment in transmission mode, more definite characterization of the crystalline structure of the deposited poly(tetrafluoroethylene) films was done with electron diffraction. The electron diffraction patterns are shown in Figure 3.7. The diffraction patterns obtained indicate a highly-oriented structure, and a number of high order spots are observed. When the sample is rotated around the rubbing direction, extra diffraction spots become apparent at 30 and 60 degrees (Figure 3.7.b). This is an indication that the sample has a hexagonal unit cell and that the close-packed poly(tetrafluoroethylene) 100 crystalline planes are parallel to the substrate as explained in Figure 3.5.b. Unit cell dimensions were calculated using the equatorial and meridian diffractions with the calibrated sample-exposure film distance. The intermolecular spacing is calculated to be 5.31 Å and the chain repeat of the 15 CF2 groups is 19.8 Å. These measurements compare modestly well with 5.55 and 19.5 Å reported by Bunn et al.[27] These results are consistent with a 157 helical chain phase IV structure which exists between 19°C and 35°C for bulk material under atmospheric pressure.[27,28] These data indicate that the rubbing deposited thin film of poly(tetrafluoroethylene) has the same structure as the crystalline bulk material under the same conditions and that their molecules lie on the surface of the glass slide with a preferred segmental orientation parallel to the rubbing direction.

As a summary for the characterization of the poly(tetrafluoroethylene) thin films, we make the following conclusions from the consistent results from both reflection infrared spectroscopy and diffraction techniques. The poly(tetrafluoroethylene) molecules lie on the surface with a preferable alignment along the rubbing direction. They assume a 157 helical chain conformation and phase IV crystalline structure with a hexagonal unit cell. Furthermore, the close-packed poly(tetrafluoroethylene) 100 crystalline planes are parallel to the substrate.

(a)

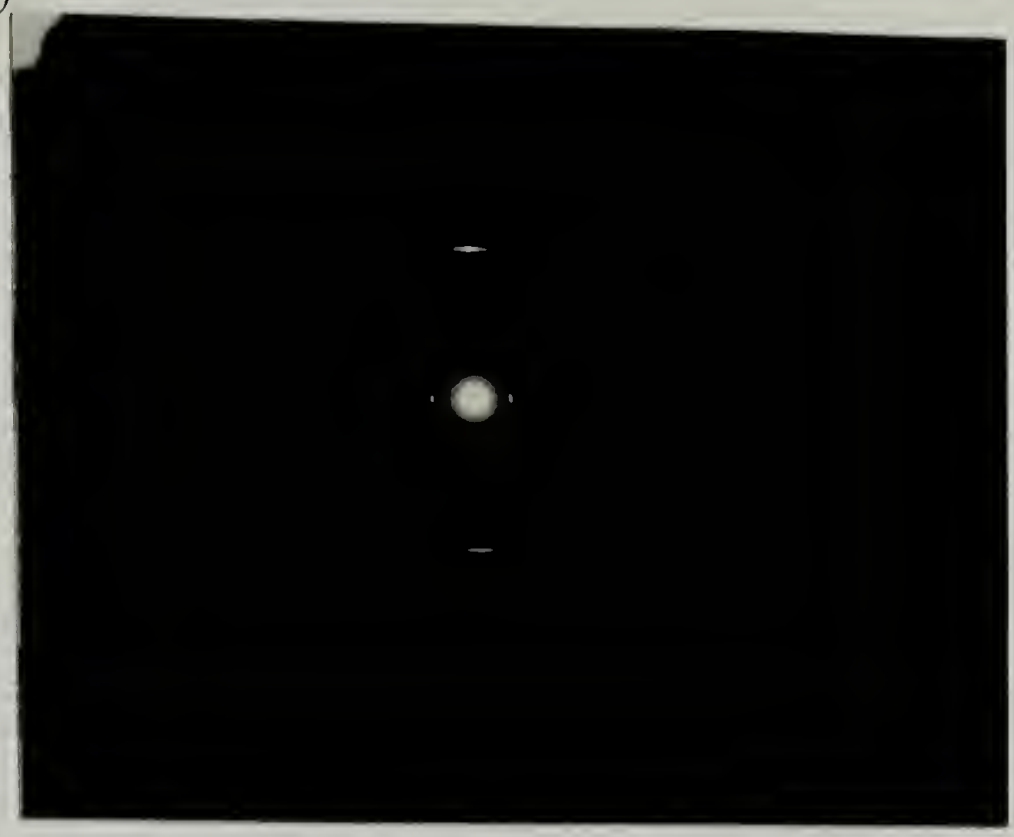

(b)

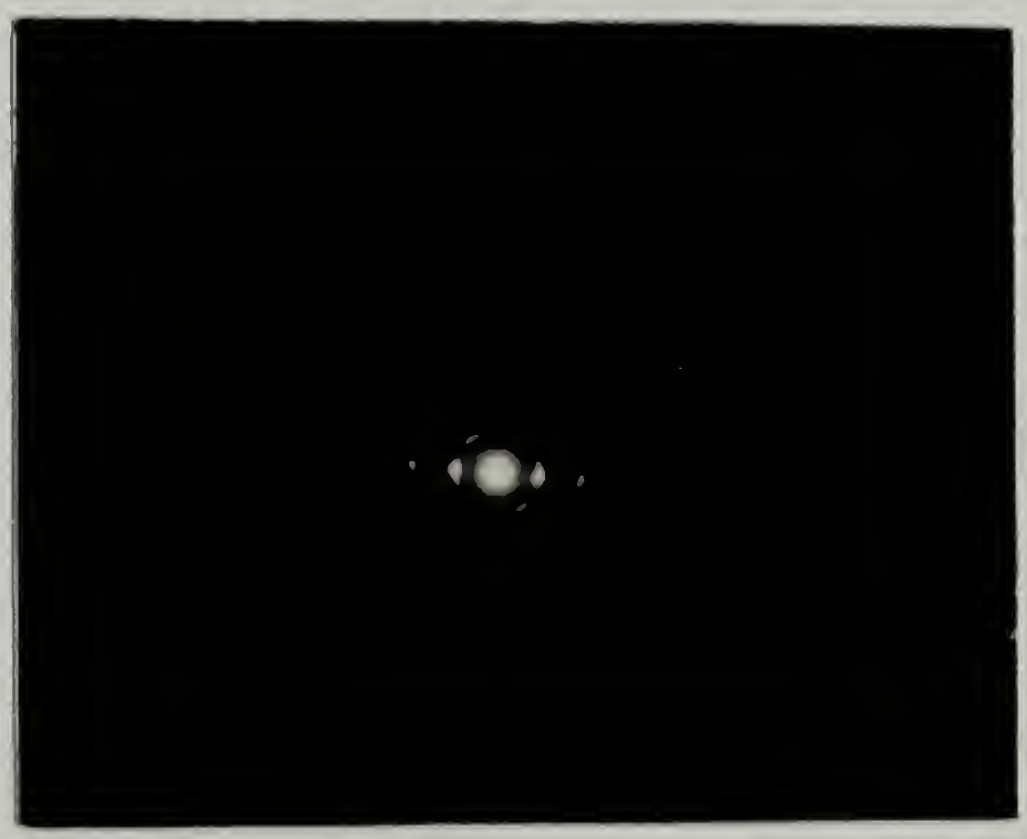

Figure 3.7 Electron diffraction patterns of the friction-deposited poly(tetrafluoroethylene) film. (a) Electron beam is normal to the film. (b) The sample is tilted around the rubbing direction.

3.3.2 Characterization of Silk Films

In order to describe quantitatively the amount of various crystallites formed, it is important to remove polarization characteristics of the spectra obtained. Therefore, the average of the two polarized spectra obtained for the incident polarization parallel and perpendicular to the rubbing direction is shown in Figure 3.8 for a silk film cast on an oriented poly(tetrafluoroethylene) substrate, and compared with isotropic silk films, e.g. films cast on glass slides or unoriented poly(tetrafluoroethylene). The isotropic films do not require this treatment since the individual polarized spectra are the same in all directions. Two polarized spectra obtained for the film cast from dilute solution (0.5 g/l) onto oriented poly(tetrafluoroethylene) surface shown in Figure 3.9 are used to calculate the average spectrum. The Amide I and II bands near 1650 and 1520 cm^{-1} exhibit multiple components. The Amide I band has a sharp maximum near 1623 cm^{-1} in all three spectra, and there are two more components at higher frequencies, near 1690 cm^{-1} (weak) and 1655 cm^{-1}. The Amide II band in the lower frequency region also has two principal components, a sharp feature centered at about 1522 cm^{1} and a broader weaker component near 1540 cm^{-1}. The Amide I and II vibrations at 1623 and 1522 cm^{-1} respectively have long been recognized as due to out-of-phase vibrations of adjacent amide groups involved in an antiparallel β pleated sheet, giving rise to a transition moment perpendicular to the chain direction.[24] The weak band at about 1690 cm^{-1} does not always occur in crystalline protein (it is missing in the spectrum of β-keratin), and was assigned by Miyazawa[24] as the Amide I vibration in which adjacent groups in antiparallel β pleated sheet move in phase with one another, giving rise to a transition moment parallel to the chain direction. The splitting between the in-phase and out-of-phase vibrations has been accounted by including a transition dipole coupling between adjacent groups.[24, 29-31] The Amide I and II bands at 1655 and 1540 cm^{-1} respectively are characteristic of disordered structures.

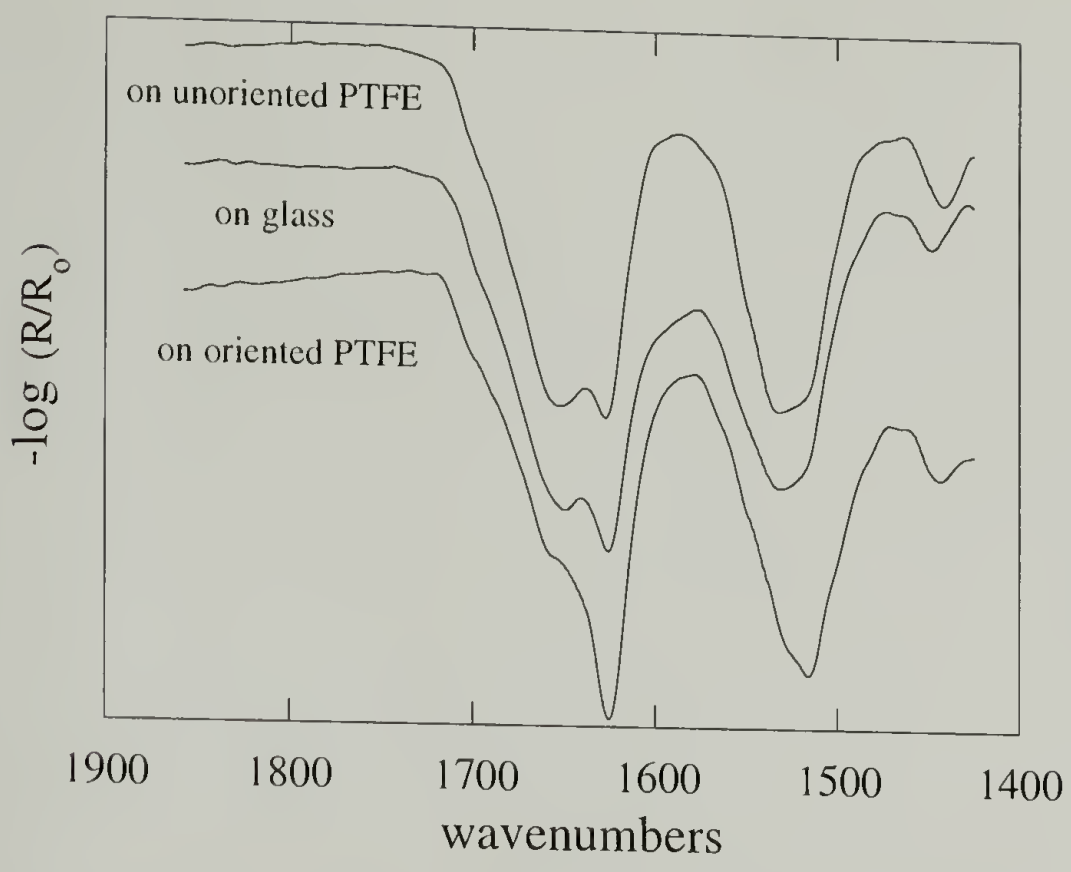

Figure 3.8 Reflectance infrared spectra of silk films cast from aqueous silk solution on different substrates.

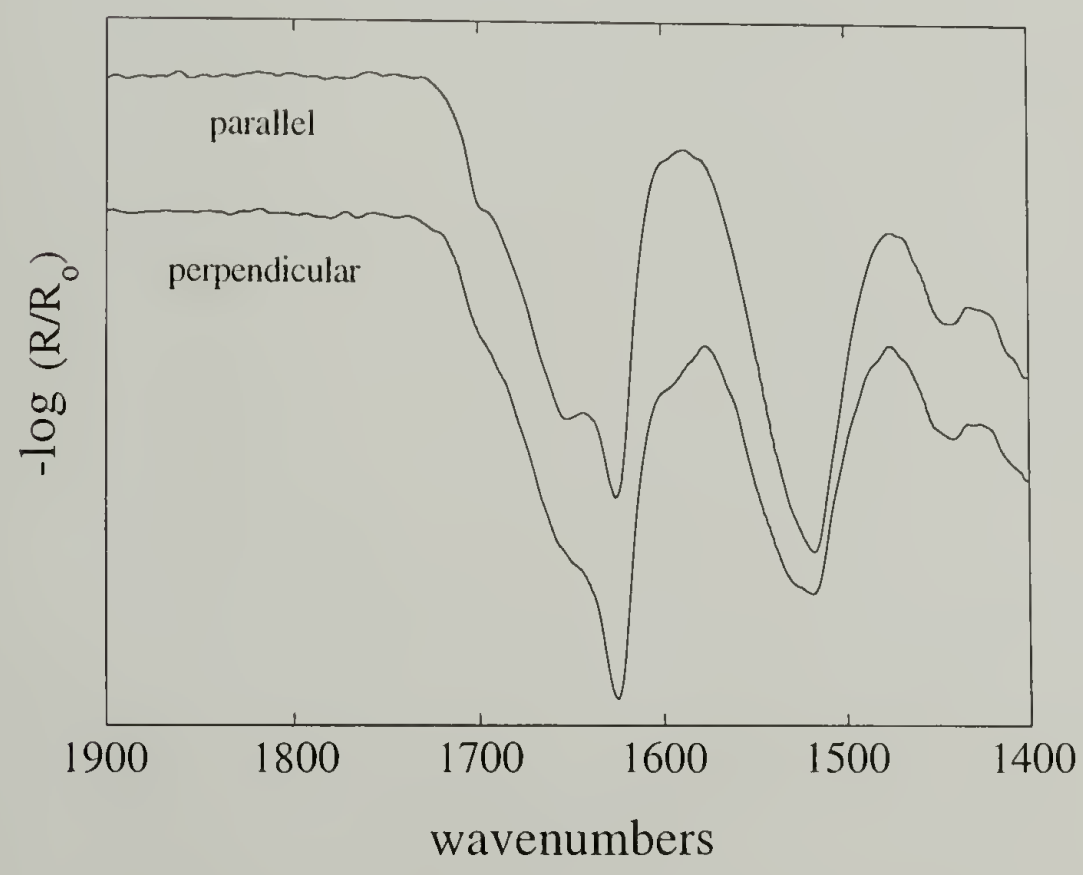

Figure 3.9 Reflectance infrared spectra of silk film cast from aqueous silk solution on oriented poly(tetrafluoroethylene) substrate, with the infrared beam polarized parallel and perpendicular to the rubbing direction.

Film cast on oriented poly(tetrafluoroethylene) substrate has a larger crystalline (silk II) content. Band deconvolution suggested that the amount of silk II structure in the film cast on oriented poly(tetrafluoroethylene) is about 55% (based on band area), while that for the film cast on glass is only about 30%. All samples contained a significant amount of disordered structure. Magoshi, et al.[5]found that films cast from solutions with concentrations less than 3% have predominantly disordered structures. The amount of disordered structure is a little larger in the film cast onto an unoriented poly(tetrafluoroethylene) surface than onto glass, consistent with the observation of Magoshi, et al.[5], that silk films cast on hydrophobic substrates have more disordered structure than films cast on hydrophilic substrates.

Polarized external reflectance infrared spectra obtained for films cast from dilute aqueous solution (0.5 g/l) onto oriented poly(tetrafluoroethylene) film are shown in Figure 3.9. The relative intensities are quite different for the two polarizations. The 1623 cm^{-1} band has the highest intensity when the rubbing direction is perpendicular to the infrared beam polarization direction. This suggests that the silk II structure has a preferred segmental orientation along the rubbing direction, i.e. parallel to the orientation of poly(tetrafluoroethylene) molecules. Deconvolution of the Amide I region shows the disordered band has much less dichroism.

Figure 3.10 compares the spectra obtained for three films cast from aqueous LiBr/silk solution on oriented poly(tetrafluoroethylene) substrate, on unoriented poly(tetrafluoroethylene) and on glass respectively. For each of these three spectra, the most intense band is broad and centered at 1630 cm^{-1}, some 5-7 cm^{-1} higher than the most intense band in the spectrum of film cast from salt-free solution. The band broadness indicates silk II crystallization with a wider distribution of chain conformation in the film cast from LiBr solution. Besides, all three samples shown in Figure 3.10 also have a broad band at 1660 cm^{-1}. This band is diagnostic for disordered chain conformations, and

entirely dominates the spectra of the films cast on the isotropic substrates like unoriented poly(tetrafluoroethylene) and on glass. Band deconvolution suggests that the film cast from LiBr solution on oriented poly(tetrafluoroethylene) substrate has about 51% β-chain conformation for silk II structure, quite close to the amount of silk II obtained from salt-free silk solution. It can also be found that the broad Amide II band maxima are at 1530-1540 cm^{-1} for the different samples. The lower frequency is found for the sample with the highest crystallinity, the higher for the samples with less crystallinity. These results show that the oriented poly(tetrafluoroethylene) surface has the ability to nucleate the silk II structure for films cast from LiBr solution, even though silk fibroin molecules assume a more contracted and disordered conformation than found in salt-free solution.[32] Furthermore, similar to the previous case where the films were cast from salt-free silk solution, the film cast on the hydrophobic surface, i.e., the isotropic poly(tetrafluoroethylene) surface has a little more disordered structure than that in the film cast on the hydrophilic glass surface.

The polarized spectra of the film cast from aqueous LiBr/silk solution on oriented poly(tetrafluoroethylene) substrate are shown in parallel and perpendicular polarization in Figure 3.11. Comparison of Figures 3.9 and 3.11 shows an especially interesting phenomenon. In Figure 3.9, for the film cast from salt-free silk solution, the greatest intensity of the 1623 cm^{-1} band is found when the electric vector of the incident infrared light is oriented perpendicular to the rubbing direction of the oriented poly(tetrafluoroethylene), indicating that the preferred segmental orientation is parallel to the rubbing direction. On the other hand, in Figure 3.11, the greatest intensity of the 1630 cm^{-1} band occurs when the orientation is parallel. Apparently, the crystalline segmental orientation of the film cast from salt-free solution is orthogonal to that of the film obtained from salt solution, a startling result.

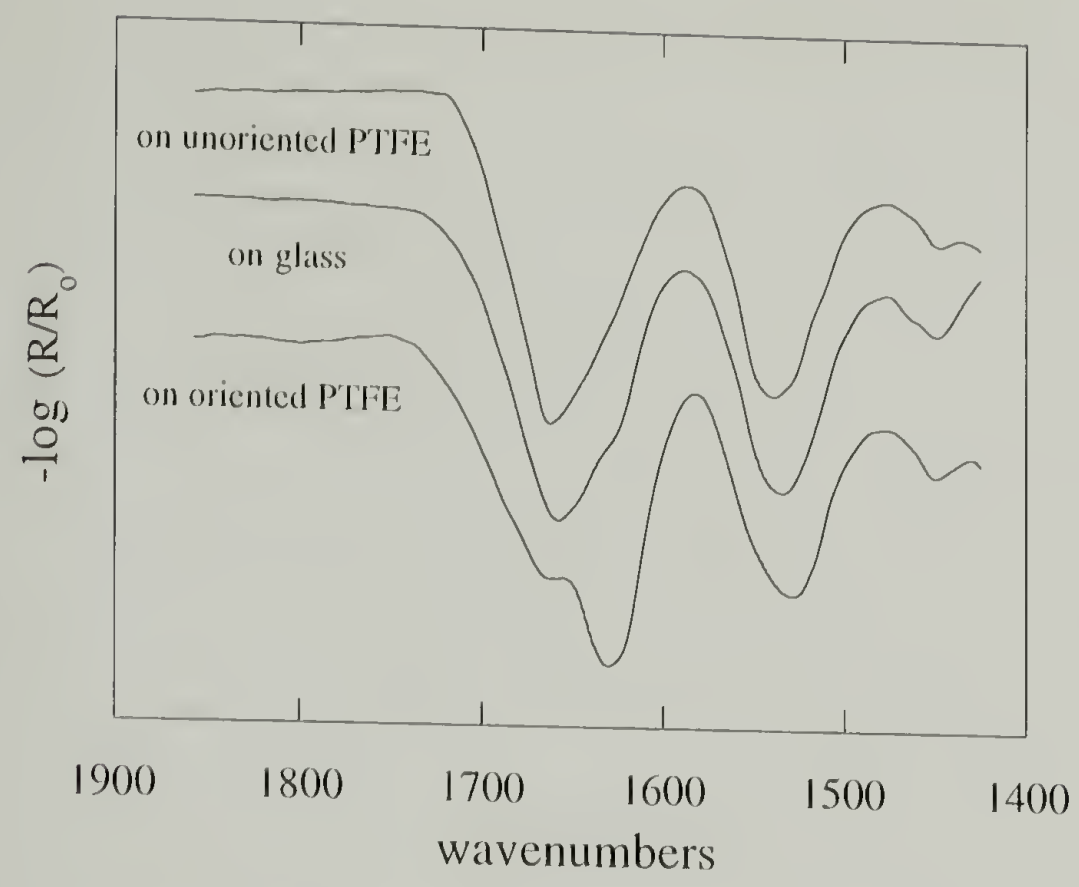

Figure 3.10 Reflectance infrared spectra of silk films cast from aqueous LiBr/silk solution on different substrates.

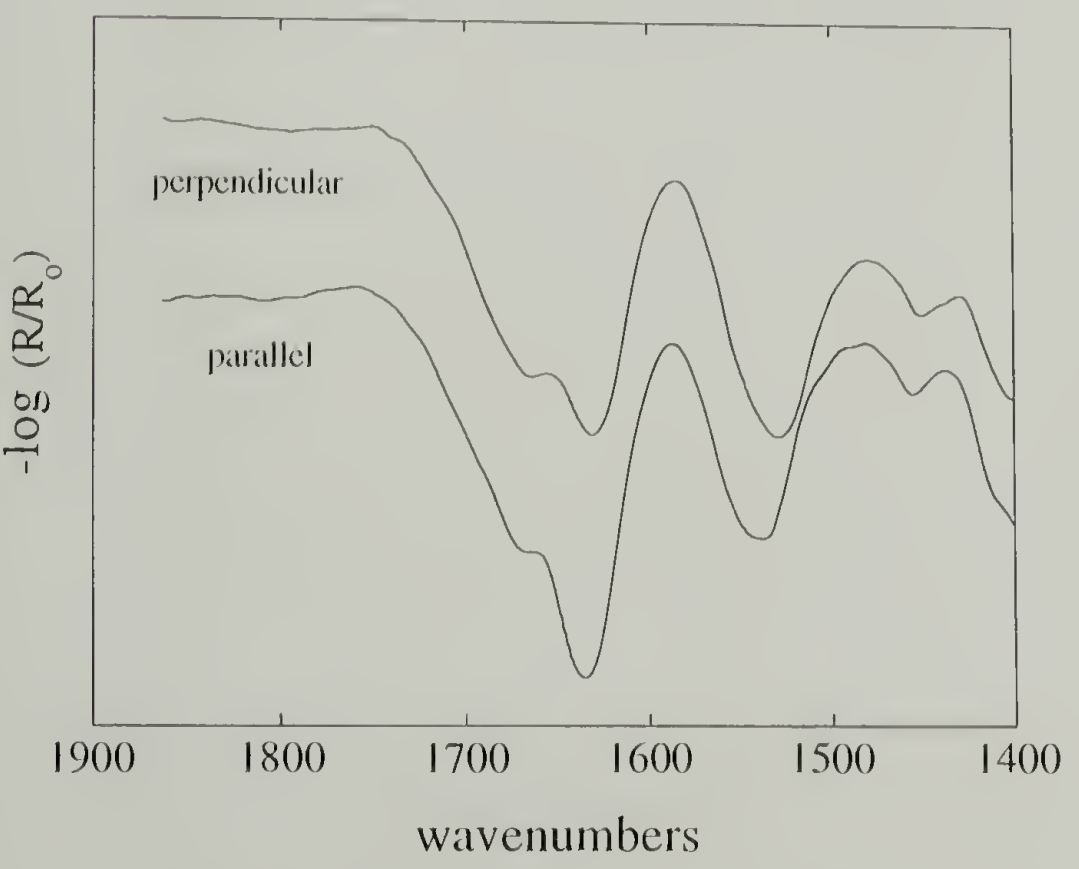

Figure 3.11 Reflectance infrared spectra of silk film cast from aqueous LiBr/silk solution on oriented poly(tetrafluoroethylene) surface, with the infrared beam polarized parallel and perpendicular to the rubbing direction.

The mechanism for the enhanced crystallization of specific forms of silk II on oriented poly(tetrafluoroethylene) is not entirely clear. Epitaxial crystallization might explain the orientation in films cast from salt-free aqueous solution, since the mismatch between the intermolecular spacing (or atomic spacing along the chain axis) of poly(tetrafluoroethylene) and that of silk fibroin molecules is only about 11%, within the usually accepted range of spacing mismatches that allows epitaxial crystallization.[33] Takahashi[34] attributed the alignment tendency of Nylon 6, polyethylene, or polycaprolactone crystals grown from the melt on drawn poly(tetrafluoroethylene) to epitaxial crystallographic interaction with similarity of atomic spacing along the chain axes of deposit and substrate polymers. The surface topography may provide another possible mechanism. The surface shows hollow ditches aligned with the rubbing direction, with lateral dimension varying from less than 5 nm to more than 1μm.[16] Polymer molecules adsorbed in these ditches perhaps can be forced to assume a stretched conformation over some distance, possibly facilitating nucleation of the silk II structure.[35]

It is possible that in films deposited from LiBr solution the chain conformation is distorted by interaction of the peptide groups with Li^+ ions. The distortion of the transition dipole coupling between adjacent peptide residues may cause a decrease in the band splittings in both the Amide I and II bands. In other words, these vibrations would move closer to the uncoupled vibrational states at higher frequencies.[36] Complex formation between lithium ions and amide groups in systems containing LiBr and polypeptides or simple amides has been proposed to explain the observed changes in vibrational spectra[36-40], and the explanation may apply here as well. Formation of a new crystallographic structure as a result of interaction with the salt for fibrous proteins immersed in high concentration of LiBr aqueous solutions has also been postulated.[40] Infrared spectral shifts in Amide I and II regions similar to the present study were also observed for nylon 6 inorganic salt mixtures.[41]

The unexpected orientation observed for the LiBr-silk crystals formed on the oriented poly(tetrafluoroethylene) film cannot be explained easily. It is clear that cross β crystals can form in polypeptides and silk[32,42,43] In those cases, the extended polypeptide chain segments are oriented perpendicular to the fiber axis. Infrared spectra obtained for those samples show the C=O and NH bonds of the peptide group are aligned approximately along the direction of stroking. The diffraction spacing and infrared frequency measured for the amide vibrations are characteristic of the β structure. Possibly crystals of a complex with LiBr form from silk/LiBr solution that are then accommodated into the ditches associated with friction transferred poly(tetrafluoroethylene) film.[16] The different crystallization behavior of silk films cast from salt-free solution and LiBr containing solution in these ditches could be due to the fact that silk molecules in solution assume a more contracted conformation in the presence of high concentration of LiBr than in salt-free solution.[32] The more compact conformation would favor intramolecular interaction enhancing nucleation in the ditches with folded-chain structures oriented along the rubbing direction.

3.4 Conclusions

Highly oriented poly(tetrafluoroethylene) films were obtained by rubbing a poly(tetrafluoroethylene) block on glass slides under pressure and at a suitable temperature. Cast silk films from either aqueous silk solution or aqueous silk-LiBr solution on the oriented poly(tetrafluoroethylene) surface exhibit more silk II structure than those cast either on glass slides or on unoriented poly(tetrafluoroethylene) surfaces under the same conditions; The silk II crystals show preferred segmental orientation along or perpendicular to the oriented poly(tetrafluoroethylene) molecules, respectively. Therefore, oriented poly(tetrafluoroethylene) films can be used as templates to control the cast film structures and their orienting ability is ascribed to epitaxial lattice matching between substrate and

deposit polymers and also to the specific surface topography. However, the resultant spatial orientation of the deposited silk molecules may as well be determined by their molecular configuration in the solution.

References

(1) Dodd, J. W.; Holliday, P.; Parker, B. E. *Polymer* **1968**, *9*, 54.

(2) Murthy, N. S.; Stamm, M.; Sibilia, J. P.; Krimm, S. *Macromolecules* **1989**, *22*, 1261.

(3) Yakhnin, E. D.; Egorova, Y. V.; Evko, E. I.; Taubman, A. B.; Lukyanovich, V. M. *J. Crystal Growth* **1969**, *5*, 184.

(4) Magoshi, J.; Kamiyama, S.; Nakamura, S. In *the Proceedings of the 7th International Wool Textile Research Conference*; Tokyo, 1985; pp 337.

(5) Magoshi, J.; Magoshi, Y.; Nakamura, S. *J. Appl. Polym. Sci.: Appl. Polym. Symp.* **1985**, *41*, 187.

(6) Magoshi, J.; Magoshi, Y.; Nakamura, S. In *Silk Polymers*; D. Kaplan, W. W. Adams, B. Farmer and C. Viney, Ed.; American Chemical Society: Washington D. C., 1994; pp 292.

(7) Asakura, T.; Yoshimizu, H.; Kakizaki, M. *Biotech. Bioeng.* **1990**, *35*, 511.

(8) Ishida, M.; Asakura, T.; Yokoi, M.; Saito, H. *Macromolecules* **1990**, *23*, 88.

(9) Magoshi, J.; Mizuide, M.; Magoshi, Y.; Takahashi, K.; Kubo, H.; Nakamura, S. *J. Polym. Sci. Polym. Phys. Ed.* **1979**, *17*, 515.

(10) Magoshi, J.; Magoshi, Y.; Nakamura, S. *J. Polym. Sci. Polym. Phys. Ed.* **1981**, *19*, 185.

(11) Yamaura, K.; Okumura, Y.; Matsuzawa, S. *J. Macromol. Sci. -Phys.* **1982**, *B21*, 49.

(12) Iizuka, E. *J. Appl. Polym. Sci.: Appl. Polym. Symp.* **1985**, *41*, 173.

(13) Magoshi, J. *Polymer* **1977**, *18*, 643.

(14) Muller, W. S.; Samuelson, L. A.; Fossey, S. A.; Kaplan, D. In *Silk Polymers*; D. Kaplan, W. W. Adams, B. Farmer and C. Viney, Ed.; American Chemical Society: Washinton D. C., 1994; pp 342.

(15) Wittman, J. C.; Smith, P. *Nature* **1991**, *352*, 414.

(16) Hansma, H.; Motamedi, F.; Smith, P.; Hansma, P.; Wittman, J. C. *Polymer* **1992**, *33*, 647.

(17) Fenwick, D.; Ihn, K. J.; Motamedi, F.; Wittman, J. C.; Smith, P. *J. Appl. Polym. Sci.* **1993**, *50*, 1151.

(18) Bamford, C. H.; Elliot, A.; Hanby, W. E. *Synthetic Polypeptides: Preparation, Structure and Properties;* Academic Press: New York, 1956, Chapt. 12.

(19) Motamedi, F.; Ihn, K. J.; Fenwick, D.; Wittmann, J.-C.; Smith, P. *J. Polym. Sci. Polym. Phys. Ed.* **1994**, *32*, 453.

(20) Ren, Y. Ph. D. Thesis, U. Massachusetts, 1995.

(21) Masetti, G.; Cabassi, F.; Morelli, G.; Zerbi, G. *Macromolecules* **1973**, *6*, 700.

(22) Zerbi, G.; Sacchi, M. *Macromolecules* **1973**, *6*, 692.

(23) Ayub, Z. H.; Arai, M.; Hirabayashi, K. *Polymer* **1994**, *35*, 2197.

(24) Miyazawa, T.; Blout, E. R. *J. Am. Chem. Soc.* **1961**, *83*, 712.

(25) Davidson, T.; Gounder, R. N. In *Adhesion and Adsorption of Polymers*; L. H. Lee, Ed.; Plenum Press: New York, 1980; Vol. 12B; pp 775.

(26) Moynihan, R. E. *J. Am. Chem. Soc.* **1959**, *81*, 1045.

(27) Bunn, C. W.; Howells, E. R. *Nature* **1954**, *174*, 549.

(28) Sperati, C. A.; Starkweather, H. W. *Adv. Polym. Sci.* **1961**, *2*, 465.

(29) Miyazawa, T. *J. Chem. Phys.* **1960**, *32*, 1647.

(30) Moore, W. H.; Krimm, S. *Biopolymers* **1976**, *15*, 2465.

(31) Abe, Y.; Krimm, S. *Biopolymers* **1972**, *11*, 1817.

(32) Iizuka, E.; Yang, J. T. *Biochemistry* **1968**, *7*, 2218.

(33) Wittmann, J. C.; Lotz, B. *J. Polym. Sci. Polym. Phys. Ed.* **1981**, *19*, 1837.

(34) Takahashi, T.; Teraoka, F.; Tsujimoto, I. *J. Macromol. Sci. -Phys.* **1976**, *B12*, 303.

(35) Binsbergen, F. L. *Polymer* **1970**, *11*, 253.

(36) Chirgadze, Y. N.; Shestopalov, B. V.; Venyaminov, S. Y. *Biopolymers* **1973**, *12*, 1337.

(37) Baddiel, C. B.; Chaudhuri, D.; Stace, B. C. *Biopolymers* **1971**, *10*, 1169.

(38) Balasubramanian, D.; Shaikh, R. *Biopolymers* **1973**, *12*, 1639.

(39) Kurtz, J.; Harrington, W. F. *J. Mol. Biol.* **1966**, *17*, 440.

(40) Mandelkern, L.; Halpin, J. C.; Diorio, A. F.; Posner, A. S. *J. Am. Chem. Soc.* **1962**, *84*, 1383.

(41) Kim, H.; Harget, P. J. *J. Appl. Phys.* **1979**, *50*, 6072.

(42) Anderson, J. M.; Chen, H. H.; Rippon, W. B.; Walton, A. G. *J. Mol. Biol.* **1972**, *67*, 459.

(43) Bradbury, E. M.; Brown, L.; Downie, A. R.; Elliott, A.; Fraser, R. D. B.; Hanby, W. E.; McDonald, T. R. R. *J. Mol. Biol.* **1960**, *2*, 276.

CHAPTER 4

CHARACTERIZATION OF CRYSTALLIZATION FROM SOLUTION OF NYLONS ON HIGHLY ORIENTED SUBSTRATES

4.1 Introduction

In this chapter we will continue to investigate the effects of oriented substrate on the crystallization behavior of nylons from solution with focus mainly on the molecular arrangement in the nylon films. As described in Chapters 1and 3, peculiar molecular arrangements may be obtained in polymer films deposited on substrates depending on the casting conditions and the interaction between polymer and the substrate. In this work, nylons will be coagulated and crystallized by various nonsolvents from solution with the presence of the oriented substrate. The molecular arrangement of the resultant films will be examined. Effects from both casting conditions (nonsolvent) and the substrate are expected to be seen in the results.

Structure and its molecular arrangement of nylon films in relation to the substrates and casting conditions have been studied. Due to its polymorphism and anisotropy in structure (e.g. hydrogen bond direction vs. intersheet direction), a variety of effects may be expected. When a solution of nylon 6 in formic acid is spread on to the (100) faces of either sodium chloride or potassium bromide at 35°C, a film in γ-crystalline form is obtained with its polar amide groups preferrentially oriented perpendicular to the plane of the film. It is thought that a considerable interaction occurs between the substrate ions and the amide groups of the polymer in the formation of the γ-crystalline form.[1] On the other hand, epitaxial crystallization of polyamides cast from m-cresol solution on to (001)

potassium chloride faces has also been found. Nylon 6 in particular was found to crystallize in the α-form with the hydrogen bonded sheets parallel to the substrate under these conditions.[2] Therefore, it should be noted the way that nylon 6 (and probably other nylon family) deposits and crystallizes on a substrate is strongly dependent on the nature of the exposed faces of the substrate and also on the casting conditions. Furthermore, when a solution of nylon 66 in formic acid or m-cresol is spread on glass or water surface, it is found that the molecules and the planes containing the hydrogen bonds tend to lie in the film plane.[3] However, recently a monolayer study on nylon 66 spread on air-water interface from a mixture of benzene and phenol indicates that the carbonyl groups tend to be vertical to the interface.[4] These examples again demonstrate the important effects of casting conditions and casting substrates on the structure of the resultant films.

The process of dissolution of a selected polymer in a solvent and subsequent precipitation of the polymer by a non-solvent under controlled conditions has been widely used in manufacturing microporous phase-inversion membranes and wet-spinning fibers. It should be noted that the coagulation process itself can also profoundly influence the molecular arrangement and also morphology in the films or membranes. Different molecular arrangement in the film of poly(p-phenylene terephthalamide) (PPTA) which is a very stiff polyamide, coagulated from sulfuric acid on glass, have been found to result from using different nonsolvents.[5] When water is used as the coagulant, the hydrogen bonded sheets and hydrogen bonds are perpendicular to the film surface. However, if other nonsolvents like methanol, ethanol or acetone is used, the hydrogen bonds and the hydrogen bonded sheets are parallel to the film surface. These results are explained on the basis of different hydrogen bonding capacity among these nonsolvents.[5] The most interesting case is the coagulation process described by Pall to prepare a nylon 66 membrane with water wettability.[6,7] This is special because nylon 66 resin as normally used (e.g. injection molded or extruded) has a critical surface tension of about 42 to 46 dyn cm^{-1}, and is thus not water wetted (the corresponding value for water is 74 dyn cm^{-1}).[6]

The reason for the water wettability is still not entirely clear. It could be due to the mode of crystallization during the membrane formation, with polar groups predominant at the pore surfaces.[6,7] Surface morphology and roughness have also been proposed to explain the wettability.[8] Whatever the case, phase separation may play an important role in determining the wettability of the resultant membranes and it may also have important implications in our study in terms of the resultant molecular arrangement on the substrate. Therefore, a brief introduction of the phase separation in the ternary system will be given next.

The mechanism of phase separation induced in the coagulation process depends on the thermodynamics of the ternary system. In Figure 4.1, the ternary phase diagram for water-formic acid-nylon 66 system at 25°C is given.[9] BC represents the crystallization line and DE the binodal line, the dashed lines being the tie lines. According to this phase diagram, a solution with composition located in ABC region will be a stable single phase. The region between the crystallization and binodal lines (i.e. BCDEF) is metastable only with respect to crystallization. Any composition in this region can only undergo precipitation by crystallization. It has been pointed out that a solution with such composition contains a significant amount of subcritical aggregates, so that the energy barrier to crystal nucleation after addition of nonsolvent is very low.[7,10] There are reports that the aforementioned nylon membranes with water wettability can be obtained only when phase separation is dominated by crystallization directly from the ternary system.[7,10,11] In the region inside the binodal envelop (region DEG), the system is metastable with respect to both liquid-liquid phase separation (unstable within the spinodal) and crystallization. As a result, both types of phase transformation are expected in this region. Usually the liquid-liquid phase separation process is favored if the solution is quenched by a pure nonsolvent. On the other hand, crystallization process will dominate if a mixture of solvent and nonsolvent is used as the coagulant. When liquid-liquid phase separation occurs, it has been observed that droplets of solvent and high concentration nonsolvent mixture are

dispersed in the solvent/polymer phase, with most polymer molecules in amorphous state distributing themselves around the droplets and later crystallization occurring at these sites.[12]

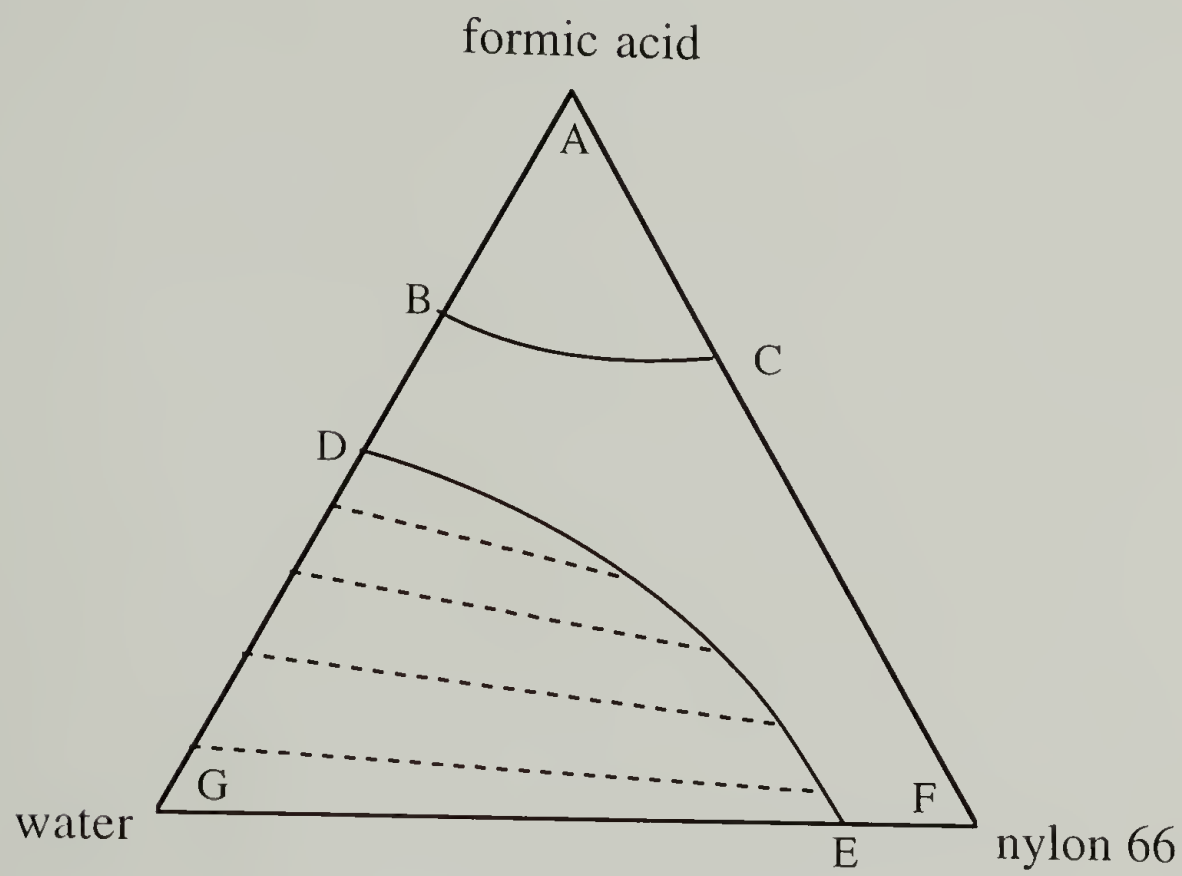

Figiure 4.1. Ternary phase diagram for water-formic acid-nylon 66 system at 25°C (from reference 9).

In this work, the resultant molecular arrangement of both nylon 6 and nylon 66 deposited on the oriented poly(tetrafluoroethylene) substrate from their dilute solutions will also be characterized and compared. Unexpectedly, differences in molecular arrangement between these two nylons are indeed observed. These differences may have implications about the formation of a water-wettable polyamide membranes. Explanations based on their phase separation behavior will be proposed.

4.2 Experimental Section

Nylon 6 (M_V=24,600) and nylon 66 (M_V=35,000) were purchased from Aldrich in pellet form. Their intrinsic viscosity was measured with a Ubbelohde viscometer at 29°C in a 90 wt% formic acid aqueous solution. The Mark-Houwink constants for molecular weight calculations are $k=22.6 \times 10^{-3}$ (ml/g), a=0.82 for nylon 6; and $k=35.3 \times 10^{-3}$ (ml/g), a=0.786 for nylon 66.[13] Nylon solutions in 90 wt% formic acid with a 0.1 wt% starting concentration were prepared and vigorously stirred for 24 hours before they were used in the coagulation experiment. The preparation procedures for oriented poly(tetrafluoroethylene) films are as described in Chapter 3. An oriented poly(tetrafluoroethylene) film was prepared accordingly and then placed floating on top of the nylon solution. Nonsolvent vapor was then introduced into the solution at room temperature to slowly change the solvent quaity. It normally took 2-3 days to observe precipitation of nylon in the bulk solution, depending on the nonsolvents. The nonsolvents used in this work included water, methanol and ethanol, with using water having taken the longest time. Precipitation of nylon 6 or nylon 66 were observed to occur not only on the oriented substrate but also on air-solution interface, in the solution and on the glass container's wall.

The nylon/poly(tetrafluoroethylene) composite film was then picked up from the solution surface and dried in air. Polarized infrared spectra of this film were obtained with a Perkin-Elmer 2000 FTIR spectrometer equipped with wide/narrow band MCT and DTGS detectors and a internal gold-grid polarizer. The sample was fixed in position while the internal polarizer was rotated to change the direction of the electric vector of the infrared beam. The corresponding wide angle X-ray diffraction (WAXD) patterns of the composite films were recorded on a Statton camera to characterize the spacial arrangement of nylon crystals on the substrate.

4.3 Results and Diseussion

4.3.1 Charaeterization of the Substrate

Although this substrate has been well eharaeterized by different teehniques in the previous chapter, it would be interesting to obtain its transmission infrared speetrum. For fluorinated compounds, there have been eonsiderable eontroversies regarding the band assignments of the 1100-1300 em^{-1} region in the infrared speetrum, mostly due to the problems of bands in this region being too intense. Normal eoordinate analysis on poly(tetrafluoroethylene) has led Liang and Krimm[14] to assign 1207 cm^{-1} band to CF_2 asymmetrieal stretehing with E_1 symmetry, and 1150 em^{-1} band to CF_2 symmetrieal stretehing also with E_1 symmetry. Sinee E_1 symmetry will give vibrations perpendieular to the chain axis for an infinitely long moleeule, both 1210 and 1150 em^{-1} bands are perpendieular bands in infrared speetrum. However, some other authors have assigned 1210 em^{-1} band to A_2 symmetry thus yielding a parallel polarization.[15-17] In this experiment the rubbing teehnique we used to prepare the poly(tetrafluoroethylene) thin film makes it possible for us to obtain its transmission infrared speetrum with absorbanee in linear range as shown in Figure 4.2. This offers us the opportunity to make unequivoeal assignments of the polarization eharaeteristies of the bands in the 1100-1300 em^{-1} region. Figure 4.2.a elearly indieates that both 1210 and 1150 em^{-1} bands are perpendieular bands and the weak shoulder at 1250 em^{-1} does not show dichroism. On the other hand, assignments of the bands in the low wavenumber region in the literature are more consistent.[14,16,18] Figure 4.2.b shows that the bands at 503 cm^{-1}, 624 em^{-1}, and 638 em^{-1} are parallel bands; the 553 em^{-1} band is a perpendieular one. It should be mentioned that the 1210, 1150, 638 and 553 em^{-1} bands have been assigned to a 15_7 helix eonformation, but the 624 cm^{-1} band has been assigned to be trans ehain eonformation.[16,18]

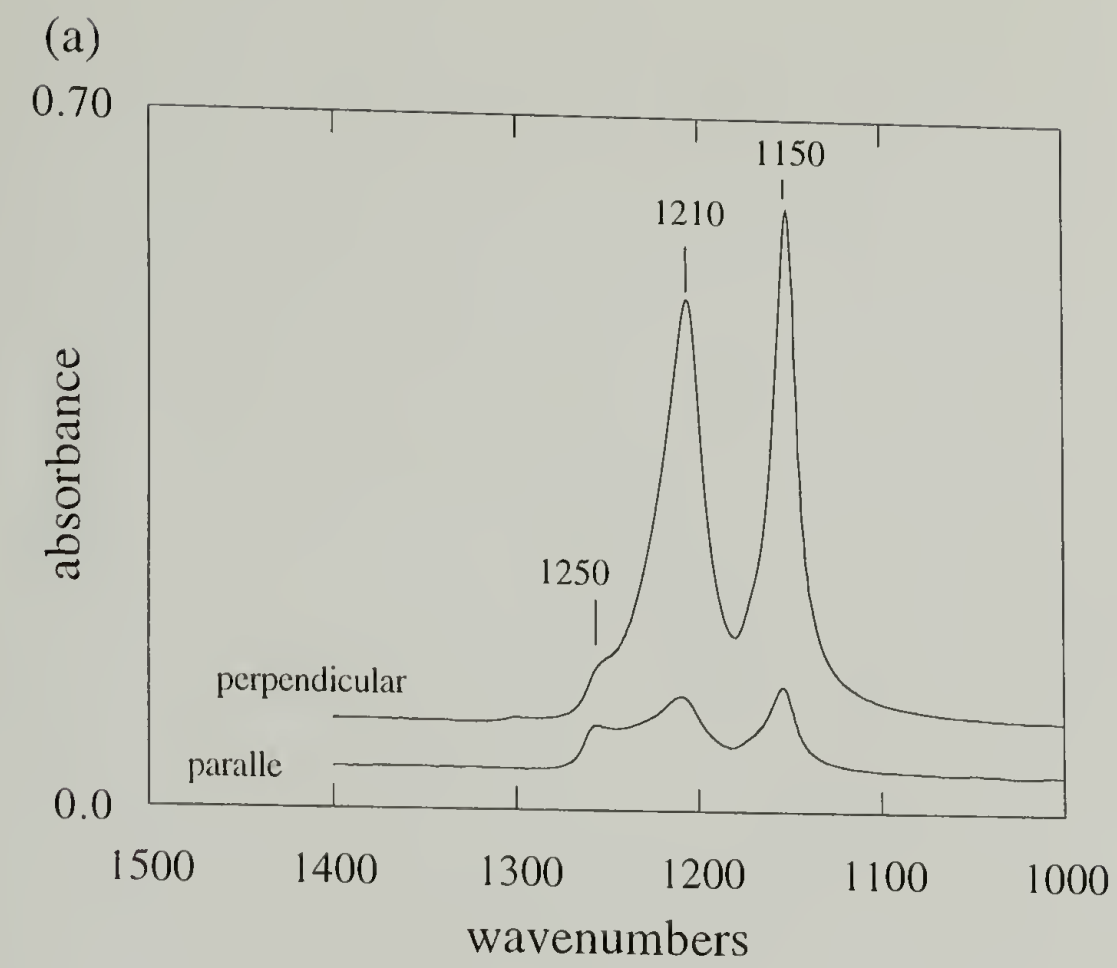

Figure 4.2. Polarized infrared spectra of the oriented poly(tetrafluoroethylene) film. Polarization is relative to the rubbing direction. (a) 1400-1000 cm^{-1} region. (b) 1000-450 cm^{-1} region.

4.3.2 Characterization of nylon films

Figure 4.3 shows the Amide I and II region of the polarized infrared spectra of nylon 6 deposited on oriented poly(tetrafluoroethylene) film from formic acid solution by using water vapor as the coagulant. The strong Amide I band at 1640 cm^{-1} shows perpendicular dichroism relative to the molecular axis of the poly(tetrafluoroethylene) substrate, and the Amide II band at 1545 cm^{-1} exhibits parallel dichroism. Their band positions also suggest an α-form crystalline chain conformation.[19] As pointed out in previous chapter that Amide I is a perpendicular band and Amide II band is a parallel band inherently, Figure 4.3 indicates that nylon 6 molecules are deposited on the oriented substrate in such a way that the chain axis is parallel to that of the poly(tetrafluoroethylene) substrate. The weak parallel Amide I band at 1666 cm^{-1} is a common feature among α-forms of nylon 2, 4, 6, 8, etc., with nylon 2 (polyglycine) having the strongest intensity.[20] It can be ascribed to the second infrared-active component resulting from the dipole moment (out-of-phase) coupling between antiparallel chains.[21,22] This assignment is supported by the absence of this band in the nylon 66 polarized spectra (shown later) since nylon 66 molecules do not have directionality and thus there is only one infrared-active Amide I band.[21,22] The polarization of this band is also in agreement with those of Amide I and II.

Two possible molecular arrangements of nylon 6 which will exhibit the polarized infrared spectra as shown in Figure 4.3 are uniaxial and uniplanar axial orientation. The latter orientation is frequently obtained in doubly oriented films which can be achieved by stretching and rolling.[19,23] The former orientation is normally found in drawn films. In both cases the chain axis of nylon 6 is parallel to that of the substrate. In the uniplanar axial case the hydrogen bonded sheets are parallel to the substrate surface. In the uniaxial case the sheets are cylindrically distributed around the chain axis. To distinguish these two cases, wide angle X-ray diffraction experiment was conducted.

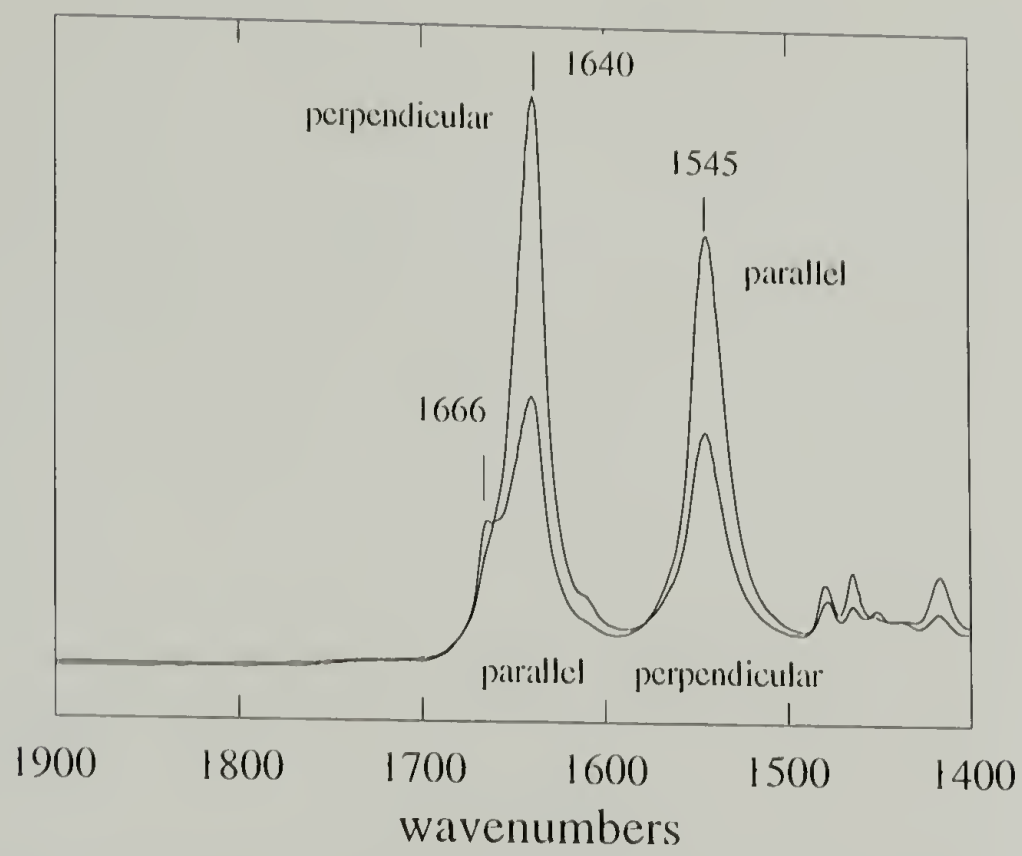

Figure 4.3 Polarized infrared spectra of nylon 6 deposited on oriented poly(tetrafluoroethylene) coagulated by water from formic acid solution. Polarization is relative to the rubbing direction.

The corresponding WAXD pattern are shown in Figure 4.4.a and Figure 4.4.b, which were obtained with the beam perpendicular to the film and the film tilted around the molecular axis respectively. The most intense and inner equatorial arches come from the intermolecular (010) or (100) reflection of poly(tetrafluoroethylene). With the X-ray beam perpendicular to the film, both (200) (hydrogen bonding direction) and (002+202) (intersheet spacing) reflection of nylon 6 are equatorial. But it is still not possible to make the distinction since both orientation will show the same pattern with such a experiment geometry. Therefore, the film was tilted around the chain axis. If the film has uniaxial orientation, such a change in geometry should not make any difference in the resultant pattern. On the other hand, if uniplanar axial orientation is the case, the tilt will produce a asymmetric effect in the pattern since one part of the given reflection is moved toward the Ewald sphere while the other is moved away from the sphere and consequently not observable. This is exactly what is observed in the pattern in Figure 4.4.b, where only one

(002+202) arc is seen. Therefore, we conclude that the α-form nylon 6 film deposited on the oriented poly(tetrafluoroethylene) substrate has a uniplanar-axial crystal texture, as illustrated in Figure 4.5.

(a)

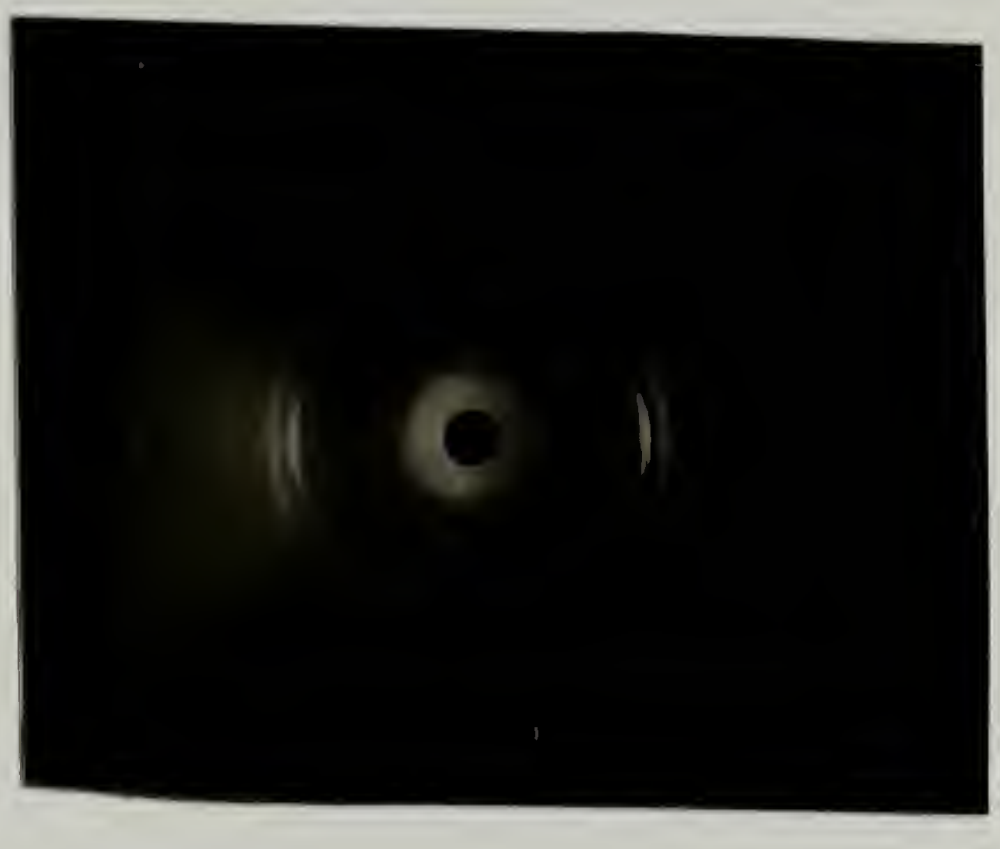

(b)

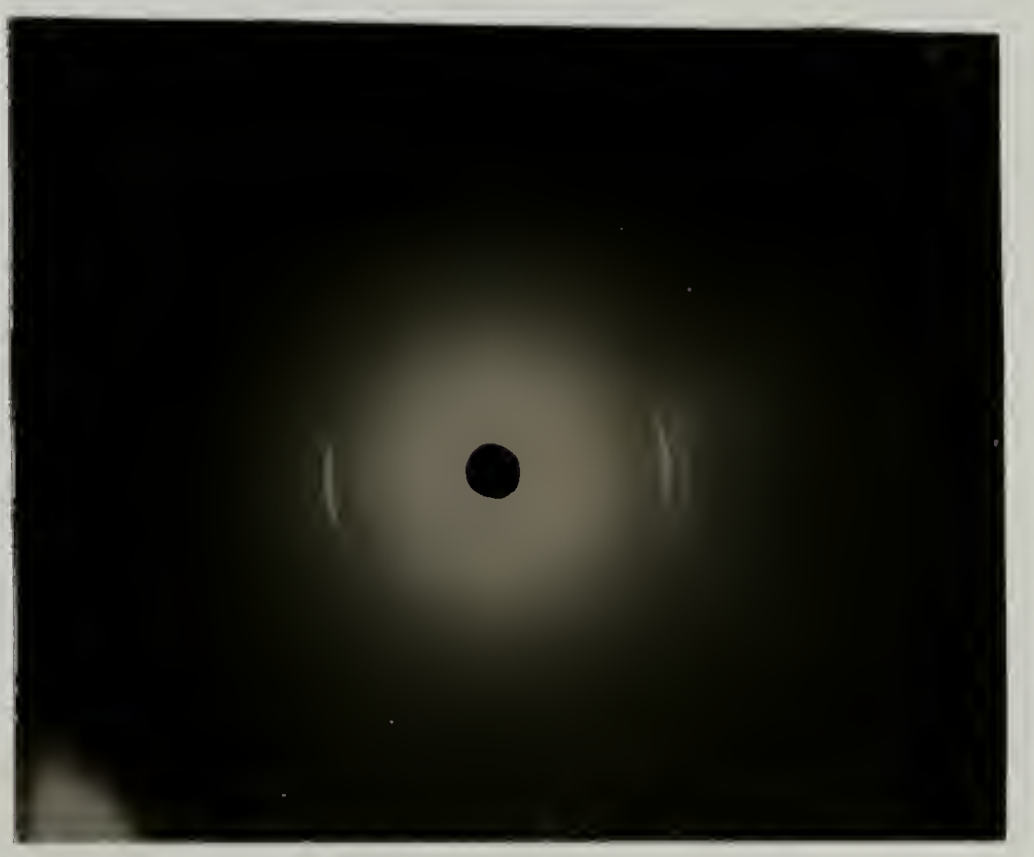

Figure 4.4 Wide angle X-ray diffraction patterns of nylon 6 deposited on oriented poly(tetrafluoroethylene) coagulated by water from formic acid solution. (a) X-ray beam is normal to the film. (b) The film is tilted about 30° around its molecular axis.

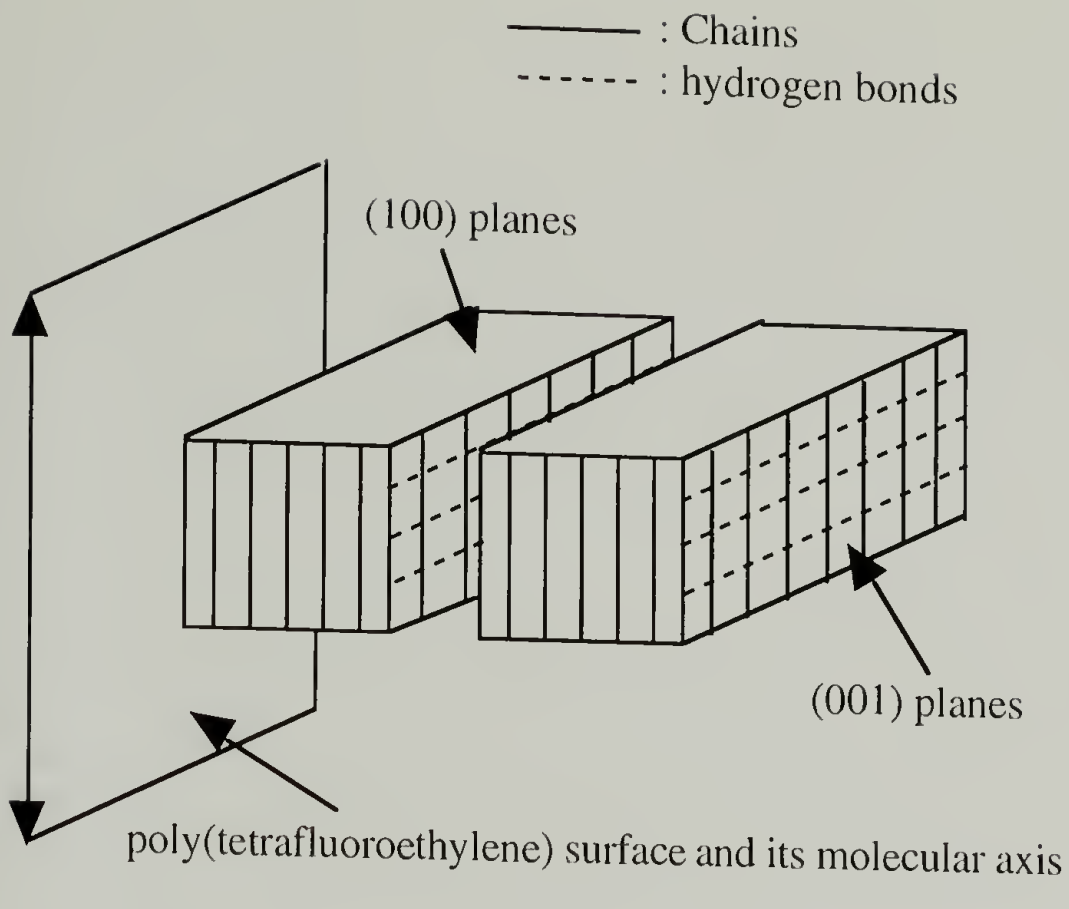

Figure 4.5 Schematic representation of the arrangement of nylon 6 crystals on the oriented poly(tetrafluoroethylene) substrate, corresponding to the sample in Figures 4.3 and 4.4.

The effect of non-solvents on the chain orientation of the nylon 6 film deposited on oriented poly(tetrafluoroethylene) substrate are shown in Figure 4.6 and Figure 4.7. As in the previous case of water as the non-solvent, using either methanol or ethanol results in films of α-form nylon 6 with their amide planes parallel to the substrate surface, preferred segmental orientation being also parallel to that of poly(tetrafluoroethylene) molecules. However, the degree of orientation is different among these three non-solvents, with the highest in the case of water and the least in ethanol case. This disparity in the degree of substrate-induced orientation could be due to the difference in crystallization rates of nylon 6 on the substrate when using various nonsolvents. It is well known that amide groups on nylon chains are protonated in protic solvents like formic acid and thus the solution exhibit polyelectrolyte properties with the nylon chains in the so called "extended coil" configuration.[24,25] For nucleation of nylon 6 crystallites to occur on the substrate,

deprotonation of the amide groups is required. This deprotonation process is favored by using nonsolvents like methanol and ethanol which have higher basicity than water. Therefore, it is assumed that when using coagulants like methanol or ethanol, the rates of deposition of polymer chains are faster; and consequently, the way they deposite on the substrate has less correlation with each other and with the molecular orientation or surface topography of the substrate.

This idea of explanation comes from the experiment where the film was obtained by coagulation with ethanol vapor from a formic acid solution containing 0.25 M salt(KCl). The corresponding polarized infrared spectra are shown in Figure 4.8. Compared with the previous figure, Figure 4.8 shows that higher degree of orientation is obtained by the addition of salts. It has been known that though nylon 6 (or nylon 66) is not soluble in alcohols at room temperature, it dissolves in mixture of alkali halide and alcohol due to the interaction of amide groups and salt/alcohol complex.[26,27] The result of this interaction is to change the role of the alcohol from that of a nonsolvent to that of a swelling agent and the deposition rate is thus decreased. This is indeed what is observed in our coagulation experiment that it takes longer for precipitation to occur when salt is added to the polymer solution. Therefore, the higher degree of orientation obtained by adding salts into the solution results from the better epitaxial correlation between the depositing polymer and the substrate, and also between two consecutive depositing layers of nylon 6 due to the slower deposition rate of the incoming layer of crystallites.

As a summary of this part of study regarding the orientation of nylon 6 on the oriented poly(tetrafluoroethylene) substrate, we found that the nylon 6 molecules lie on the substrate with their chain axis preferably aligned with that of the substrate. Besides, the degree of orientation of nylon 6 depends on the nonsolvents used as the coagulants, with water inducing the highest orientation and ethanol the least.

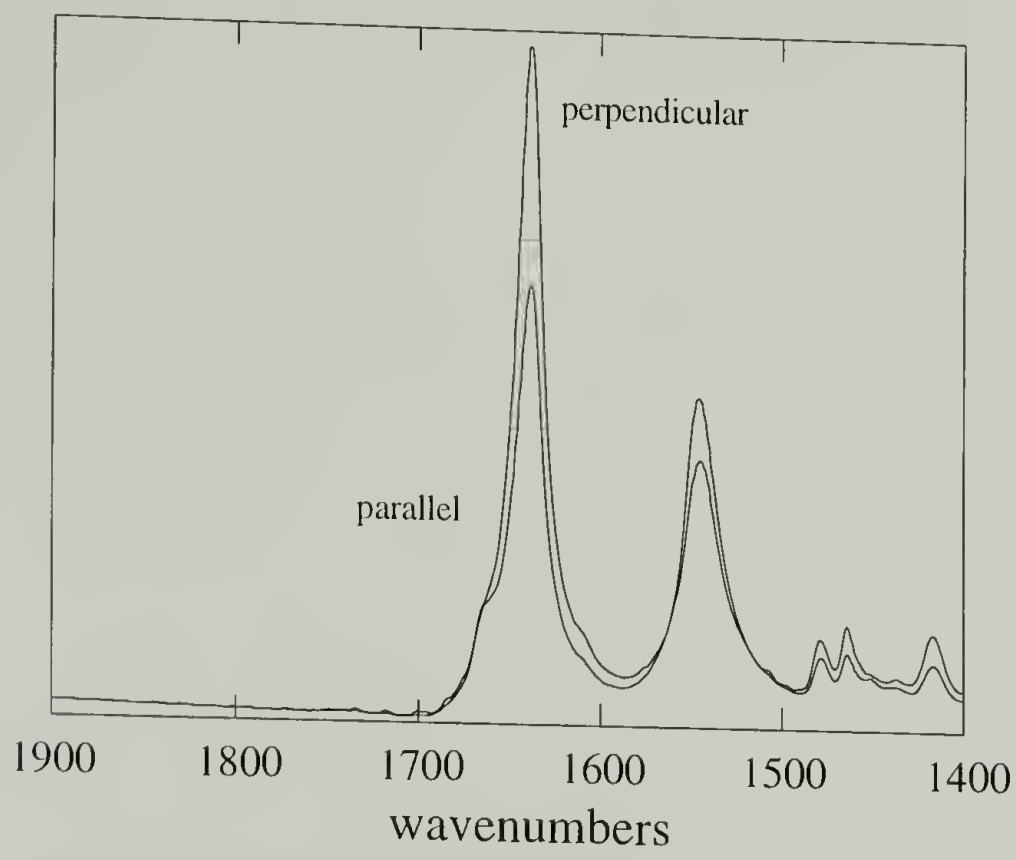

Figure 4.6 Polarized infrared spectra of nylon 6 deposited on oriented poly(tetrafluoroethylene) coagulated by methanol vapor from formic acid solution. Polarization is relative to the rubbing direction.

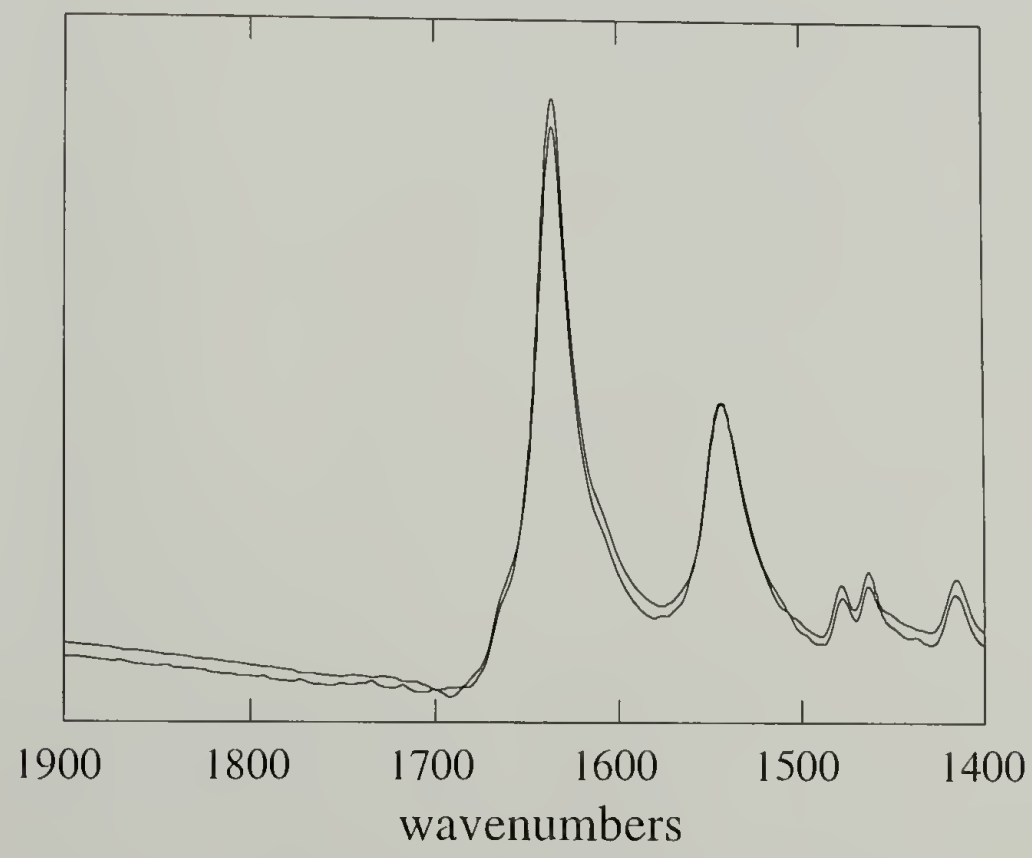

Figure 4.7 Polarized infrared spectra of nylon 6 deposited on oriented poly(tetrafluoroethylene) coagulated by ethanol vapor from formic acid solution.

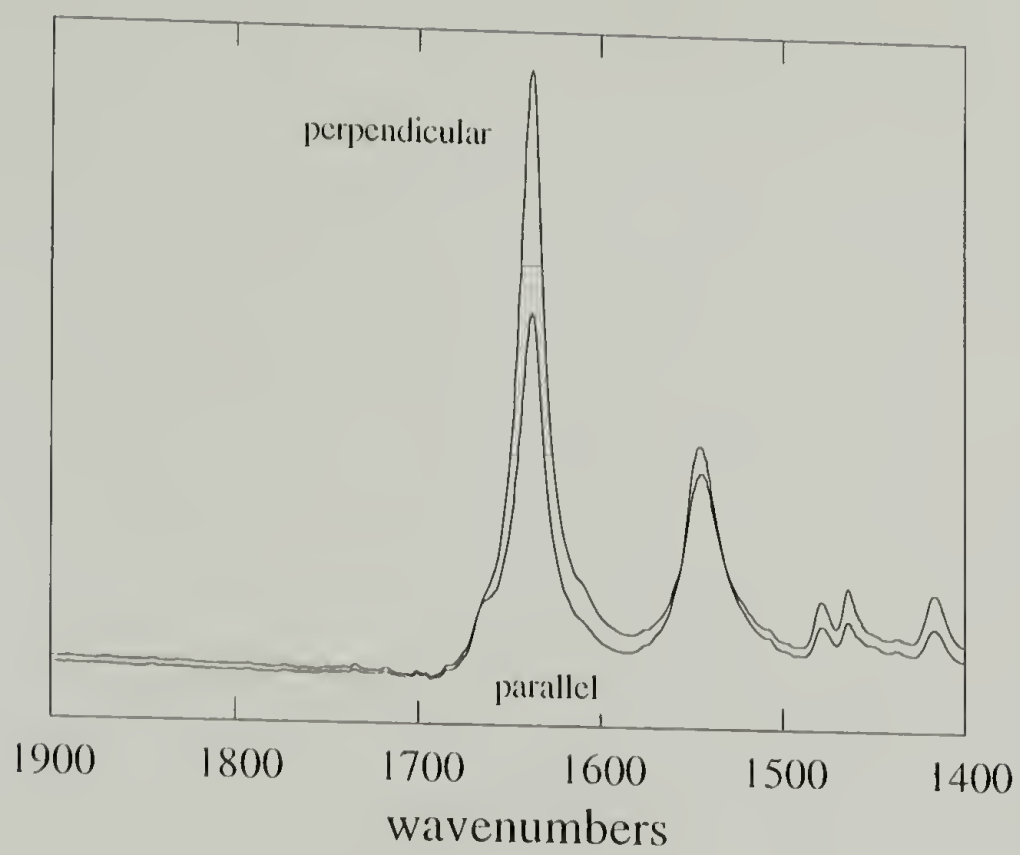

Figure 4.8 Polarized infrared spectra of nylon 6 deposited on oriented poly(tetrafluoroethylene) coagulated by ethanol vapor from formic acid/KCl solution. Polarization is relative to the rubbing direction.

The same experiments were also conducted with nylon 66 at the same concentration. In Figure 4.9 are shown the polarized infrared spectra of nylon 66 deposited on oriented poly(tetrafluoroethylene) substrate coagulated by water vapor from formic acid solution. There is only one Amide I band observed at 1634 cm^{-1} for nylon 66. This result confirms the previous assignment for the weak parallel Amide I band at 1666 cm^{-1} for nylon 6 to the dipole moment coupling between two antiparallel chains. Due to the symmetry of nylon 66 chains, only two amide groups from one chain needs to be considered. Therefore, there is no interchain coupling and thus only one infrared active band observed.[21,22] Compared with the Amide I band frequency of nylon 6 at 1640 cm^{-1}, the lower Amide I band frequency at 1634 cm^{-1} indicates stronger hydrogen bonding strength in nylon 66.

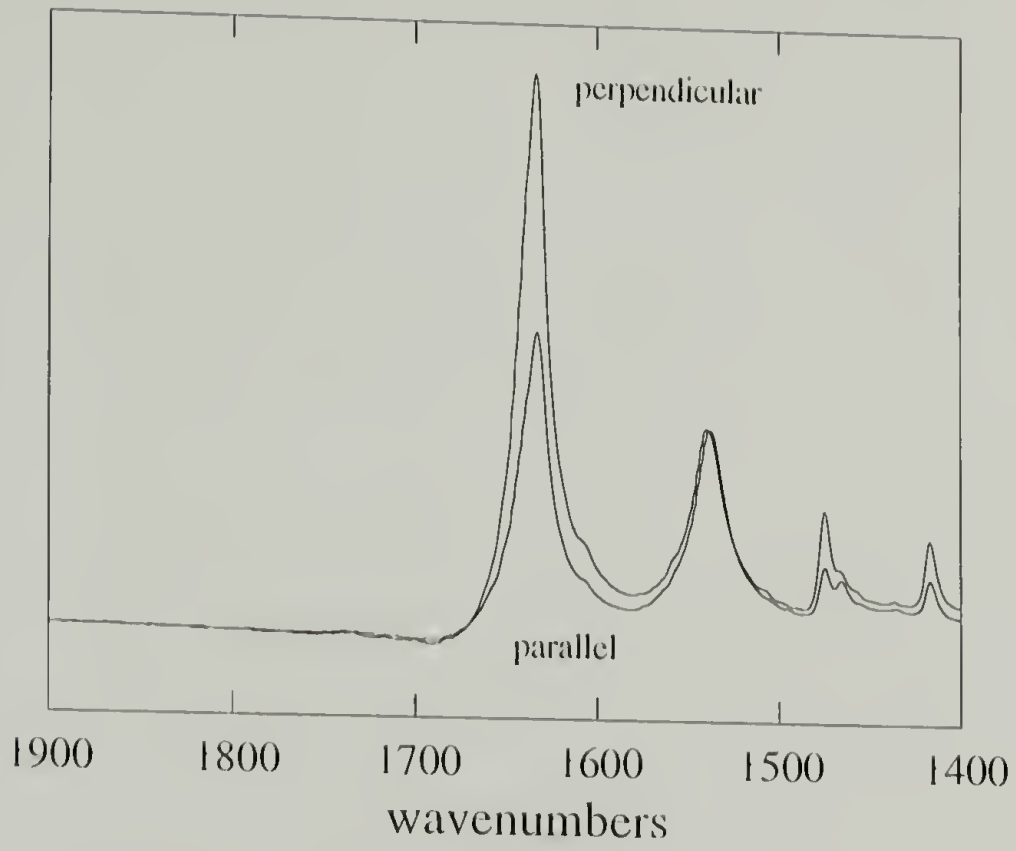

Figure 4.9 Polarized infrared spectra in Amide I and II region of nylon 66 deposited on oriented poly(tetrafluoroethylene) coagulated by water from formic acid solution. Polarization is relative to the rubbing direction.

Regarding the orientation relationship of the nylon 66 film with respect to the substrate, the results are quite unexpected. As can be seen in Figure 4.9, the Amide I band shows perpendicular dichroism; however, interestingly the Amide II band does not show the corresponding parallel dichroism as in the nylon 6 case shown in Figure 4.3 and exhibits a little perpendicular dichroism. This is an indication that the hydrogen-bonded amide planes are not parallel to that of the oriented poly(tetrafluoroethylene) substrate. Similar polarized spectra have been found in doubly oriented films of nylons.[19] We, therefore, also propose the same structure model as that in doubly oriented nylon films as illustrated in Figure 4.10. The nylon 66 film deposited on oriented poly(tetrafluoroethylene) substrate has such a morphology that the hydrogen bonding sheets are perpendicular to the substrate plane with the hydrogen bonding direction

perpendicular to that of the poly(tetrafluoroethylene) molecules; in other words, the nylon 66 molecules are preferably erect on the substrate. This is quite different from the orientation found in nylon 6 where the molecules lie on the substrate. This morphology is also similar to what is usually observed in crystal mats filtered from crystal suspensions with additional preferred orientation in hydrogen bonding direction. This picture gains further support from the dichroism of the Amide V band at 690 cm^{-1}, which has considerable contribution from out-of-plane deformation of N-H bond and thus inherently is a perpendicular band.[19,28] On the contrary, as shown in Figure 4.11 the Amide V band exhibits parallel dichroism relative to the chain axis of the substrate which is consistent with the proposed picture.

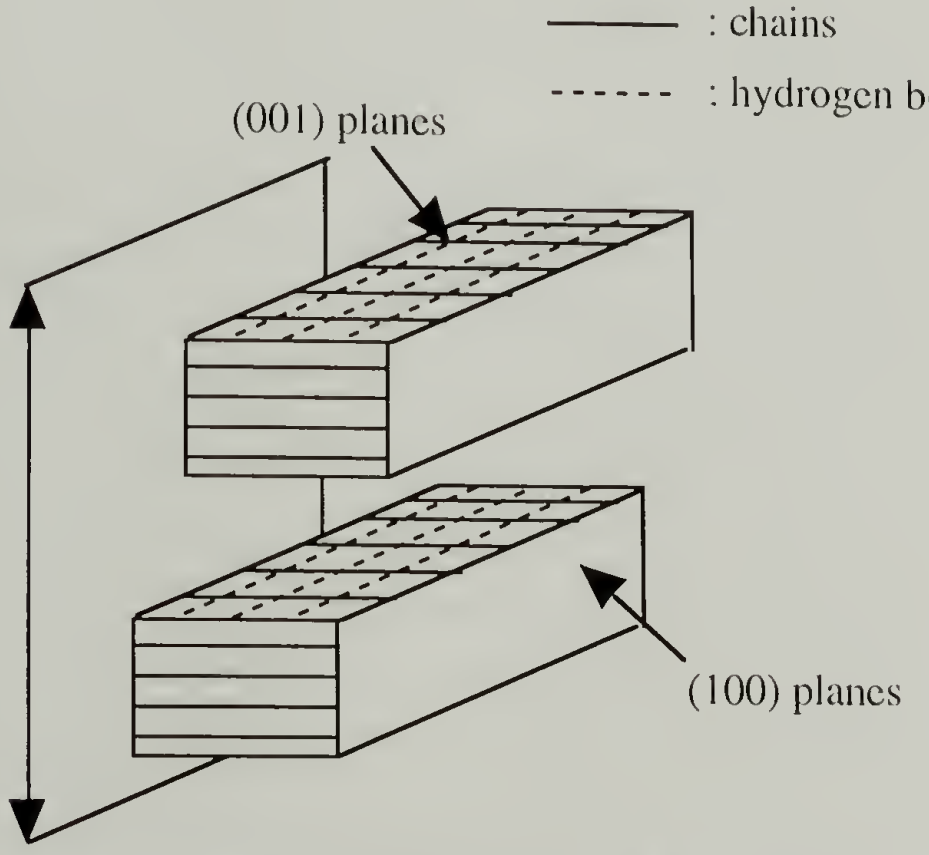

Figure 4.10 Schematic representation of the arrangement of nylon 66 crystals on the oriented poly(tetrafluoroethylene) substrate, corresponding to the sample in Figure 4.9.

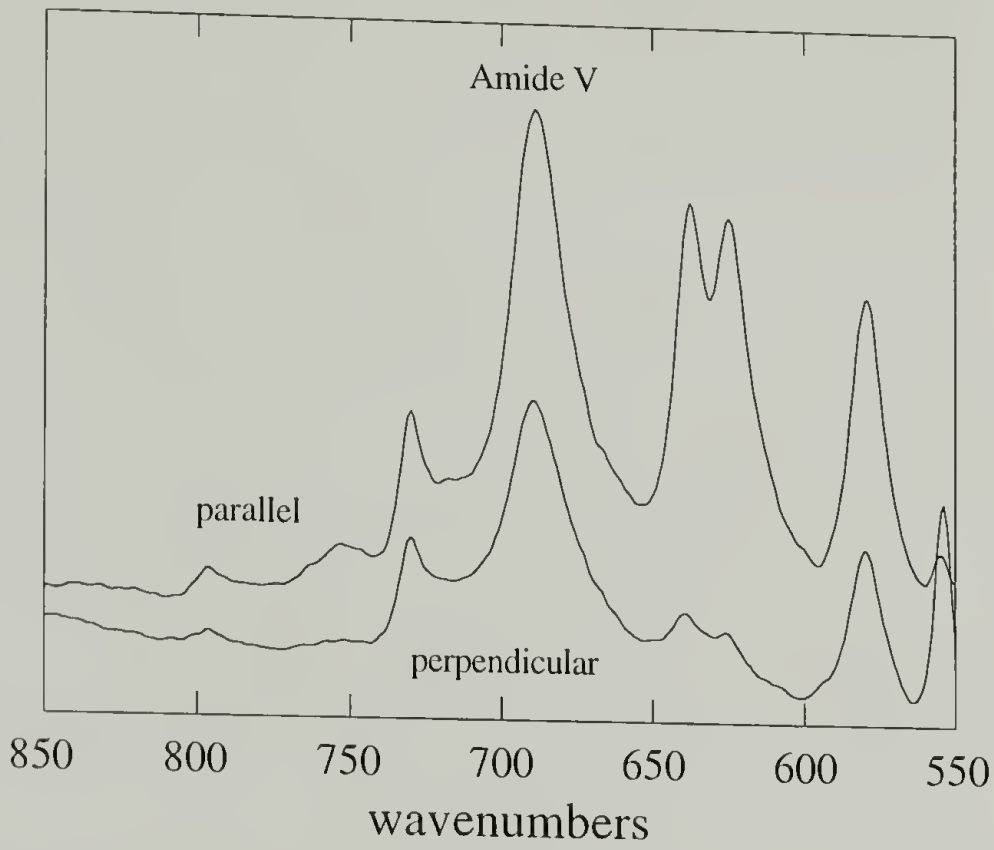

Figure 4.11 Polarized infrared spectra in Amide V region of nylon 66 deposited on oriented poly(tetrafluoroethylene) coagulated by water from formic acid solution. Polarization is relative to the rubbing direction.

The corresponding X-ray pattern for the nylon 66 film exhibiting the previous infrared spectra is shown in Figure 4.12. Again, the most intense and inner equatorial arches come from the intermolecular (010) or (100) reflection of poly(tetrafluoroethylene). However, the splittings in the reflections from nylon 66 crystals are quite different from those of nylon 6. The splittings of (100) reflection (from hydrogen bonds spacing) into four off-axis arches suggest a double orientation (uniplanar axial) among the hydrogen bonding sheets..[19] Furthermore, the meridian location of the weak (010+110) reflection (from spacing between hydrogen bonded sheets) establishes that the hydrogen bonding sheets are arranged as illustrated in Figure 4.11.

Figure 4.12 Wide angle X-ray diffraction patterns of nylon 66 deposited on oriented poly(tetrafluoroethylene) coagulated by water from formic acid solution. X-ray beam is normal to the film.

The effects of non-solvents on the orientation characteristics of nylon 66 on the oriented poly(tetrafluoroethylene) substrate are the same as observed in the case of nylon 6. Figure 4.13 and Figure 4.14 show that using different nonsolvents only affect the degree of orientation in the films but not the mode of orientation since only dichroism of Amide I band is observed. And again, the degree of orientation is the least when ethanol is used as the coagulant and the highest in the case of water. We again attribute this trend to the difference in deposition rates caused by these non-solvents since this is also confirmed with addition of salts to decrease the crystallization rate of the polymer on the substrate. However, the difference in orientation exhibited by nylon 6 and nylon 66 remains to be answered.

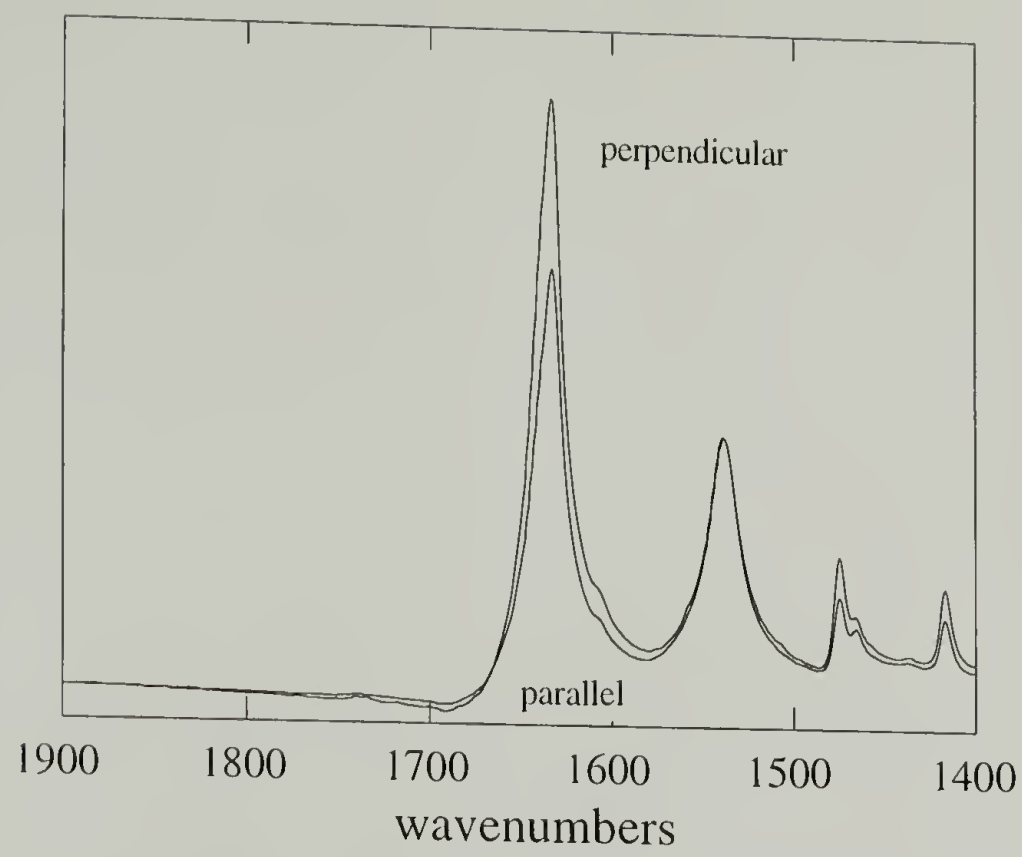

Figure 4.13 Polarized infrared spectra of nylon 66 deposited on oriented poly(tetrafluoroethylene) coagulated by methanol vapor from formic acid solution. Polarization is relative to the rubbing direction.

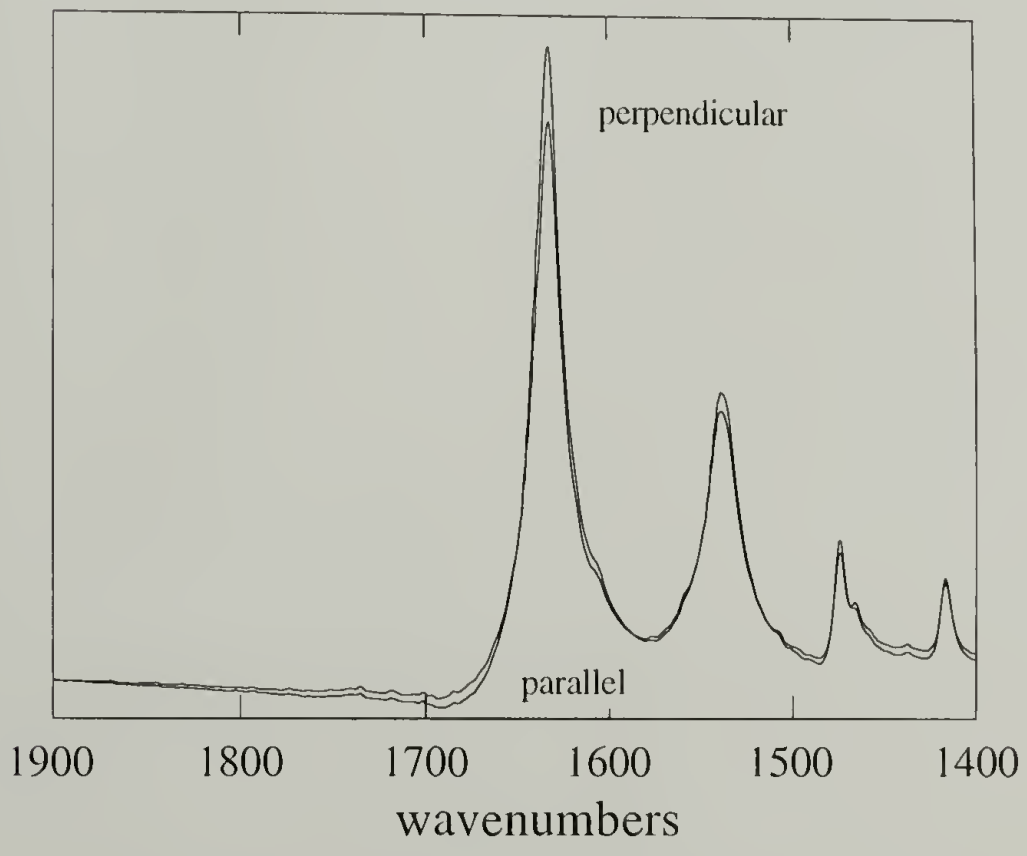

Figure 4.14 Polarized infrared spectra of nylon 66 deposited on oriented poly(tetrafluoroethylene) coagulated by ethanol vapor from formic acid solution. Polarization is relative to the rubbing direction.

A fundamental difference between nylon 6 and nylon 66 is that the latter crystallizes faster than the former.[29] This may be reflected in their phase diagram especially in the dilute polymer concentration region. In Figure 4.15, the corresponding ternary phase diagram for nylon 6 is illustrated.[9] It can be seen that in the low concentration region, the composition of the mixture could be easily changed into the binodal region (GDE) without staying in the crystallization-metastable region (BCDEF). Since our experiment is conducted in this low concentration region, the phase separation behavior is different when these two nylons are precipitated from the solution. Therefore, the molecular configurations of the nylons in the solution, which is at the point of incipient precipitation, are also different. In the case of liquid-liquid demixing (i.e. nylon 6), the polymer molecules are in amorphous form; on the other hand, in the case of demixing due to crystallization of nylon 66, the solution contains a large amount of segmental aggregates of subcritical size.[7,10] As we have shown in Chapter 3. the molecular configuration of the depositing polymer can determine the mode of deposition and thus the resultant spatial orientation. Consequently, the different phase separation behavior may as well be the underlying reason for the different molecular arrangements in these two nylon films deposited on the oriented substrate.

To be more certain of this explanation, we check the following question. If this conclusion is true, then we should be able to change the molecular arrangement in the film simply by changing the phase separation behavior. This is done by directly injecting nonsolvent into the polymer solution so that precipitation is quickly induced. This would have the effect of suppressing nucleation and thus crystallization of either nylon directly from the solution[10], since the starting polymer concentration does not allow much nucleation to occur on its own and besides deprotonation is required for nucleation, which takes longer induction time than liquid-liquid demixing.[10] Our expectation is confirmed. As shown in Figure 4.16, by this way of coagulation of nylon 66, we can obtain a nylon 66 film with the same orientation characteristics as nylon 6,i.e. both Amide I and Amide II

bands show dichroism, indicating that the amide planes preferrentially rest on the substrate plane. Therefore, the phase separation behavior and thus the configuration of the depositing entity is indeed the controlling factor of the resultant molecular arrangement on the substrate.

As was mentioned in the introduction section, a nylon membrane with water wettability can be cast only under the condition that the phase separation phenomenon is predominated by the crystallization of the nylon directly from the solution. Our results may thus carry the implication that, as Pall[6,7] suggested, the water wettability of commercial nylon membranes may derive from their special molecular arrangement at the membrane surface due to the crystallization of polymer directly from the solution instead of their surface topography (roughness porosity etc.). However, the reason why in such a case the given molecular arrangement is favored is not clear yet.

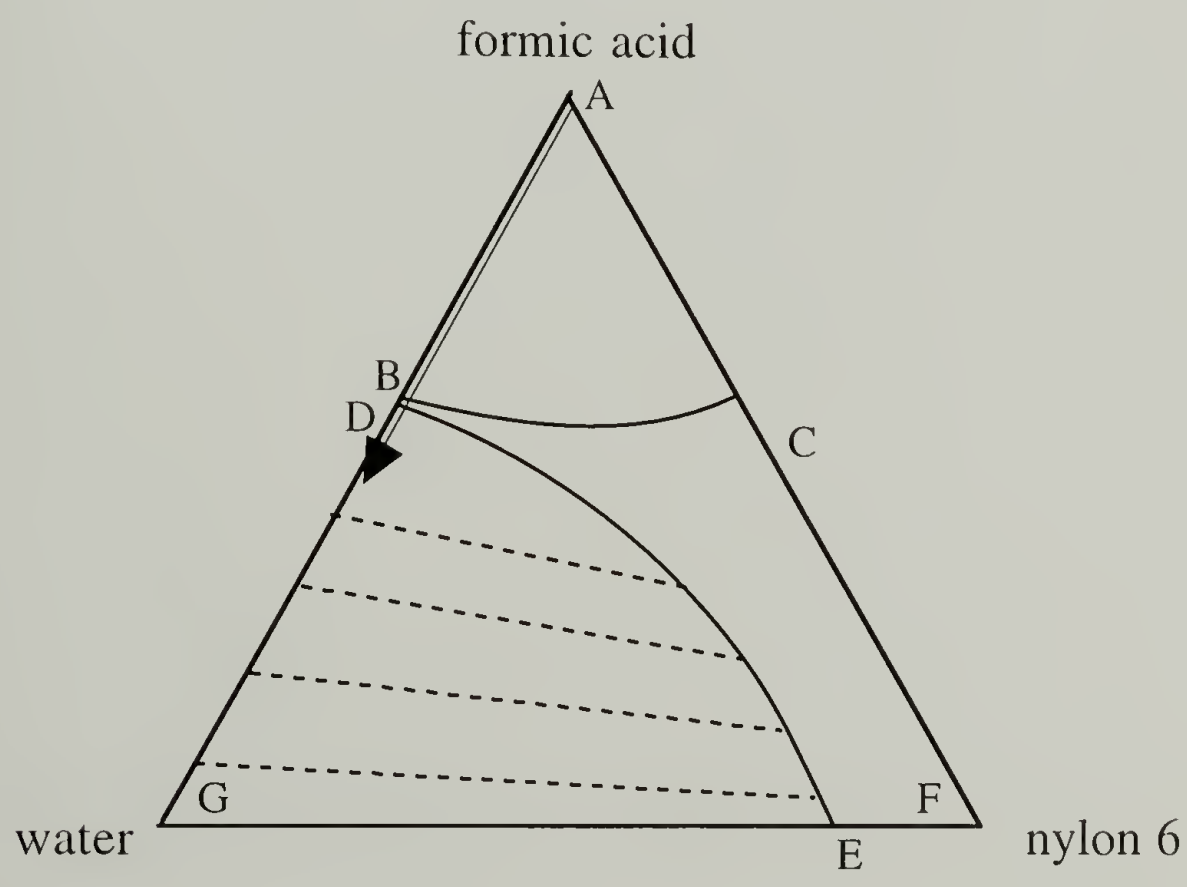

Figure 4.15 Ternary phase diagram for water-formic acid-nylon 6 system at 25°C (from reference 9). The arrow indicates the route of composition change in our experiment.

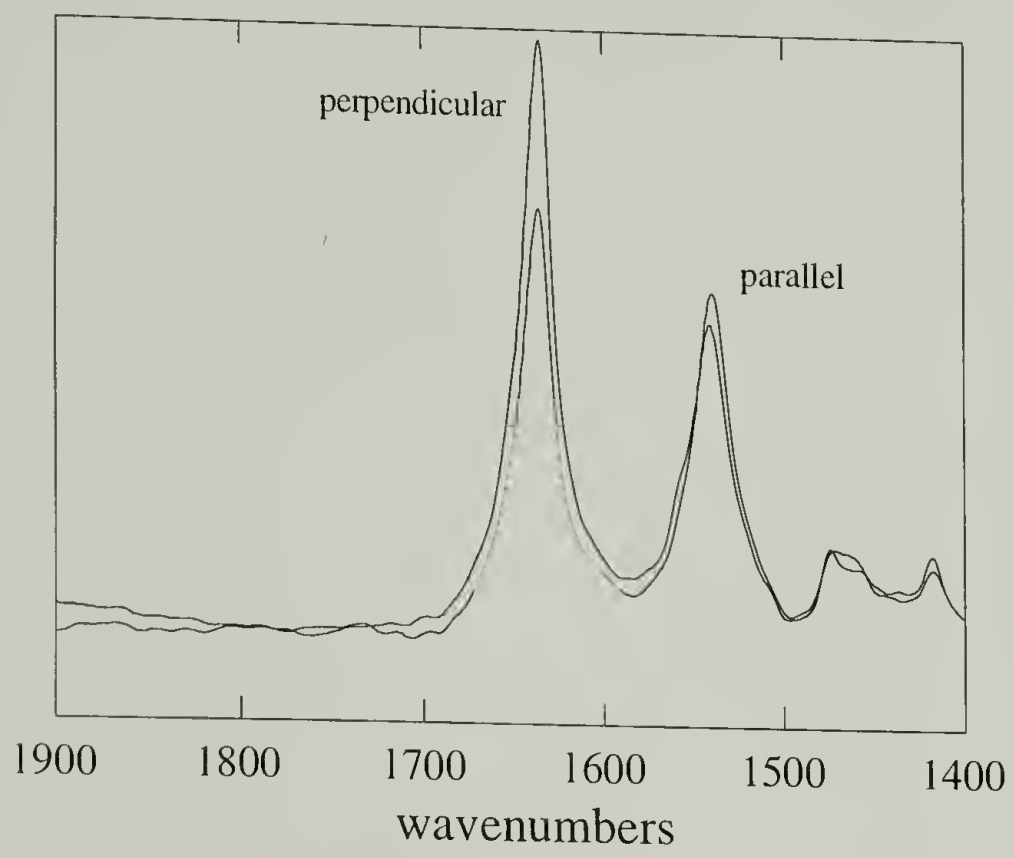

Figure 4.16 Polarized infrared spectra of nylon 66 deposited on oriented poly(tetrafluoroethylene) coagulated by quenching the formic acid solution with water. Polarization is relative to the rubbing direction.

4.4 Conclusions

In the presence of oriented poly(tetrafluoroethylene) films, both nylon 6 and nylon 66 were precipitated from their formic acid solutions by introducing different nonsolvents in their vapor phase. The resultant molecular arrangements of the nylon films on the substrate were characterized with polarized infrared spectroscopy and WAXD. Nonsolvents were found to have effects only on the degree of orientation in the films of both nylon 6 and nylon 66 with the same trend, i.e. the highest orientation achieved when water was used; and the least when ethanol was used. The modes of deposition of molecules are quite different between nylon 6 and nylon 66. For nylon 6, the molecular arrangement is such that the preferred segmental orientation is parallel to that of the poly(tetrafluoroethylene) molecules with their amide planes also parallel to the substrate.

However, for nylon 66, both of the molecules and the amide planes are preferably erect on the substrate with the preferred hydrogen bonding direction perpendicular to the poly(tetrafluoroethylene) molecules. This difference is supposed to be due to their different phase separation behavior, with the liquid-liquid phase separation predominant in the case of nylon 6 and with phase separation through crystallization for nylon 66. This conclusion may bear important implications in the mechanism of forming water-wettable nylon membranes.

References

(1) Dodd, J. W.; Holliday, P.; Parker, B. E. *Polymer* **1968**, *9*, 54.

(2) Fischer, E. W.; Willems, J. *J. Makromol. Chem.* **1966**, *99*, 85.

(3) Keller, H. H. *J. Polym. Sci.* **1959**, *36*, 361.

(4) Wang, L. F.; Kuo, J. F.; Chen, C. Y. *Colloid Polym. Sci.* **1995**, *273*, 16.

(5) Haraguchi, K.; Kajiyama, T.; Takayanagi, M. *J. Appl. Polym. Sci.* **1979**, *23*, 903.

(6) Pall, D. B.; Kirnbauer, E. A.; Allen, B. T. *Colloids and Surfaces* **1980**, *1*, 235.

(7) Pall, D. B., U. S. Patent 4,340,479, 1982.

(8) Knight, R. A.; Hazlett, T.; Gryte, C. C. In *Polym. Solns., Blends, and Interf.*; I. Noda and D. N. Rubingh, Ed.; Elsevier: Amsterdam, 1992; pp 299.

(9) Cheng, L.-P.; Dwan, A.-H.; Gryte, C. C. *J. Polym. Sci. Polym. Phys. Ed.* **1994**, *32*, 1183.

(10) Cheng, L.-P.; Dwan, A.-H.; Gryte, C. C. *J. Polym. Sci. Polym. Phys. Ed.* **1995**, *33*, 211.

(11) Marinaccio, P. J.; Knight, R. A., U. S. Patent 3,876,738, 1975.

(12) Kesting, R. E. *Synthetic Polymeric Membranes;* John Wiley & Sons, Inc.: New York, 1985, Chapt. 7.

(13) Brandrup, J.; Immergut, E. H. *Polymer Handbook*; John Wiley and Sons, Inc.: New York, 1975, Chapt. IV.

(14) Liang, C. Y.; Krimm, S. *J. Chem. Phys.* **1956**, *25*, 563.

(15) Boerio, F. J.; Koenig, J. L. *J. Chem. Phys.* **1970**, *52*, 4826.

(16) Moynihan, R. E. *J. Am. Chem. Soc.* **1959**, *81*, 1045.

(17) Rabolt, J. F.; Fanconi, B. *Macromolecules* **1978**, *11*, 740.

(18) Masetti, G.; Cabassi, F.; Morelli, G.; Zerbi, G. *Macromolecules* **1973**, *6*, 700.

(19) Arimoto, H. *J. Polym. Sci. A* **1964**, *2*, 2283.

(20) Bradbury, E. M.; Elliott, A. *Polymer* **1963**, *4*, 47.

(21) Miyazawa, T. *J. Chem. Phys.* **1960**, *32*, 1647.

(22) Miyazawa, T.; Blout, E. R. *J. Am. Chem. Soc.* **1961**, *83*, 712.

(23) Lewis, E. L. V.; Ward, I. M. *J. Macrom. Sci.* **1980**, *B18*, 1.

(24) Schaefgen, J. R.; Trivisonno, C. *J. Am. Chem. Soc.* **1951**, *73*, 4580.

(25) Tuzar, Z.; Kratochvil, P.; Bohdanecky, M. *Adv. Polym. Sci.* **1979**, *30*, 117.

(26) Nakajima, A.; Tanaami, K. *Polym. J.* **1973**, *5*, 248.

(27) Hattori, M.; Saito, M.; Okajima, K.; Kamide, K. *Polym. J.* **1995**, *27*, 631.

(28) Cannon, C. G. *Spectrochim. Acta* **1960**, *16*, 302.

(29) Khanna, Y. P. *Polym. Sci. Eng.* **1990**, *30*, 1615.

CHAPTER 5

General Results and Recommendations for Future Work

5.1 General Results

In this thesis we examine both the stabilizing and destabilizing effects of enviroment on the crystalline structure of biopolymers. The main characterization techniques include infrared spectroscopy and diffraction methods both in transmission and reflection modes. The results are herein summarized.

In Chapter 2, the effects of moisture sorption on the structure of a biosynthesized model polypeptide was investigated. The model polypeptide used in the hydration study has a lamellar structure with uniform lamellar thickness, a folding surface decorated with carboxylic acid or carboxylate functional groups and a crystalline core with β-sheet chain conformation. The accessibility of the structure to water was determined by following the deuteration kinetics. Its regular structure makes it possible to separate the various structure-related hydration events. The structure was found to be changed by moisture sorption in a sequential way. The folding surface functionality is hydrated most quickly followed by the expansion of crystalline core in the intersheet distance. The crystalline chain conformation is the last to be changed from β-sheet to disordered after the intersheet expansion is large enough to make the crystalline phase accessible to water. The expansion is proposed to be due to unfavorable surface energetics induced by the incorporation of water molecules on the folding surface. Comparison of hydration-induced structural changes between two polypeptides with different lamellar thickness support this

explanation. The change in chain conformation is ascribed to the direct interaction of water and peptide units.

In contrast to the potential destabilization effects of the environment (moisture) on crystalline structure described in Chapter 2, we examine the stabilization effects of an oriented substrate on the formation of nuclei and crystallites of silk fibroin even in the presence of extensive water-silk interaction. The oriented substrate used in the study of substrate-induced crystallization was prepared by rubbing a poly(tetrafluoroethylene) block on a glass slide at constant temperature and load. Silk fibroin known to be unable to crystallize from dilute aqueous solution with or without salt is found to crystallize in silk II form on this oriented substrate. The orientation and chain conformation of silk fibroin crystals thus formed are characterized with external reflection infrared spectroscopy. When salt-free aqueous silk solution is used, the preferred segmental orientation of silk fibroin is parallel to that of the oriented poly(tetrafluoroethylene) substrate. However, if lithium bromide solution is used, the orientation will be perpendicular to that of the substrate. Both lattice matching and surface topography are possible nucleation mechanism for the oriented crystallization in the salt-free case. On the other hand, surface topography is considered the only reason for the case with perpendicular orientation. Which mechanism(s) will be favored depends on the molecular configuration of silk fibroin in the solution prior to deposition.

In Chapter 4, we continue to study the crystallization behavior of nylon 6 and nylon 66 from formic acid solution induced by various nonsolvents in the presence of the oriented poly(tetrafluoroethylene) film. For either nylon, different degrees of orientation is achieved by using different nonsolvents, with the highest orientation obtained by using water and the least by using ethanol. This difference is supposed to be due to the different deposition rates caused by these nonsolvents. Different types of molecular arrangement are found in the films of two nylons deposited on the oriented substrate. Nylon 6 exhibits uniplanar

axial orientation with its hydrogen-bonded sheets parallel to the substrate surface and chain axis parallel to that of the substrate. On the other hand, nylon 66 shows a peculiar molecular arrangement with its hydrogen-bonded sheets preferably erect on the substrate and their hydrogen bonds perpendicular to the substrate molecular axis. This difference in molecular arrangement is supposed to be due to the different phase separation behavior between these two polymers. This conclusion may carry the implication that water wettability of commercial nylon membranes, which are inherently hydrophobic, may derive from their special molecular arrangement instead of their surface topography (roughness, porosity etc.).

5.2 Recommended Future Work

For the work on the hydration behavior of the model polypeptide, it would be interesting to pursue more work on similar polypeptides with various crystalline stem lengths. A critical stem length might exist for the hydration-induced structural changes to occur.

As stated in Chapter 3 and 4, the molecular configuration of the depositing polymer in the solution is crucial in determining the resultant spatial orientation. Therefore, the molecular parameters of nylons, for examole radius of gyration, characteristic ratio, in the mixture of solvent and nonsolvent at the point of incipient precipitation are useful in evaluating the deposition mechanism. These data can be obtained from light scattering and viscosity measurement. Furthermore, the characterization of the structure and orientation of nylon films formed on different substrates with different hydrophilicity and those formed at the nonsolvent vapor-formic acid solution interface will also be helpful in understanding the mechanism of formation of peculiar molecular arrangement of nylon films.

To further understand the origin of the water-wettability of commercial nylon membranes, the chemical composition and physical structure (e.g. chain conformation and orientation) at the membrane surface should be examined. X-ray photoelectron spectroscopy (XPS) and polarized attenuated total reflection (ATR) infrared spectroscopy can be used for the characterization purpose. Besides, depth-profiling of the molecular arrangement of nylon films deposited on substrates are particularly important in illuminating the effects of substrate and interface on the structural orientation.

BIBLIOGRAPHY

(1) Abe, Y.; Krimm, S. *Biopolymers* **1972**, *11*, 1817.

(2) Anderson, J. M.; Chen, H. H.; Rippon, W. B.; Walton, A. G. *J. Mol. Biol.* **1972**, *67*, 459.

(3) Arimoto, H. *J. Polym. Sci. A* **1964**, *2*, 2283.

(4) Asakura, T.; Yoshimizu, H.; Kakizaki, M. *Biotech. Bioeng.* **1990**, *35*, 511.

(5) Ayub, Z. H.; Arai, M.; Hirabayashi, K. *Polymer* **1994**, *35*, 2197.

(6) Baddiel, C. B.; Chaudhuri, D.; Stace, B. C. *Biopolymers* **1971**, *10*, 1169.

(7) Balasubramanian, D.; Shaikh, R. *Biopolymers* **1973**, *12*, 1639.

(8) Bamford, C. H.; Elliot, A.; Hanby, W. E. *Synthetic Polypeptides: Preparation, Structure and Properties*; Academic Press: New York, 1956, Chapt. 12.

(9) Binsbergen, F. L. *Polymer* **1970**, *11*, 253.

(10) Blout, E. R.; DE Loze, C.; Asadourian, A. *J. Am. Chem. Soc.* **1961**, *83*, 1895.

(11) Boerio, F. J.; Koenig, J. L. *J. Chem. Phys.* **1970**, *52*, 4826.

(12) Bolton, B. A.; Scherer, J. R. *J. Phys. Chem.* **1989**, *93*, 7635.

(13) Bradbury, E. M.; Brown, L.; Downie, A. R.; Elliott, A.; Fraser, R. D. B.; Hanby, W. E.; McDonald, T. R. R. *J. Mol. Biol.* **1960**, *2*, 276.

(14) Bradbury, E. M.; Elliott, A. *Polymer* **1963**, *4*, 47.

(15) Brandrup, J.; Immergut, E. H. *Polymer Handbook*; John Wiley and Sons, Inc.: New York, 1975, Chapt. IV.

(16) Broza, G.; Rieck, V.; Kawaguchi, A.; Petermann, J. *J. Mater. Sci.* **1985**, *23*, 2623.

(17) Brunauer, S.; Emmett, P. H.; Teller, E. *J. Am. Chem. Soc.* **1938**, *60*, 309.

(18) Bubeck, R. A.; Kramer, E. J. *J. Appl. Phys.* **1971**, *42*, 4631.

(19) Bull, H. *J. Am. Chem. Soc.* **1944**, *64*, 751.

(20) Bunn, C. W.; Howells, E. R. *Nature* **1954**, *174*, 549.

(21) Campbell, G. A. *J. Polym. Sci. B* **1969**, *7*, 629.

(22) Cannon, C. G. *Spectrochim. Acta* **1960**, *16*, 302.

(23) Careri, G.; Giansanti, A. *Biopolymers* **1979**, *18*, 1187.

(24) Carr, S. H.; Colket, W. C. *J. Colloid Interf. Sci.* **1969**, *31*, 328.

(25) Cheng, L.-P.; Dwan, A.-H.; Gryte, C. C. *J. Polym. Sci. Polym. Phys. Ed.* **1994**, *32*, 1183.

(26) Cheng, L.-P.; Dwan, A.-H.; Gryte, C. C. *J. Polym. Sci. Polym. Phys. Ed.* **1995**, *33*, 211.

(27) Chirgadze, Y. N.; Ovsepyan, A. M. *Biopolymers* **1972**, *11*, 2179.

(28) Chirgadze, Y. N.; Shestopalov, B. V.; Venyaminov, S. Y. *Biopolymers* **1973**, *12*, 1337.

(29) Chirgadze, Y. N.; Brazhnikov, E. V.; Nevskaya, N. A. *J. Mol. Biol.* **1976**, *102*, 781.

(30) D'Arcy, R. L.; Watt, I. C. *Trans. Faraday Soc.* **1969**, *66*, 1236.

(31) Davidson, T.; Gounder, R. N. In *Adhesion and Adsorption of Polymers*; L. H. Lee, Ed.; Plenum Press: New York, 1980; Vol. 12B; pp 775.

(32) Dodd, J. W.; Holliday, P.; Parker, B. E. *Polymer* **1968**, *9*, 54.

(33) Fenwick, D.; Ihn, K. J.; Motamedi, F.; Wittman, J. C.; Smith, P. *J. Appl. Polym. Sci.* **1993**, *50*, 1151.

(34) Fischer, E. W.; Willems, J. *J. Makromol. Chem.* **1966**, *99*, 85.

(35) Flory, P. J. *J. Chem. Phys.* **1942**, *10*, 51.

(36) Fraser, R. D. B.; MacRae, T. P.; Stewart, F. H. C.; Suzuki, E. *J. Mol. Biol.* **1965**, *11*, 706.

(37) Fraser, R. D. B.; MacRae, T. P. *Conformation in Fibrous Proteins*; Academic Press: New York, 1973.

(38) Fuzek, J. F. In *Water in Polymers*; S. P. Rowland, Ed.; ACS Symposium Series 127: Washington, D. C., 1980; pp 515.

(39) Gohil, R. M. *J. Polym. Sci. Polym. Phys. Ed.* **1985**, *23*, 1713.

(40) Greenspan, L. *J. Res. Nat. Bur. Standards* **1977**, *81A*, 89.

(41) Gross, B.; Petermann, J. *J. Mater. Sci.* **1984**, *19*, 105.

(42) Hansma, H.; Motamedi, F.; Smith, P.; Hansma, P.; Wittman, J. C. *Polymer* **1992**, *33*, 647.

(43) Haraguchi, K.; Kajiyama, T.; Takayanagi, M. *J. Appl. Polym. Sci.* **1979**, *23*, 903.

(44) Hattori, M.; Saito, M.; Okajima, K.; Kamide, K. *Polym. J.* **1995**, *27*, 631.

(45) Hayward, D. O.; Trapnell, B. M. W. *Chemisorption*; Butterworths: London, 1964.

(46) Huggins, M. L. *Ann. N. Y. Acad. Sci.* **1943**, *44*, 431.

(47) Iizuka, E.; Yang, J. T. *Biochemistry* **1968**, *7*, 2218.

(48) Iizuka, E. *J. Appl. Polym. Sci.: Appl. Polym. Symp.* **1985**, *41*, 173.

(49) Inoue, K.; Hoshino, S. *J. Polym. Sci., Polym. Phys. Ed.* **1976**, *14*, 1513.

(50) Ishida, M.; Asakura, T.; Yokoi, M.; Saito, H. *Macromolecules* **1990**, *23*, 88.

(51) Jesser, W. A.; Kuhlmann-Wilsdorf, D. *Phys. Stat. Solidi* **1967**, *19*, 95.

(52) Kawasaki, K.; Sekita, Y.; Kanoue, K. *J. Colloid Sci.* **1962**, *17*, 865.

(53) Keller, H. H. *J. Polym. Sci.* **1959**, *36*, 361.

(54) Kesting, R. E. *Synthetic Polymeric Membranes;* John Wiley & Sons, Inc.: New York, 1985, Chapt. 7.

(55) Khanna, Y. P. *Polym. Sci. Eng.* **1990**, *30*, 1615.

(56) Kim, H.; Harget, P. J. *J. Appl. Phys.* **1979**, *50*, 6072.

(57) Kitchener, A.; Vincent, J. F. V. *J. Mater. Sci.* **1987**, *22*, 1385.

(58) Knight, R. A.; Hazlett, T.; Gryte, C. C. In *Polym. Solns., Blends, and Interf.*; I. Noda and D. N. Rubingh, Ed.; Elsevier: Amsterdam, 1992; pp 299.

(59) Kojima, M.; Satake, H. *J. Polym. Sci. Polym. Phys. Ed.* **1984**, *22*, 285.

(60) Koutsky, J. A.; Walton, A. G.; Baer, E. *J. Polym. Sci. A-2* **1966**, *4*, 611.

(61) Krejchi, M. T.; Atkins, E. D. T.; Waddon, A. J.; Fournier, M. J.; Mason, T. L.; Tirrell, D. A. *Science* **1994**, *265*, 1427.

(62) Krimm, S.; Bandekar, J. *Adv. Protein Chem.* **1986**, *38*, 181.

(63) Kuntz, I. D. *J. Am. Chem. Soc.* **1971**, *93*, 516.

(64) Kuntz, I. D.; Kauzmann, W. *Adv. Protein Chem.* **1974**, *28*, 239.

(65) Kurtz, J.; Harrington, W. F. *J. Mol. Biol.* **1966**, *17*, 440.

(66) Kusanagi, H.; Yukawa, S. *Polymer* **1994**, *35*, 5637.

(67) Kutsumizu, S.; Nagao, N.; Tadano, K.; Tachino, H.; Hirasawa, E.; Yano, S. *Macromolecules* **1992**, *25*, 6829.

(68) Lee, I. H.; Schultz, J. M. *J. Mater. Sci.* **1988**, *23*, 4237.

(69) Lenormant, H.; Baudras, A.; Blout, E. R. *J. Am. Chem. Soc.* **1958**, *80*, 6191.

(70) Lewis, E. L. V.; Ward, I. M. *J. Macrom. Sci. -Phys.* **1980**, *B18*, 1.

(71) Liang, C. Y.; Krimm, S. *J. Chem. Phys.* **1956**, *25*, 563.

(72) Lotz, B.; Wittmann, J. C. *J. Polym. Sci. Polym. Phys. Ed.* **1986**, *24*, 1559.

(73) Lowry, S. R.; Mauritz, K. A. *J. Am. Chem. Soc.* **1980**, *102*, 4665.

(74) Magoshi, J. *Polymer* **1977**, *18*, 643.

(75) Magoshi, J.; Mizuide, M.; Magoshi, Y.; Takahashi, K.; Kubo, H.; Nakamura, S. *J. Polym. Sci. Polym. Phys. Ed.* **1979**, *17*, 515.

(76) Magoshi, J.; Magoshi, Y.; Nakamura, S. *J. Polym. Sci. Polym. Phys. Ed.* **1981**, *19*, 185.

(77) Magoshi, J.; Magoshi, Y.; Nakamura, S. *J. Appl. Polym. Sci.: Appl. Polym. Symp.* **1985**, *41*, 187.

(78) Magoshi, J.; Kamiyama, S.; Nakamura, S. In *7th International Wool Textile Research Conference*; Tokyo, 1985; pp 337.

(79) Magoshi, J.; Magoshi, Y.; Nakamura, S. In *Silk Polymers*; D. Kaplan, W. W. Adams, B. Farmer and C. Viney, Ed.; American Chemical Society: Washington D. C., 1994; pp 292.

(80) Mandelkern, L.; Halpin, J. C.; Diorio, A. F.; Posner, A. S. *J. Am. Chem. Soc.* **1962**, *84*, 1383.

(81) Marinaccio, P. J.; Knight, R. A. U. S. Patent 3,876,738, 1975.

(82) Marsh, R. E.; Corey, R. B.; Pauling, L. *Biochim. Biophys. Acta* **1955**, *16*, 1.

(83) Masetti, G.; Cabassi, F.; Morelli, G.; Zerbi, G. *Macromolecules* **1973**, *6*, 700.

(84) McLaren, A. D.; Rowen, J. W. *J. Polym. Sci.* **1951**, *7*, 289.

(85) Michielsen, S. *J. Appl. Polym. Sci.* **1994**, *52*, 1081.

(86) Miyazawa, T. *J. Chem. Phys.* **1960**, *32*, 1647.

(87) Miyazawa, T.; Blout, E. R. *J. Am. Chem. Soc.* **1961**, *83*, 712.

(88) Moore, W. H.; Krimm, S. *Biopolymers* **1976**, *15*, 2465.

(89) Motamedi, F.; Ihn, K. J.; Fenwick, D.; Wittmann, J.-C.; Smith, P. *J. Polym. Sci. Polym. Phys. Ed.* **1994**, *32*, 453.

(90) Moynihan, R. E. *J. Am. Chem. Soc.* **1959**, *81*, 1045.

(91) Muller, W. S.; Samuelson, L. A.; Fossey, S. A.; Kaplan, D. In *Silk Polymers*; D. Kaplan, W. W. Adams, B. Farmer and C. Viney, Ed.; American Chemical Society: Washinton D. C., 1994; pp 342.

(92) Murthy, N. S.; Stamm, M.; Sibilia, J. P.; Krimm, S. *Macromolecules* **1989**, *22*, 1261.

(93) Nakajima, A.; Tanaami, K. *Polym. J.* **1973**, *5*, 248.

(94) Nishio, Y.; Yamane, T.; Takahashi, T. *J. Macromolec. Sci. -Phys.* **1984**, *B23*, 17.

(95) Oono, T.; Kumamaru, F.; Kajiyama, T.; Takayanagi, M. *Rep. Prog. Polym. Phys. Japan* **1981**, *24*, 193.

(96) Painter, P. C.; Coleman, M. M. *Biopolymers* **1978**, *17*, 2475.

(97) Pall, D. B.; Kirnbauer, E. A.; Allen, B. T. *Colloids and Surfaces* **1980**, *1*, 235.

(98) Pall, D. B. U. S. Patent 4,340,479, 1982.

(99) Pashley, D. W. *Advan. Phys.* **1956**, *5*, 173.

(100) Pethig, R. *Dielectric and Electronic Properties of Biological Materials*; John Wiley and Sons: New York, 1979, pp 119.

(101) Pineri, M. H.; Escoubes, M.; Roche, G. *Biopolymers* **1978**, *17*, 2799.

(102) Pool, P. L.; Finney, J. L. *Biopolymers* **1983**, *22*, 255.

(103) Pool, P. L.; Finney, J. L. *Biopolymers* **1984**, *23*, 1647.

(104) Puffr, R. J.; Sebenda, J. J. *J. Polym. Sci. C.* **1967**, *16*, 79.

(105) Puffr, R. *Kolloid-Z. Z. Polym* **1968**, *222*, 130.

(106) Rabolt, J. F.; Fanconi, B. *Macromolecules* **1978**, *11*, 740.

(107) Reimschuessel, H. K. *J. Polym. Sci., Polym. Chem. Ed.* **1978**, *16*, 1229.

(108) Ren, Y. Ph. D. Thesis, U. Massachusetts, 1995.

(109) Rowen, J. W.; Simha, R. *J. Phys. Chem.* **1949**, *53*, 921.

(110) Rupley, J. A.; Yang, P.-H.; Tollin, U. In *Water in Polymers*; S. P. Rowland, Ed.; ACS Symposium Series 127: Washington, D. C., 1980; pp 111.

(111) Schaefgen, J. R.; Trivisonno, C. *J. Am. Chem. Soc.* **1951**, *73*, 4580.

(112) Shmueli, U.; Traub, W. *J. Mol. Biol.* **1965**, *12*, 205.

(113) Sperati, C. A.; Starkweather, H. W. *Adv. Polym. Sci.* **1961**, *2*, 465.

(114) Susi, H.; Timasheff, S. N.; Stevens, L. *J. Biol. Chem.* **1967**, *242*, 5460.

(115) Takahashi, T.; Teraoka, F.; Tsujimoto, I. *J. Macromol. Sci. -Phys.* **1976**, *B12*, 303.

(116) Teeter, M. M. *Annu. Rev. Biophys. Biophys. Chem.* **1991**, *20*, 577.

(117) Tirrell, D.; Grossman, S.; Vogl, O. *Makromol.Chem.* **1979**, *180*, 721.

(118) Tsuboi, M.; Nakanishi, M. *Adv. Biophys.* **1979**, *12*, 101.

(119) Tuzar, Z.; Kratochvil, P.; Bohdanecky, M. *Adv. Polym. Sci.* **1979**, *30*, 117.

(120) Vergalati, C.; Imberty, A.; Perez, S. *Macromolecules* **1993**, *26*, 4420.

(121) Verma, A.; Deopura, B. L.; Sengupta, A. K. *Text. Res. J.* **1984**, *54*, 92.

(122) Vollrath, F.; Edmonds, D. T. *Nature* **1989**, *340*, 305.

(123) Walton, A. G.; Carr, S. H.; Baer, E. *Polymer Preprints* **1968**, *9*, 603.

(124) Wang, L. F.; Kuo, J. F.; Chen, C. Y. *Colloid Polym. Sci.* **1995**, *273*, 16.

(125) Willems, J. *Experientia* **1967**, *23*, 409.

(126) Wittmann, J. C.; Lotz, B. *J. Polym. Sci. Polym. Phys. Ed.* **1981**, *19*, 1837.

(127) Wittmann, J. C.; Smith, P. *Nature* **1991**, *352*, 414.

(128) Wunderlich, B. *Macromolecular Physics, Crystal Structure, Morphology, Defects*; Academic Press: New York, 1973; Vol. 1.

(129) Yakhnin, E. D.; Egorova, Y. V.; Evko, E. I.; Taubman, A. B.; Lukyanovich, V. M. *J. Crystal Growth* **1969**, *5*, 184.

(130) Yamaura, K.; Okumura, Y.; Matsuzawa, S. *J. Macromol. Sci. -Phys.* **1982**, *B21*, 49.

(131) Zerbi, G.; Sacchi, M. *Macromolecules* **1973**, *6*, 692.